NEW MOLECULAR TOOLS FOR DOLLAR SPOT DETECTION AND THE GENETIC MAKEUP, BIOLOGICAL CONTROL EFFICACY, AND NITROUS OXIDE EMISSION MITIGATION OF TRICHODERMA T22

by

KYARI ASTER OLEANDER

(Under the Direction of Alfredo D. Martinez-Espinoza)

ABSTRACT

This dissertation explores several research topics and aspects, including molecular assay design, genomic analysis, and biological experimental design in two pathosystems. Dollar spot is the costliest turfgrass pathogen worldwide and rapidly causes damage that affects turfgrass quality and value. *Clarireedia jacksonii* and *C. monteithiana* are the two most common species that cause dollar spot in the United States, and rapid pathogen detection is required for management. This research included designing, testing, and optimizing two novel dollar spot detection assays. In three hours, a co-dominant cleaved amplified polymorphic sequences (CAPS) assay can detect and differentiate the two species, *C. jacksonii* and *C. monteithiana*. A portable colorimetric probe-based loop-mediated isothermal amplification (LAMP) assay can detect both U.S. species found in grass samples within 1.2 hours. These tools allow for faster, more precise dollar spot detection and will help turfgrass managers make better decisions. Switching from pathogen detection to disease protection, *Trichoderma* is a biological control fungus that forms protective symbiotic rhizosphere relationships. The *Trichoderma* strain T22 has been used for decades, but little research has been performed to understand its genomic background. This research included

sequencing the protoplast fusion participants, T12 and T95, and comparing those genomes to the resulting T22 genome. This study found that T22 does not have genomic contributions from T95 supported by single nucleotide polymorphisms or structural variants. Additionally, the genetic differences between T12 and T22 were examined and detailed to aid future research in enhancing *Trichoderma* biocontrol. Continuing to evaluate plant and ecosystem protection, this research also investigated using *Trichoderma* T22 to manage the nitrous oxide (N_2O) emissions of the fungal pathogen *Fusarium verticillioides* (*Fv*). N_2O is a potent greenhouse gas released by fungi during agricultural use that contributes to global warming and systemic nitrogen loss. Results found that T22 produces N_2O in some specific conditions and can mitigate *Fv* N_2O emissions in others. Additionally, both strains produced small amounts of N_2O in the soil settings tested. These results show that T22 has promise as an N_2O mitigator but requires more research and potential genetic modification to remove N_2O production potential.

INDEX WORDS: *Trichoderma, Fusarium, Clarireedia,* Biological control, Nitrous oxide, Pathogen detection

NEW MOLECULAR TOOLS FOR DOLLAR SPOT DETECTION AND THE GENETIC MAKEUP, BIOLOGICAL CONTROL EFFICACY, AND NITROUS OXIDE EMISSION MITIGATION OF TRICHODERMA T22

by

KYARI ASTER OLEANDER

B.S., The University of Tennessee, 2016

M.S., The University of Tennessee, 2019

A Dissertation Submitted to the Graduate Faculty of The University of Georgia in Partial Fulfillment of the Requirements for the Degree

DOCTOR OF PHILOSOPHY

ATHENS, GEORGIA

2025

NEW MOLECULAR TOOLS FOR DOLLAR SPOT DETECTION AND THE GENETIC MAKEUP, BIOLOGICAL CONTROL EFFICACY, AND NITROUS OXIDE EMISSION MITIGATION OF TRICHODERMA T22

by

KYARI ASTER OLEANDER

Major Professor:	Alfredo D. Martinez-Espinoza
Committee:	James W. Buck
	Shavannor Smith
	Gerald Henry

Electronic Version Approved:

Ron Walcott
Vice Provost for Graduate Education and Dean of the Graduate School
The University of Georgia
May 2025

DEDICATION

To the dreamers, wishers, hopers, and lovers.

To the readers, teachers, thinkers, and fighters.

To the uncommon and unknowing,

I dedicate this work to those who are curious and ever-growing.

ACKNOWLEDGEMENTS

I want to acknowledge those who helped me along my academic career. This includes friends, colleagues, mentors, and many more. I want to thank TMRU at USDA-ARS; this unit has been my home for the last four years, and I'm thankful for your continual support. I want to thank the University of Georgia Plant Pathology Department and the Society of Aspiring Plant Pathologists for the community and support they provided. I especially want to thank those who helped through three advisor changes, several project changes, a campus change, and all other aspects of my journey. I could not have done this without the guidance of others. I hope all those who supported me know that I am eternally grateful.

TABLE OF CONTENTS

Page

LIST OF TABLES

Page

LIST OF FIGURES

Page

CHAPTER 1

INTRODUCTION AND LITERATURE REVIEW

Turfgrass – Importance, Benefits, and General Summary

Turfgrasses are bred and cultivated for low mowing heights and are used worldwide for lawns, recreation, and commercial use. Turfgrass covers over 50 million acres of land nationwide, surpassing all but four food crops in total acreage (Morris 2003, USDA 2019). The turfgrass industry is responsible for over 800,000 jobs and is valued at $100 billion to the U.S. economy (Haydu et al. 2006, Shaddox et al. 2022). Turfgrass has long been associated with increased human health and positive environmental benefits. Green spaces reduce stress and depression symptoms and improve cognitive skills and physical activity (Beard and Green 1994, Frumkin 2001, Barrett et al. 2014, Beyer et al. 2014). Turfgrass can reduce overland water flow, contributing to erosion and chemical runoff (Morton et al. 1988, Gross et al. 1991). It has also been shown to reduce atmospheric temperatures and decrease heat island effects in urban spaces, decreasing indoor cooling costs (Wang et al. 2016, Amani-Beni et al. 2018, Braun et al. 2024). Turfgrass exhibits unique growth patterns, and its management requirements set turfgrass apart from most cropping systems. Turfgrass management primarily aims to maintain visual and functional quality (Morris and Shearman 1998). The exact goals vary depending on the turfgrass use, but visual characteristics typically include density, color, uniformity, texture, and smoothness, while functional characteristics include rigidity, rooting, resiliency, and elasticity (Morris and Shearman 1998).

Depending on their photosynthetic metabolism, turfgrass species are considered cool-season or warm-season. Cool-season grasses fix carbon dioxide (CO_2) into a 3-carbon molecule using ribulose-1,5-bisphosphate (RuBP) carboxylase during the C_3 cycle (Ehleringer and Cerling 2002). In contrast, warm-season grasses fix carbon dioxide into 4-carbon molecules using phosphoenolpyruvate (PEP) carboxylase in the C_4 cycle (Ehleringer and Cerling 2002). The terms cool-season and C_3 grasses along with warm-season and C_4 grasses are used interchangeably. The optimal temperature range for cool-season and warm-season grasses follows their naming pattern, with cool-season grass growth being optimal at 15 to 24 °C (59 to 75 °F) and warm-season grass growth optimal at 26 to 35 °C (78 to 95 °F) (Huang and Jiang 2002, Christians et al. 2016). C_3 grasses grow primarily in spring and fall, with slow or no growth in summer (Huang and Jiang 2002). Meanwhile, C_4 grasses grow from late spring through early fall (Christians et al. 2016). Climate maps can help determine the suitability of a cool- or warm-season grass for a specific area, while the presence of both cool and warm-season grasses overlap in the transition zone (Cook and Ervin 2010, Christians et al. 2016). Other factors, such as the salinity of the soil or disease resistance, may also significantly affect turfgrass selection (Hatfield 2017). Many resources can be used to help select the ideal turfgrass for an area such as the local county extension office or the NTEP website https://www.ntep.org (Casler and Duncan 2003, Christians et al. 2016).

Turfgrass management can vary depending on the use and function of a particular stand. Turfgrass used for sports requires the most maintenance, while recreational landscapes may receive less management inputs. Proper fertilization is key to turfgrass management and includes regular applications of macro- (nitrogen, phosphorus, potassium) and micronutrients (iron, zinc, copper, manganese, boron, chloride, molybdenum, and nickel) (Carrow et al. 2002). Micronutrient deficiencies are uncommon in turfgrass and can be treated if symptoms arise (McCarty 2011). The

turfgrass must be actively growing to utilize the fertilizer nutrients; therefore, application scheduling is different for cool- and warm-season turfgrasses.

Irrigation requirements may vary depending on the environmental conditions, turfgrass species, and soil type. The combined water loss from the soil surface (evaporation) and from the plant (transpiration) can be used to calculate the water needs of the turfgrass (Ehleringer and Cerling 2002, Christians et al. 2016). C_4 turfgrasses will have lower evapotranspiration rates because they have better photosynthetic efficiency than C_3 turfgrasses. All turfgrasses can close stomata in response to heat stress, but C_4 plants will maintain higher CO_2 levels within their cells due to physical separation of CO_2 fixation (Ehleringer and Cerling 2002). The amount and timing of irrigation varies, but it is typically best performed in the early hours to reduce evaporative loss and reduce periods of leaf wetness that can promote disease (Christians et al. 2016).

Mowing is the removal of shoot tissue from the turfgrass canopy. This stresses the plant as it removes photosynthetic tissue and causes wounds, but it is essential to turfgrass management. Mowing requirements vary depending on the turfgrass species and purpose, but typically, no more than one-third of the desired height is removed at one time (Reicher 2006). The direction in which turfgrass grows and leans, otherwise known as grain, affects golf ball movement on putting greens, so mowing patterns are often rotated to keep plants vertically oriented (Beard 2002). Turfgrass cultivation, including aerification and verticutting, is performed to alleviate soil compaction and reduce thatch (Reicher 2006). However, these practices can also temporarily decrease turfgrass stand density and create ports for disease entrance through wounding (Reicher 2006). Topdressing with soil or sand is often performed after cultivation to fill the holes and smooth the surface (Davis 1978).

Dollar Spot – Summarizing the Most Common Turfgrass Pathogen

Plant diseases cause significant losses within cropping systems, including turfgrass. Fungi, nematodes, viruses, and bacteria cause most plant diseases. However, turfgrass diseases are primarily caused by fungal pathogens, with over 150 fungal species causing turfgrass diseases (Couch 1995). Over $80 million, or 20% of the national fungicide market, is spent annually on turfgrass pathogens (Nelson and Boehm 2002, Vargas 2018). In the U.S., fungicides are used in turfgrass more than other commodities. Most turfgrass pathogens are either foliar or crown and root diseases, mainly managed culturally or chemically (Vargas 2018). Fungicides are grouped by their mode of action (MOA), which is defined by how the active ingredient disrupts the pathogen. Turfgrass fungal management includes 11 of the 13 major fungicide FRAC codes, with four of them in use for dollar spot management (FRAC, https://www.frac.info/home). Rotating through various FRAC codes throughout a growing season is encouraged to reduce the potential for fungicide resistance (Young and Patton 2010).

Dollar spot is a widespread foliar disease that has been reported in allturfgrass species. Dollar spot is a fungal infection caused by *Clarireedia* spp. that create small, blighted, sunken patches that decrease playability and aesthetic value (Couch 1995). The lesions begin as individual spots on the leaves but coalesce into 2- to 3-inch sunken patches the size of a half-dollar coin (Smiley et al. 2005, Vargas 2018). Fluffy, gray mycelia can sometimes be observed in the early morning when the turfgrass is covered in dew (Smiley et al. 2005). This sign can be confused with other pathogens, such as *Pythium* and *Rhizoctonia*, but can be distinguished with microscopy (Allen et al. 2005, Vargas 2018). Dollar spot does not produce spores for dissemination but is primarily transported via infected tissues, animals, equipment, water, and wind (Smiley et al. 2005).

Dollar spot causes disease on more than 40 hosts, primarily in Poaceae grass family (Walsh et al. 1999). Due to its widespread distribution and host range, dollar spot is the most economically important turfgrass pathogen (Couch 1995, Vargas 2018). It's estimated that 70% of fungicide applications on golf courses go towards managing dollar spot, anthracnose, and brown patch, with ten or more fungicide applications each year (Bonos et al. 2006, Hammerschmidt 2018). While some cultivars and species are more tolerant, there are no sources of complete disease resistance to dollar spot (Walsh et al. 1999).

The species taxonomy for dollar spot had been debated for almost a century due to its apparent lack of sexual structures (Monteith 1927, Bennett 1937, Whetzel 1945, Carbone and Kohn 1993). The fungal pathogens that cause dollar spot are now classified as the genus *Clarireedia* within the *Rutstroemiaceae* family (Salgado-Salazar et al. 2018). The reclassification was made based on ITS, calmodulin, and Mcm7 (Salgado-Salazar et al. 2018). When renamed in 2018, there were four species: *C. homoeocarpa*, *C. benettii*, *C. jacksonii*, and *C. monteithiana*. *C jacksonii* and *C. monteithiana* are both globally distributed, while *C. homoeocarpa* and *C. benettii* are both mostly restricted to the United Kingdom (Salgado-Salazar et al. 2018). Since 2018, three more species have been added, *C. paspali* and *C. aff. paspali* (Hu et al. 2019, Bahri et al. 2023) and *C. hainanense* (Zhang et al. 2022), all found in China and Hawaii. Initially, *C. jacksonii* and *C. monteithiana* were both thought to be host-specific, where *C. jacksonii* infected C_3 hosts and *C. monteithiana* infected C_4 hosts (Salgado-Salazar et al. 2018); however, pathogenicity assays found that both *C. jacksonii* and *C. monteithiana* could infect both C_3 and C_4 grasses (Aynardi et al. 2019, Sapkota et al. 2020).

The most critical factor in disease management is accurate diagnosis (Agrios 2005). This can be particularly difficult in grasses. There are often symptom overlaps that can lead to

misdiagnosis. Factors such as site history, cultivar or species, season, climate, signs, and symptomology play a role in correct diagnosis. *Clarireedia* can be identified with PCR, but that is time-consuming and requires laboratory equipment that a turfgrass manager is not likely to possess (Salgado-Salazar et al. 2018). *Clarireedia* does not have any reliable morphological features to differentiate between species (Salgado-Salazar et al. 2018). DNA sequencing of CaM, Mcm7, EF-1α genes, or the ITS region via PCR can differentiate the species with SNPs, but this is an expensive process taking several days. A need was identified to differentiate between the species more quickly and to have a portable diagnosis method. These needs were both addressed by the research detailed in this dissertation.

Trichoderma – A Readily Transformable Rhizosphere Competent Biocontrol and Biofertilizing Fungus

Trichoderma was first characterized from soil and plant debris in 1794 (Persoon 1794). As of 2019, over 300 species of *Trichoderma have been* identified (Marik et al. 2019). *Trichoderma* is one of the most frequently isolated soil fungi, with 10^1-10^3 culturable propagules per gram in most temperate and tropical soils, and is often considered an indicator of soil health (Harman et al. 2004, Lange 2014). *Trichoderma* species are not limited to soil and have been found on tree bark and in algae and sponges in aquatic systems (Gal-Hemed et al. 2011, Mukherjee et al. 2014, Song et al. 2018). Some species of *Trichoderma* do not have sexual phases, while others have the teleomorph previously named *Hypocrea* (Druzhinina and Kubicek 2005, Druzhinina et al. 2010). While some strains form plant symbiotic relationships that have made *Trichoderma* famous for biocontrol and biofertilizer use, others thrive mainly as saprotrophs (Contreras-Cornejo et al. 2009).

Some *Trichoderma* strains are rhizosphere competent, meaning they colonize the plant rhizosphere, form mutualistic relationships with the plant roots, and improve plant growth. *Trichoderma* is endophytic and will colonize in and around the roots of many host plants (Harman et al. 2004, Bailey and Melnick 2013). *Trichoderma* and the plant interact through this physical contact or release of chemicals like volatile organic compounds (VOCs) and key plant metabolites, including phytoalexins and phytohormones (Contreras-Cornejo et al. 2009, Manganiello et al. 2018, Villalobos-Escobedo et al. 2020). Root colonization of *Trichoderma* induces both local and systemic resistance that helps the plants defend against future pathogen attacks (Djonovic et al. 2006). Evidence shows that *T. virens* receives sucrose from the plant to support fungal growth (Vargas et al. 2009). Generally, plants with *Trichoderma* in their rhizosphere will have more developed root systems with more root hairs, lateral roots, and a higher total surface area than those without the symbiont. Some strains colonize specific portions of a root system, such as the root hairs or tips. Notably, some strains of *Trichoderma*, including our primary strain of interest, T22, colonize and affect the entire root system. It is estimated from metabolomic studies that there are over 100 organic compounds that *Trichoderma spp*. secrete during interactions with other organisms (Sharma et al. 2017).

Trichoderma spp. that suppress soil-borne plant pathogens via mycoparasitism will sense the presence of a host-pathogen fungus, grow towards it, penetrate it, and kill it for nutrients and other resources. *Trichoderma* produces many degrative enzymes for mycoparasitism, including chitinases, proteases, and glucanases (Zimand et al. 1996, Harman et al. 2004). *Trichoderma* also produces siderophores to chelate iron while depriving other microorganisms of this needed nutrient, weakening the target and increasing its susceptibility to attack (Contreras-Cornejo et al. 2020). Many *Trichoderma* species are non-pathogenic opportunistic plant symbionts that can be

used as low-cost, effective biocontrol and biofertilizer agents. The yield improvements from *Trichoderma* as a biofertilizer can be dramatic; for example, an $8 treatment of *Trichoderma* led to yield improvements of over $400 per hectare (Harman 2011). These symbionts can be added to many different pathosystems without impairing other beneficial microorganisms or impacting soil biotic equilibrium. *Trichoderma* symbiosis leads to plant resistance to a range of plant pathogens, increased absorption of nutrients, increased abiotic stress tolerance, and stimulation of various metabolite biosynthesis, including plant growth regulators, siderophores, and antibiotics (Kuć 2001, Van Wees et al. 2008, Fu et al. 2021). Several hundred strains of *Trichoderma* have been used commercially as biocontrol agents (Singh et al. 2009). The number of strains with commercial use varies from country to country, with India having around 250 strains (Singh et al. 2009). In the United States, ten EPA PC codes contain 13 unique *Trichoderma* strains used for biopesticides.

Trichoderma afroharzianum T22 is a biocontrol and biofertilizer strain reportedly produced via protoplast fusion that has been sold worldwide as RootShield to manage various fungi and Oomycota since the early 1990s (Harman et al. 1993). T22 is labeled for control of *Pythium, Rhizoctonia, Fusarium, Thielaviopsis,* and *Cylindrocladium* and is used on a vast range of plant hosts, including corn, turfgrass, and ornamentals. T22 was generated using protoplast fusion of two complementary auxotrophic mutants of T12 and T95 (Stasz et al. 1988). T12 was selected for biocontrol efficacy, while T95 was chosen for rhizosphere competency (Stasz et al. 1988, Sivan and Harman 1991). The protoplast fusion goal was a combination of these two traits. The selected strain, T22, outcompeted the parental strains in several key characteristics, including biocontrol efficacy, rhizosphere competency, and growth rate (Harman et al. 1993). The two fusion participant strains were never genetically characterized. Understanding the genotypes of these parental strains was the goal of Objective 2 in this dissertation. This, in turn, will give an insight

into the participation of each strain and how their combination resulted in an increased biocontrol potential.

Trichoderma has been transformed using several methods to study the organism and produce better biocontrol strains. Genome modification of *Trichoderma* is most reported through polyethylene glycol (PEG) mediated transformation of protoplasts (see Wang et al. 2022 for a review of *Trichoderma* transformation techniques) (Cai et al. 2021, Wang et al. 2022). While not a transformation, this is similar to the method used to create T22, using PEG-mediated protoplast fusion of two strains of interest (Stasz et al. 1988, Herrera-Estrella et al. 1990). *Trichoderma* can also be transformed using *Agrobacterium tumefaciens*-mediated transformation (ATMT) of conidia, protoplasts, or mycelia for random insertion or homologous recombination (Elena et al. 2006, Cai et al. 2021, Wang et al. 2022). ATMT efficiency in *T. reesei* was much higher (5x to 10x more transformants) when using protoplasts compared to conidia (Zhong et al. 2007). Electroporation and biolistic bombardment have also been used in *Trichoderma* transformation but are not as common as the other methods (Te'o et al. 2002, Kim and Miasnikov 2013, Wang et al. 2022).

Trichoderma is a potential N_2O emitter, but some strains have been used to reduce overall N_2O emissions in some crop environments through its biofertilizer capabilities. There have been several studies on fungi regarding their ability to produce N_2O (Lavrent'ev et al. 2008, Mothapo et al. 2013, Jirout 2015, Maeda et al. 2015, Mothapo et al. 2015). Generally, *Trichoderma* is considered a potential denitrifier, with some strains capable of producing high amounts of N_2O and others not (Maeda et al. 2015). These results have been examined in soil and/or in vitro. However, many reports on mitigating N_2O emissions use *Trichoderma* as a biofertilizer and different nitrogen inputs such as agricultural wastewater or biochar, instead of conventional

fertilizer sources, to reduce N_2O emissions (Kashyap et al. 2017, Xu et al. 2018, Sani et al. 2020, Geng et al. 2021, Wang et al. 2021). Tea plants are often used for this research in fields and greenhouse settings. Tea fields have a much higher (9.4 ± 6.2 times) N_2O flux when compared to woodlands, and these N_2O emissions can be mitigated with *Trichoderma* biofertilizer application (Xu et al. 2014, Xu et al. 2017). Most of this change is attributed to the difference in nitrogen sources. Still, it shows promise in using *Trichoderma* as a biofertilizer and other tools to mitigate agricultural N_2O emissions. Further studies are needed to determine if N_2O emissions can be reduced with *Trichoderma* application and traditional inorganic nitrogen sources.

Trichoderma's Use Within Turfgrass Systems

Trichoderma has been studied as a management strategy for several different turfgrass pathogens. Turfgrass, especially sports fields, can be a high-input crop with large amounts of fertilizer and pesticides used to manage growth, recovery, and health. In 2021, turf nitrogen inputs in the golf course sector alone were projected to be approximately 54,000 tons in the U.S., with approximately 1.58 lbs. of nitrogen added per 1,000 ft² (GCSAA 2022). In addition, the dependence on chemical pesticides in turfgrass management has increased in recent years (GCSAA 2022). There is a low threshold for damage in sports fields and golf courses. Many turfgrass pathogens, such as dollar spot, rapidly spread causing significant reductions in turfgrass aesthetics and health. These factors have made biocontrol agents, such as *Trichoderma,* an appealing potential management strategy against various turfgrass pathogens. Strains of *Trichoderma*, including T22, have been used to manage *Rhizoctonia solani* (Lo et al. 1996, Mocioni et al. 2003, Coelho et al. 2021), *Clarireedia* spp. (formally *Sclerotinia homoeocarpa*) (Lo et al. 1998, Carey et al. 2011, Coelho et al. 2021), *Pythium graminicola* (Lo et al. 1998), *Nigrospora sphaerica* (Zhang et al. 2021), *Bipolaris peregianensis* (TariqJaveed et al. 2021), and

various plant parasitic nematodes (TariqJaveed et al. 2021). However, the literature is inconclusive regarding whether *Trichoderma* T22 can manage dollar spot. For example, dollar spot, previously *Sclerotinia homoeocarpa,* is now known to be several *Clarireedia* spp., which may cause the inconsistency in T22 dollar spot management results (Lo et al. 1998, Carey et al. 2011, Coelho et al. 2021). *Trichoderma* as a biofertilizer has also been examined with positive results in turfgrass systems, particularly for surviving environmental stressors such as drought (Patakioutas et al. 2014, TariqJaveed et al. 2021). While the research proposed here is mainly proof of concept, we expect these results could most likely be transferable to a turfgrass system.

The Nitrogen Cycle, Denitrification, and Nitrous Oxide Emissions in Agriculture

Nitrogen in environments like in soil, travels through the nitrogen cycle and is reduced or oxidized by microbes through nitrogen fixation, ammonification, decomposition, nitrification, denitrification, and assimilation. These processes take nitrogen through various steps from being fully reduced (amines) to being fully oxidized (nitrate) (Stein and Klotz 2016). Nitrogen is the most limiting plant nutrient. For most cropping systems, excluding legumes with "nitrogen fixing" bacterial symbiotes, this nutrient is added as a reactive nitrogen source (Signor and Cerri 2013). For all other plants, nitrogen becomes available in the soil through added fertilizer, lightning, or the aerobic and anaerobic breakdown of organic material. Fourteen million metric tons of ammonia are consumed each year in the U.S., with 88% of that being attributed to fertilizer use in the form of directly applying urea, ammonium nitrates, ammonium phosphates, and other nitrogen compounds derived from atmospheric nitrogen (Survey 2023). This nitrogen is primarily produced using Haber-Bosch's conversion of atmospheric nitrogen and hydrogen to ammonia ($N_2 + 3H_2 \rightarrow 2NH_3$) under very high pressure and heat (Haber and Le Rossignol 1913). Plants or other organisms will uptake this available nitrogen, leaving the system through volatilization, denitrification,

leaching, or runoff (Petrovic 1990). The nitrogen amount utilized by plants varies depending on the planting system and crop (Glass 2003, Stevens et al. 2005).

Denitrification is the biological process of redox reactions from nitrate (NO_3^-) and nitrite (NO_2^-) to atmospheric nitrogen (N_2) or nitrous oxide (N_2O). This process occurs in both prokaryotes and eukaryotes, with bacteria, archaea, and fungi being relevant soil denitrifiers. The enzymes responsible for denitrification include dissimilatory nitrate reductase (dNAR), dissimilatory nitrite reductase (dNIR), nitric oxide reductase (NOR; p450nor), and nitrous oxide reductase (NOS) (Figure 1.1). Nitrous oxide reductase (NOS) is only present in prokaryotes. Fungi lacks NOS, so they produce N_2O as a final product without further reduction in dinitrogen. To be considered a fungal denitrifier, a strain must have the genomic presence and function of dNIR and NOR to convert NO_2^- to N_2O (Shoun et al. 2012).

Oakley (2023) examined the genus *Fusarium* for pathway genes, and among the strains investigated (73), approximately 85% had at least a portion of the denitrification pathway (Oakley BA 2025). There were various pathway combinations, but all strains with any portion of the denitrification pathway contained NOR (Oakley BA 2025). Most of the strains with NOR also contained dNIR (Oakley BA 2025). dNAR was present in about 31% of the strains examined (Oakley BA 2025). This is not true of all genera within Hypocreales but suggests many species of *Fusarium* are denitrifiers. Maeda et al. (2015) found that N_2O-emitting fungal species were primarily in the order Hypocreales. Most isolates produced more N_2O at a neutral pH with ≤ 10% atmospheric O_2 (Lavrent'ev et al. 2008, Maeda et al. 2015). Additionally, fungi with high N_2O emissions were primarily associated with intensively managed soil systems, like agriculture. Many of these species are saprotrophs distributed throughout the soil, an environment that can often be hypoxic and trigger denitrification.

Nitrous oxide has about 300 times the warming potential of CO_2 (pound for pound) and an atmospheric lifetime of 116 ± 9 years (Prather et al. 2015, EPA 2023). An atmospheric lifetime is defined as the average time an N_2O molecule will stay in the atmosphere before it is removed by a sink or destroyed by chemical reactions (EPA 2023). Nitrous oxide concentration in the atmosphere has increased from 270 ppb before the Industrial Revolution to 334 ppb in 2021 (Pachauri and Reisinger 2007, Galloway et al. 2008, Signor and Cerri 2013, Wuebbles 2017). It is currently estimated that about 50% of the world's population is nitrogen fertilizer dependent, and the agricultural need for nitrogen fertilizers is expected to increase with rising population, so the atmospheric N_2O concentration is also likely to increase (Galloway et al. 2008, Walling and Vaneeckhaute 2020). With 73% of N_2O emissions directly derived from agricultural soil management, there is a need to mitigate agricultural soil nitrogen emissions (EPA 2023).

Many studies have explored when N_2O is released in agricultural fields and what environmental conditions affect N_2O release. These studies often use closed air chambers directly above the soil that capture N_2O, and either are read in the field with automated systems or collected in syringes and taken back to a laboratory for gas chromatography (Cates Jr. and Keeney 1987, Wagner-Riddle et al. 1997, Ma et al. 2010, Yang et al. 2012, Amadi et al. 2016, Zhou et al. 2017, Johnson and Barbour 2019, Fiorini et al. 2020). Fortunately, many of these studies were in maize, one of our crops of interest (Cates Jr. and Keeney 1987, Wagner-Riddle et al. 1997, Ma et al. 2010, Johnson and Barbour 2019, Fiorini et al. 2020), with rice being another common crop for N_2O studies (Yang et al. 2012, Zhou et al. 2017). There are specifically high spikes after fertilization with inorganic nitrogen fertilizers and heavy rains (Zhou et al. 2017). The type of nitrogen applied also impacts N_2O emission levels, with organic sources like manure generally taking longer to break down than inorganic sources like ammonium. This longer breakdown time means less of an

emission spike immediately after fertilizing. It allows for the crop to use nitrogen over time instead of losing a significant portion immediately after fertilization. Maize is a crop with high nitrogen input needs, and most of the N_2O emission studies examined if different nitrogen sources impacted N_2O emissions. Rice patties are flooded for much of their growth, explaining why rice has also been well-studied for N_2O emissions. Many of these studies also explore carbon dioxide and methane emissions, but those are outside the scope of this dissertation. These studies generally have several static chambers set up in field within each treatment where they take samples 3-5 times over 0 to 30 minutes after chamber closure. Most published studies took samples mid-morning once or twice weekly, with additional samples taken daily for the first week after fertilization (Zhou et al. 2017). Publications varied from monitoring over one season to seven years. There are also several reports showing that heavily managed turfgrass, such as golf courses and sports fields, have similar N_2O emissions as agriculture, with homeowner and urban turfgrass systems releasing around half the emissions of agricultural settings (Maggiotto et al. 2000, Li et al. 2013, van Delden et al. 2016, Braun and Bremer 2018).

The previous study by Maeda et al. (2015) found that *F. verticillioides* produced N_2O in malt medium and sterile soil (60% water holding capacity) spiked with sodium nitrite (Maeda et al. 2015). A recent study from Oakley 2023 reported that cultures inoculated with *Fv*Δ*nor1* deletion mutants in *Fusarium verticillioides* produced 50-fold less N_2O compared to the wild-type (Oakley 2023). *F. verticillioides* was selected as a model in the Oakley 2023 study, as it has single copies of each of the three essential denitrification genes and is a corn pathogen of interest. Mutants, add-back transformants, and sexual crosses were produced, and the N_2O emissions were quantified. Growth rates of the various deletion and add-back strains were not statistically different from the wild type. That study asserts that *NOR1* could be a valuable target for eliminating fungal-

derived agricultural N_2O emissions. It also asserts that since 50% of applied fertilizer is lost due to soil processes and environmental conditions, inhibiting fungal N_2O emissions could reduce nitrogen fertilizer loss and subsequent applications, saving growers money and giving ecological benefits (Hirel et al. 2011). My research aims to explore potential N_2O emission mitigation using *Trichoderma*, a well-documented biocontrol agent, to reduce N_2O emitting fungal soil populations.

Fusarium verticillioides **– The Pathogen and Nitrous Oxide Emitter**

Fusarium verticillioides (Fv) is a mycotoxigenic fungal pathogen of maize, a staple crop for both human and animal feed, worldwide (Baldwin et al. 2014). *F. verticillioides* is capable of causing disease throughout the maize life cycle, including seedling blight and rots of stalk, root, kernel, seed, and ears (Blacutt et al. 2018). *F. verticillioides* infection is often associated with host tissue damage typically caused by either insect feeding or mechanically (Duncan and Howard 2009). As a pathogen, *F. verticillioides* can cause a reduction in yield and produce fumonisin secondary metabolites that are toxic to humans and animals (Presello et al. 2008, Duncan and Howard 2009). *F. verticillioides* is often an asymptomatic maize endophyte that is still mycotoxigenic, actively contributing to fumonisin contamination (Nelson et al. 1993, Duncan and Howard 2009).

Many species of *Fusarium* can colonize plant debris and persist in soils for about two years, typically on crop residues (Nelson et al. 1994, Blacutt et al. 2018, Paugh and Gordon 2021). Warm and dry temperate field conditions are optimal for *F. verticillioides* and fumonisin production (Santiago et al. 2015). Root rot and seedling blight can develop if seedlings are germinated under conducive conditions in *F. verticillioides*-infested soils. If the conditions are not conducive to disease, *F. verticillioides* can form asymptomatic, systemic, endophytic infections in maize. Later infections can occur if there is plant wounding for *F. verticillioides* to enter the stalks or ears. Ear

rot occurs most often under wet conditions post-silking. After these infections, *F. verticillioides* can colonize, form conidia, and disperse, serving as subsequent primary inoculum (Blacutt et al. 2018).

Current management strategies for *F. verticillioides* maize colonization include reducing insect feeding and biocontrol seed coatings. Insect feeding in maize can be decreased with *Bt* transgenic maize and earlier planting dates (Wu 2006, Parsons and Munkvold 2012). Pereira et al. used *Bacillus amyloliquefaciens, Microbacterium oleovorans,* and *Enterobacter hormaechei* to reduce *F. verticillioides* infection in maize grain (Pereira et al. 2007, Pereira et al. 2010). *Trichoderma* has also been used as a mycoparasitic biocontrol against *F. verticillioides* (Ferrigo et al. 2014, Ferrigo et al. 2014, Galletti et al. 2020, Cuervo-Parra et al. 2022). Several strains of Trichoderma have been used to manage *F. verticillioides* in maize, including the commercially available strain of interest for our research, *T. harzianum* T22 (Ferrigo et al. 2014). T22 colonizes the maize roots and enhances activation of the SA- and JA/ET-dependent defense responses to help combat *F. verticillioides* disease incidence (Ferrigo et al. 2014, Ferrigo et al. 2014). Cultural practices such as crop rotation, tillage, and residue destruction may also help reduce *F. verticillioides* primary inoculum.

Fusarium verticillioides, along with many other species in the Hypocreales, produce N_2O (Shoun et al. 1992, Lavrent'ev et al. 2008, Mothapo et al. 2013, Maeda et al. 2015, Mothapo et al. 2015). *F. verticillioides* produces N_2O in agricultural soil (Maeda et al. 2015). As detailed previously, Oakley (2023) found that *Fv*Δ*nor1* deletion mutant cultures produce drastically less N_2O than wild-type cultures without affecting fungal growth. This research aims to use *F. verticillioides* as a model organism to determine if *Trichoderma*, a well-documented biocontrol agent, can reduce N_2O emissions by managing *F. verticillioides*, with or without genetic

manipulation. Additionally, we aim to gain a better genetic understanding of the biocontrol strain T22 and a better understanding of N_2O emissions from *Trichoderma* strains.

Rationale

Dollar spot is the costliest turfgrass disease worldwide. For turfgrass management within the U.S., *C. jacksonii* and *C. monteithiana* must be detected quickly, with as little expense and time as possible. This allows for rapid response to decrease damage and management costs. New assays are needed to make these goals achievable.

T22 is a crucial *Trichoderma* strain used for decades, but little is known about the parental line genetics. This information can help inform future line selection and genetic modifications for biocontrol production. Genetic testing on the parental strains is needed to better understand this important strain.

Nitrous oxide is a major fungal emission of concern for its greenhouse warming effects. There is a need to explore new management strategies for fungal N_2O emissions in agricultural soil.

Research Objectives

This research used molecular biology techniques to create new disease detection assays for turfgrass dollar spot management. This research also used fungal genetics and biological techniques to further understand the genetic background of the *Trichoderma* strain T22 and its potential use for fungal N_2O emission management. The following were objectives for this research:

1. Objective one: Develop specific, sensitive, and rapid molecular assays for turfgrass dollar spot detection and species identification.

2. Objective two: Evaluate the genomic structure and protoplast participant contribution to *Trichoderma* strain T-22 through whole genome SNP analysis of reported protoplast fusion participants.
3. Objective three: Test the use of *Trichoderma* biocontrol agent T22 to reduce fungal N_2O production in fertilized soils.

These findings allow for more rapid speciation differentiation between *C. jacksonii* and *C. monteithiana* in lab settings and for more rapid identification of these species with a portable diagnosis method. These findings also give a genetic understanding of the commercially available and widely used *Trichoderma* T22. Additionally, the potential for using T22 as a fungal N_2O emission mitigator was examined using its ability to manage *Fusarium verticillioides.*

References

Agrios, G. (2005). Plant Pathology. London, UK, Elsevier Academic Press.

Allen, T., A. Martinez and L. Burpee (2005). "Dollar spot of turfgrass." Plant Health Instr doi **101094**.

Amadi, C. C., K. C. J. Van Rees and R. E. Farrell (2016). "Soil–atmosphere exchange of carbon dioxide, methane and nitrous oxide in shelterbelts compared with adjacent cropped fields." Agriculture, Ecosystems & Environment **223**: 123-134.

Amani-Beni, M., B. Zhang and J. Xu (2018). "Impact of urban park's tree, grass and waterbody on microclimate in hot summer days: A case study of Olympic Park in Beijing, China." Urban Forestry & Urban Greening **32**: 1-6.

Aynardi, B., M. Jiménez-Gasco and W. Uddin (2019). "Effects of isolates of Clarireedia jacksonii and Clarireedia monteithiana on severity of dollar spot in turfgrasses by host type." European Journal of Plant Pathology **155**: 817-829.

Bahri, B. A., R. K. Parvathaneni, W. T. Spratling, H. Saxena, S. Sapkota, P. L. Raymer and A. D. Martinez-Espinoza (2023). "Whole genome sequencing of Clarireedia aff. paspali reveals potential pathogenesis factors in Clarireedia species, causal agents of dollar spot in turfgrass." Front Genet **13**: 1033437.

Bailey, B. A. and R. L. Melnick (2013). The endophytic *Trichoderma*. *Trichoderma*: Biology and applications, CABI Wallingford UK**:** 152-172.

Baldwin, T. T., N. C. Zitomer, T. R. Mitchell, A.-M. Zimeri, C. W. Bacon, R. T. Riley and A. E. Glenn (2014). "Maize seedling blight induced by *Fusarium verticillioides*: accumulation off fumonisin B1 in leaves without colonization of the leaves." Journal of Agricultural and Food Chemistry **62**(9): 2118-2125.

Barrett, M. A., D. Miller and H. Frumkin (2014). "Parks and health: aligning incentives to create innovations in chronic disease prevention." Preventing chronic disease **11**: E63.

Beard, J. B. (2002). Turf Management for Golf Courses. Chelsea, MI, Ann Arbor Press.

Beard, J. B. and R. L. Green (1994). "The role of turfgrasses in environmental protection and their benefits to humans." Journal of environmental quality **23**(3): 452-460.

Bennett, F. (1937). "Dollar spot disease of turf and its causal organism Sclerotinia homoeocarpa n. sp."

Beyer, K. M., A. Kaltenbach, A. Szabo, S. Bogar, F. J. Nieto and K. M. Malecki (2014). "Exposure to neighborhood green space and mental health: evidence from the survey of the health of Wisconsin." International journal of environmental research and public health **11**(3): 3453-3472.

Blacutt, A. A., S. E. Gold, K. A. Voss, M. Gao and A. E. Glenn (2018). "*Fusarium verticillioides*: Advancements in understanding the toxicity, virulence, and niche

adaptations of a model mycotoxigenic pathogen of maize." Phytopathology **108**(3): 312-326.

Bonos, S. A., B. B. Clarke and W. A. Meyer (2006). "Breeding for disease resistance in the major cool-season turfgrasses." Annu. Rev. Phytopathol. **44**(1): 213-234.

Braun, R. C. and D. J. Bremer (2018). "Nitrous oxide emissions in turfgrass systems: a review." Agronomy Journal **110**(6): 2222-2232.

Braun, R. C., P. Mandal, E. Nwachukwu and A. Stanton (2024). "The role of turfgrasses in environmental protection and their benefits to humans: Thirty years later." Crop Science **64**(6): 2909-2944.

Cai, F., C. P. Kubicek and I. S. Druzhinina (2021). Genetic transformation of *Trichoderma* spp. Biofuels and Biodiesel, Springer**:** 171-185.

Carbone, I. and L. M. Kohn (1993). "Ribosomal DNA sequence divergence within internal transcribed spacer 1 of the Sclerotiniaceae." Mycologia **85**(3): 415-427.

Carey, K., A. Porter, E. Lyons and K. Jordan (2011). *Trichoderma harzianum* as a biocontrol for dollar spot disease (*Sclerotinia homoeocarpa*) on creeping bentgrass turf-2011 trial. 2011 Annual Research Report, Guelph Turfgrass Institute.

Carrow, R. N., D. V. Waddington and P. E. Rieke (2002). Turfgrass soil fertility & chemical problems: Assessment and management, John Wiley & Sons.

Casler, M. D. and R. R. Duncan (2003). Turfgrass biology, genetics, and breeding, John Wiley & Sons.

Cates Jr., R. L. and D. R. Keeney (1987). "Nitrous oxide production throughout the year from fertilized and manured maize fields." Journal of Environmental Quality **16**(4): 443-447.

Christians, N. E., A. J. Patton and Q. D. Law (2016). Fundamentals of turfgrass management, John Wiley & Sons.

Coelho, L., M. Reis, C. Guerrero and L. Dionísio (2021). "Biological control of turfgrass diseases with organic composts enriched with *Trichoderma atroviride*." Biological Control **159**: 104620.

Contreras-Cornejo, H. A., L. Macías-Rodríguez, C. Cortés-Penagos and J. López-Bucio (2009). "*Trichoderma virens*, a plant beneficial fungus, enhances biomass production and promotes lateral root growth through an auxin-dependent mechanism in *Arabidopsis*." Plant Physiol **149**(3): 1579-1592.

Contreras-Cornejo, H. A., L. Macías-Rodríguez, E. del-Val and J. Larsen (2020). "Interactions of *Trichoderma* with plants, insects, and plant pathogen microorganisms: Chemical and molecular bases." Co-evolution of Secondary Metabolites: 263-290.

Cook, T. W. and E. H. Ervin (2010). "Lawn ecology." Urban ecosystem ecology **55**: 153-178.

Couch, H. B. (1995). Diseases of turfgrasses.

Cuervo-Parra, J. A., V. H. Pérez España, E. A. Zavala-González, M. Peralta-Gil, J. E. Aparicio Burgos and T. Romero-Cortes (2022). "*Trichoderma asperellum* strains as potential biological control agents against *Fusarium verticillioides* and *Ustilago maydis* in maize." Biocontrol Science and Technology **32**(5): 624-647.

Davis, W. B. (1978). "Pros and cons of frequent sand topdressing." Calif. Turfgrass Cult **28**: 25-29.

Djonovic, S., C. Howell and C. Kenerley (2006). "Sm1, a proteinaceous elicitor secreted by the biocontrol fungus *Trichoderma virens* induces plant defense responses and systemic resistance." Mol Plant Microbe Interact **19**: 838-853.

Druzhinina, I. and C. P. Kubicek (2005). "Species concepts and biodiversity in *Trichoderma* and *Hypocrea:* From aggregate species to species clusters?" J Zhejiang Univ Sci B **6**(2): 100-112.

Druzhinina, I. S., C. P. Kubicek, M. Komoń-Zelazowska, T. B. Mulaw and J. Bissett (2010). "The *Trichoderma harzianum* demon: Complex speciation history resulting in coexistence of hypothetical biological species, recent agamospecies and numerous relict lineages." BMC Evol Biol **10**(1): 1-14.

Duncan, K. E. and R. J. Howard (2009). "Biology of maize kernel infection by *Fusarium verticillioides*." Molecular Plant-Microbe Interactions **23**(1): 6-16.

Ehleringer, J. R. and T. E. Cerling (2002). "C3 and C4 photosynthesis." Encyclopedia of global environmental change **2**(4): 186-190.

Elena, C. R., V. J. Antonio, H. M. Rosa, M. Enrique and G. Santiago (2006). "A comparison of the phenotypic and genetic stability of recombinant *Trichoderma* spp. generated by protoplast-and *Agrobacterium*-mediated transformation." Journal of Microbiology **44**(4): 383-395.

EPA, U. S. E. P. A. (2023). "Overview of greenhouse gases." EPA, from https://www.epa.gov/ghgemissions/overview-greenhouse-gases.

Ferrigo, D., A. Raiola, E. Piccolo, C. Scopel and R. Causin (2014). "*Trichoderma harzianum* T22 induces in maize systemic resistance against *Fusarium verticillioides*." Journal of Plant Pathology **96**(1).

Ferrigo, D., A. Raiola, R. Rasera and R. Causin (2014). "*Trichoderma harzianum* seed treatment controls *Fusarium verticillioides* colonization and fumonisin contamination in maize under field conditions." Crop Protection **65**: 51-56.

Fiorini, A., S. C. Maris, D. Abalos, S. Amaducci and V. Tabaglio (2020). "Combining no-till with rye (*Secale cereale* L.) cover crop mitigates nitrous oxide emissions without decreasing yield." Soil and Tillage Research **196**: 104442.

Frumkin, H. (2001). "Beyond toxicity: human health and the natural environment." American journal of preventive medicine **20**(3): 234-240.

Fu, J., Y. Xiao, Y. F. Wang, Z. H. Liu, Y. F. Zhang and K. J. Yang (2021). "*Trichoderma asperellum* alters fungal community composition in saline–alkaline soil maize rhizospheres." Soil Sci Soc Am J **85**(4): 1091-1104.

Gal-Hemed, I., L. Atanasova, M. Komon-Zelazowska, I. S. Druzhinina, A. Viterbo and O. Yarden (2011). "Marine isolates of *Trichoderma* spp. as potential halotolerant agents of biological control for arid-zone agriculture." Applied and Environmental Microbiology **77**(15): 5100-5109.

Galletti, S., R. Paris and S. Cianchetta (2020). "Selected isolates of *Trichoderma gamsii* induce different pathways of systemic resistance in maize upon *Fusarium verticillioides* challenge." Microbiological research **233**: 126406.

Galloway, J. N., A. R. Townsend, J. W. Erisman, M. Bekunda, Z. Cai, J. R. Freney, L. A. Martinelli, S. P. Seitzinger and M. A. Sutton (2008). "Transformation of the nitrogen cycle: Recent trends, questions, and potential solutions." Science **320**(5878): 889-892.

GCSAA, G. C. S. A. o. A. (2022). 2022 nutrient use and management practices on U.S. golf courses. Golf Course Environmental Profile. **Phase III, Volume ll**.

GCSAA, G. C. S. A. o. A. (2022). A continued investigation into pest management practices on U.S. golf courses. Golf Course Environmental Profile. **Phase III, Volume llI**.

Geng, Y., Y. Yuan, Y. Miao, J. Zhi, M. Huang, Y. Zhang, H. Wang, Q. Shen, J. Zou and S. Li (2021). "Decreased nitrous oxide emissions associated with functional microbial genes under bio-organic fertilizer application in vegetable fields." Pedosphere **31**(2): 279-288.

Glass, A. D. (2003). "Nitrogen use efficiency of crop plants: physiological constraints upon nitrogen absorption." Critical reviews in plant sciences **22**(5): 453-470.

Gross, C. M., J. Angle, R. Hill and M. Welterlen (1991). Runoff and sediment losses from tall fescue under simulated rainfall, Wiley Online Library.

Haber, F. and R. Le Rossignol (1913). "Über die technische Darstellung von Ammoniak aus den Elementen." Zeitschrift für Elektrochemie und angewandte physikalische Chemie **19**(2): 53-72.

Hammerschmidt, R. (2018). Biology, Etiology, and Management of Dollar Spot in Turfgrasses. In: National Information Management & Support System. **NC1208**.

Harman, G. E. (2011). "*Trichoderma*—not just for biocontrol anymore." Phytoparasitica **39**(2): 103-108.

Harman, G. E., C. R. Howell, A. Viterbo, I. Chet and M. Lorito (2004). "*Trichoderma* species—opportunistic, avirulent plant symbionts." Nature Rev Microbiol **2**(1): 43-56.

Harman, G. E., T. E. Stasz and N. F. Weeden (1993). Fused biocontrol agents. United States, Cornell Research Foundation Inc. **US5260213A**.

Hatfield, J. (2017). "Turfgrass and climate change." Agronomy Journal **109**(4): 1708-1718.

Haydu, J. J., A. W. Hodges and C. R. Hall (2006). "Economic impacts of the turfgrass and lawncare industry in the United States: FE632/FE632, 4/2006." Edis **2006**(7).

Herrera-Estrella, A., G. H. Goldman and M. Van Montagu (1990). "High-efficiency transformation system for the biocontrol agents, *Trichoderma* spp." Molecular Microbiology **4**(5): 839-843.

Hirel, B., T. Tétu, P. J. Lea and F. Dubois (2011). "Improving nitrogen use efficiency in crops for sustainable agriculture." Sustainability **3**(9): 1452-1485.

Hu, J., Y. Zhou, J. Geng, Y. Dai, H. Ren and K. Lamour (2019). "A new dollar spot disease of turfgrass caused by Clarireedia paspali." Mycological progress **18**: 1423-1435.

Huang, B. and Y. Jiang (2002). "Irrigation management and heat tolerance." Golf Course Management **70**: 49-52.

Jirout, J. (2015). "Nitrous oxide productivity of soil fungi along a gradient of cattle impact." Fungal Ecology **17**: 155-163.

Johnson, J. M. F. and N. W. Barbour (2019). "Stover harvest did not change nitrous oxide emissions in two Minnesota fields." Agronomy Journal **111**(1): 143-155.

Kashyap, P. L., P. Rai, A. K. Srivastava and S. Kumar (2017). "Trichoderma for climate resilient agriculture." World Journal of Microbiology and Biotechnology **33**(8): 155.

Kim, S. and A. Miasnikov (2013). Method for introducing nucleic acids into fungal cells. US, Danisco US Inc. **US20100304468A1**.

Kuć, J. (2001). "Concepts and direction of induced systemic resistance in plants and its application." Eur J Plant Pathol **107**: 7-12.

Lange, L. (2014). "The importance of fungi and mycology for addressing major global challenges." IMA Fungus **5**(2): 463-471.

Lavrent'ev, R., S. Zaitsev, I. Sudnitsyn and A. Kurakov (2008). "Nitrous oxide production by fungi in soils under different moisture levels." Moscow University soil science bulletin **63**(4): 178-183.

Li, X., F. Hu, D. Bowman and W. Shi (2013). "Nitrous oxide production in turfgrass systems: Effects of soil properties and grass clipping recycling." Applied Soil Ecology **67**: 61-69.

Lo, C., E. Nelson and G. Harman (1996). "Biological control of turfgrass diseases with a rhizosphere competent strain of *Trichoderma harzianum*." Plant Disease.

Lo, C. T., E. B. Nelson, C. K. Hayes and G. E. Harman (1998). "Ecological studies of transformed *Trichoderma harzianum* strain 1295–22 in the rhizosphere and on the phylloplane of creeping bentgrass." Phytopathology **88**(2): 129-136.

Ma, B. L., T. Y. Wu, N. Tremblay, W. Deen, M. J. Morrison, N. B. McLaughlin, E. G. Gregorich and G. Stewart (2010). "Nitrous oxide fluxes from corn fields: on-farm assessment of the amount and timing of nitrogen fertilizer." Global Change Biology **16**(1): 156-170.

Maeda, K., A. Spor, V. Edel-Hermann, C. Heraud, M.-C. Breuil, F. Bizouard, S. Toyoda, N. Yoshida, C. Steinberg and L. Philippot (2015). "N2O production, a widespread trait in fungi." Scientific Reports **5**(1): 1-7.

Maggiotto, S., J. Webb, C. Wagner-Riddle and G. Thurtell (2000). Nitrous and nitrogen oxide emissions from turfgrass receiving different forms of nitrogen fertilizer, Wiley Online Library.

Manganiello, G., A. Sacco, M. R. Ercolano, F. Vinale, S. Lanzuise, A. Pascale, M. Napolitano, N. Lombardi, M. Lorito and S. L. Woo (2018). "Modulation of tomato response to

Rhizoctonia solani by *Trichoderma harzianum* and its secondary metabolite harzianic acid." Front Microbiol **9**: 1966.

Marik, T., C. Tyagi, D. Balázs, P. Urbán, Á. Szepesi, L. Bakacsy, G. Endre, D. Rakk, A. Szekeres and M. A. Andersson (2019). "Structural diversity and bioactivities of peptaibol compounds from the *Longibrachiatum* clade of the filamentous fungal genus *Trichoderma*." Front Microbiol **10**: 1434.

McCarty, L. B. (2011). Best golf course management practices: construction, watering, fertilizing, cultural practices, and pest management strategies to maintain golf course turf with minimal environmental impact, Prentice Hall.

Mocioni, M., P. Titone, A. Garibaldi and M. Gullino (2003). "Efficacy of different fungicides against *Rhizoctonia* brown patch and *Pythium* blight on turfgrass in Italy." Communications in agricultural and applied biological sciences **68**(4 Pt B): 511-517.

Monteith, J. (1927). "Can you identify brown patch." The National Greenkeeper **6**: 7-11.

Morris, K. (2003). "National turfgrass research initiative." National Turfgrass Federation, Inc., and National Turfgrass Evaluation Program, Beltsville.

Morris, K. N. and R. C. Shearman (1998). NTEP turfgrass evaluation guidelines. NTEP turfgrass evaluation workshop, Beltsville, MD.

Morton, T., A. Gold and W. Sullivan (1988). Influence of overwatering and fertilization on nitrogen losses from home lawns, Wiley Online Library.

Mothapo, N., H. Chen, M. A. Cubeta, J. M. Grossman, F. Fuller and W. Shi (2015). "Phylogenetic, taxonomic and functional diversity of fungal denitrifiers and associated N2O production efficacy." Soil Biology and Biochemistry **83**: 160-175.

Mothapo, N. V., H. Chen, M. A. Cubeta and W. Shi (2013). "Nitrous oxide producing activity of diverse fungi from distinct agroecosystems." Soil Biology and Biochemistry **66**: 94-101.

Mukherjee, A., A. Sampath Kumar, S. Kranthi and P. Mukherjee (2014). "Biocontrol potential of three novel *Trichoderma* strains: isolation, evaluation and formulation." Biotechnology **4**: 275-281.

Nelson, E. B. and M. J. Boehm (2002). "Compost-induced suppression of turf grass diseases." BioCycle **43**(6): 51-51.

Nelson, P. E., A. E. Desjardins and R. D. Plattner (1993). "Fumonisins, mycotoxins produced by *Fusarium* species: biology, chemistry, and significance." Annual Review of Phytopathology **31**(1): 233-252.

Nelson, P. E., M. C. Dignani and E. J. Anaissie (1994). "Taxonomy, biology, and clinical aspects of *Fusarium* species." Clinical Microbiology Reviews **7**(4): 479-504.

Oakley, B. A. (2023). Denitrification in *Fusarium*: A crossroads between fungal biology and emission of a major greenhouse gas.

Oakley BA, G. M., Gu X, Gold SE, and Glenn AE. (2025). "Phylogenetic and phylogenomic characterization of denitrification-associated proteins in *Fusarium verticillioides*." To be submitted to Frontiers in Microbiology.

Pachauri, R. K. and A. Reisinger (2007). "Climate change 2007: Synthesis report. Contribution of working groups I, II and III to the fourth assessment report of the Intergovernmental Panel on Climate Change." Climate Change 2007. Working Groups I, II and III to the Fourth Assessment.

Parsons, M. and G. Munkvold (2012). "Effects of planting date and environmental factors on *Fusarium* ear rot symptoms and fumonisin B1 accumulation in maize grown in six North American locations." Plant Pathology **61**(6): 1130-1142.

Patakioutas, G., D. Dimou, O. Kostoula, P. Yfanti, D. Kyrkas, P. Baltzoi, I. Tsirogiannis, N. Ntoulas and P. Nektarios (2014). Turfgrass root system inoculation and colonization by a mycorrhizal fungus and other symbiotic micro-organisms and evaluation of its effects on green turf cover and growth. XXIX International Horticultural Congress on Horticulture: Sustaining Lives, Livelihoods and Landscapes (IHC2014): III 1122.

Paugh, K. R. and T. R. Gordon (2021). "Survival of *Fusarium oxysporum* f. sp. *lactucae* on crop residue in soil." Plant Disease **105**(4): 912-918.

Pereira, P., A. Nesci, C. Castillo and M. Etcheverry (2010). "Impact of bacterial biological control agents on fumonisin B1 content and *Fusarium verticillioides* infection of field-grown maize." Biological Control **53**(3): 258-266.

Pereira, P., A. Nesci and M. Etcheverry (2007). "Effects of biocontrol agents on *Fusarium verticillioides* count and fumonisin content in the maize agroecosystem: Impact on rhizospheric bacterial and fungal groups." Biological Control **42**(3): 281-287.

Persoon, C. H. (1794). "Disposita methodical fungorum." Romers Neues Mag Bot **1**: 81-128.

Petrovic, A. M. (1990). "The fate of nitrogenous fertilizers applied to turfgrass." Journal of Environmental Quality **19**(1): 1-14.

Prather, M. J., J. Hsu, N. M. DeLuca, C. H. Jackman, L. D. Oman, A. R. Douglass, E. L. Fleming, S. E. Strahan, S. D. Steenrod, O. A. Søvde, I. S. Isaksen, L. Froidevaux and B. Funke (2015). "Measuring and modeling the lifetime of nitrous oxide including its variability." Journal of Geophysical Research **120**(11): 5693-5705.

Presello, D. A., G. Botta, J. Iglesias and G. H. Eyhérabide (2008). "Effect of disease severity on yield and grain fumonisin concentration of maize hybrids inoculated with *Fusarium verticillioides*." Crop Protection **27**(3): 572-576.

Reicher, Z., Patton, A. J., Bigelow, C. A. and Voigt, T. (2006). Mowing, thatching, aerifying, and rolling turf. Purdue University Cooperative Extension. P. University. West Lafayette, IN, Purdue University. **Bul. AY-8-W**.

Salgado-Salazar, C., L. A. Beirn, A. Ismaiel, M. J. Boehm, I. Carbone, A. I. Putman, L. P. Tredway, B. B. Clarke and J. A. Crouch (2018). "Clarireedia: A new fungal genus comprising four pathogenic species responsible for dollar spot disease of turfgrass." Fungal Biology **122**(8): 761-773.

Sani, M. N. H., M. Hasan, J. Uddain and S. Subramaniam (2020). "Impact of application of *Trichoderma* and biochar on growth, productivity and nutritional quality of tomato under reduced NPK fertilization." Annals of Agricultural Sciences **65**(1): 107-115.

Santiago, R., A. Cao and A. Butrón (2015). "Genetic factors involved in fumonisin accumulation in maize kernels and their implications in maize agronomic management and breeding." Toxins **7**(8): 3267-3296.

Sapkota, S., A. Martinez-Espinoza, E. Ali, C. Vermeer and B. Bahri (2020). "Taxonomical identification of Clarireedia species causing dollar spot disease of turfgrass in Georgia." Plant Disease **104**(11): 3063.

Shaddox, T. W., J. B. Unruh, M. E. Johnson, C. D. Brown and G. Stacey (2022). "Water use and management practices on US golf courses." Crop, Forage & Turfgrass Management **8**(2): e20182.

Sharma, V., R. Salwan and P. Sharma (2017). "The comparative mechanistic aspects of *Trichoderma* and probiotics: scope for future research." Physiological and Molecular Plant Pathology **100**: 84-96.

Shoun, H., S. Fushinobu, L. Jiang, S.-W. Kim and T. Wakagi (2012). "Fungal denitrification and nitric oxide reductase cytochrome P450nor." Philosophical Transactions of the Royal Society B: Biological Sciences **367**(1593): 1186-1194.

Shoun, H., D.-H. Kim, H. Uchiyama and J. Sugiyama (1992). "Denitrification by fungi." FEMS Microbiology Letters **94**(3): 277-281.

Signor, D. and C. E. P. Cerri (2013). "Nitrous oxide emissions in agricultural soils: A review." Pesquisa Agropecuária Tropical **43**: 322-338.

Singh, H., B. Singh, S. Singh, S. Singh and B. Sarma (2009). "Biological control of plant diseases: Status and prospects." Recent Advances in Biopesticides: Biotechnological Applications; New India Pub.: New Delhi, India **322**.

Sivan, A. and G. Harman (1991). "Improved rhizosphere competence in a protoplast fusion progeny of *Trichoderma harzianum*." Microbiol **137**(1): 23-29.

Smiley, R., P. Dernoeden and B. Clarke (2005). "Compendium of turfgrass diseases."

Song, Y.-P., X.-H. Liu, Z.-Z. Shi, F.-P. Miao, S.-T. Fang and N.-Y. Ji (2018). "Bisabolane, cyclonerane, and harziane derivatives from the marine-alga-endophytic fungus *Trichoderma asperellum* cf44-2." Phytochemistry **152**: 45-52.

Stasz, T., G. Harman and N. Weeden (1988). "Protoplast preparation and fusion in two biocontrol strains of *Trichoderma harzianum*." Mycologia **80**(2): 141-150.

Stein, L. Y. and M. G. Klotz (2016). "The nitrogen cycle." Current Biology **26**(3): R94-R98.

Stevens, W., R. Hoeft and R. L. Mulvaney (2005). "Fate of nitrogen-15 in a long-term nitrogen rate study: II. Nitrogen uptake efficiency." Agronomy Journal **97**(4): 1046-1053.

Survey, U. S. G. (2023). Mineral commodity summaries 2023. Mineral Commodity Summaries. Reston, VA**:** 210.

TariqJaveed, M., T. Farooq, A. S. Al-Hazmi, M. D. Hussain and A. U. Rehman (2021). "Role of *Trichoderma* as a biocontrol agent (BCA) of phytoparasitic nematodes and plant growth inducer." Journal of Invertebrate Pathology **183**: 107626.

Te'o, V., P. Bergquist and K. Nevalainen (2002). "Biolistic transformation of *Trichoderma reesei* using the Bio-Rad seven barrels Hepta Adaptor system." Journal of Microbiological Methods **51**(3): 393-399.

USDA (2019). Crop Acreage Data.

van Delden, L., E. Larsen, D. Rowlings, C. Scheer and P. Grace (2016). "Establishing turf grass increases soil greenhouse gas emissions in peri-urban environments." Urban Ecosystems **19**(2): 749-762.

Van Wees, S. C., S. Van der Ent and C. M. Pieterse (2008). "Plant immune responses triggered by beneficial microbes." Curr Opin Plant Biol **11**(4): 443-448.

Vargas, J. M. (2018). Management of turfgrass diseases, CRC Press.

Vargas, W. A., J. C. Mandawe and C. M. Kenerley (2009). "Plant-derived sucrose is a key element in the symbiotic association between *Trichoderma virens* and maize plants." Plant Physiology **151**(2): 792-808.

Villalobos-Escobedo, J. M., S. Esparza-Reynoso, R. Pelagio-Flores, F. López-Ramírez, L. F. Ruiz-Herrera, J. López-Bucio and A. Herrera-Estrella (2020). "The fungal NADPH

oxidase is an essential element for the molecular dialog between *Trichoderma* and *Arabidopsis*." Plant J **103**(6): 2178-2192.

Wagner-Riddle, C., G. W. Thurtell, G. K. Kidd, E. G. Beauchamp and R. Sweetman (1997). "Estimates of nitrous oxide emissions from agricultural fields over 28 months." Canadian Journal of Soil Science **77**(2): 135-144.

Walling, E. and C. Vaneeckhaute (2020). "Greenhouse gas emissions from inorganic and organic fertilizer production and use: A review of emission factors and their variability." Journal of Environmental Management **276**: 111211.

Walsh, B., S. S. Ikeda and G. J. Boland (1999). "Biology and management of dollar spot (*Sclerotinia homoeocarpa*); an important disease of turfgrass." HortScience **34**(1): 13-21.

Walsh, B., S. S. Ikeda and G. J. Boland (1999). "Biology and management of dollar spot (Sclerotinia homoeocarpa): An important disease of turfgrass." HortScience **34**(1): 14.

Wang, C., B. Amon, K. Schulz and B. Mehdi (2021). "Factors that influence nitrous oxide emissions from agricultural soils as well as their representation in simulation models: A review." Agronomy **11**(4): 770.

Wang, Y., H. Chen, L. Ma, M. Gong, Y. Wu, D. Bao and G. Zou (2022). "Use of CRISPR-Cas tools to engineer *Trichoderma* species." Microbial Biotechnology **15**(10): 2521-2532.

Wang, Z.-H., X. Zhao, J. Yang and J. Song (2016). "Cooling and energy saving potentials of shade trees and urban lawns in a desert city." Applied Energy **161**: 437-444.

Whetzel, H. H. (1945). "A synopsis of the genera and species of the Sclerotiniaceae, a family of stromatic inoperculate discomycetes." Mycologia **37**(6): 648-714.

Wu, F. (2006). "Mycotoxin reduction in *Bt* corn: potential economic, health, and regulatory impacts." Transgenic Research **15**: 277-289.

Wuebbles, D. J., D.W. Fahey, K.A. Hibbard, D.J. Dokken, B.C. Stewart, and T.K. Maycock, eds. (2017). Climate science special report: Fourth National Climate Assessment, volume I. . U. U. S. G. C. R. Program).

Xu, S., S. Feng, H. Sun, S. Wu, G. Zhuang, Y. Deng, Z. Bai, C. Jing and X. Zhuang (2018). "Linking N2O emissions from biofertilizer-amended soil of tea plantations to the abundance and structure of N2O-reducing microbial communities." Environmental Science & Technology **52**(19): 11338-11345.

Xu, S., X. Fu, S. Ma, Z. Bai, R. Xiao, Y. Li and G. Zhuang (2014). "Mitigating nitrous oxide emissions from tea field soil using bioaugmentation with a *Trichoderma viride* biofertilizer." The Scientific World Journal **2014**: 793752.

Xu, S., S. Zhou, S. Ma, C. Jiang, S. Wu, Z. Bai, G. Zhuang and X. Zhuang (2017). "Manipulation of nitrogen leaching from tea field soil using a *Trichoderma viride* biofertilizer." Environmental Science and Pollution Research **24**(36): 27833-27842.

Yang, S., S. Peng, J. Xu, Y. Luo and D. Li (2012). "Methane and nitrous oxide emissions from paddy field as affected by water-saving irrigation." Physics and Chemistry of the Earth, Parts A/B/C **53-54**: 30-37.

Young, J. and A. Patton (2010). A guide to fungicide resistance in turf systems, [Cooperative Extension Service], University of Arkansas, US Department of ….

Zhang, H., Y. Dong, Y. Zhou, J. Hu, K. Lamour and Z. Yang (2022). "Clarireedia hainanense: a new species is associated with dollar spot of turfgrass in Hainan, China." Plant Disease **106**(3): 996-1002.

Zhang, W., J.-y. Yang, X. Lu, J.-m. Lin and X.-l. Niu (2021). "A preliminary study of the antifungal activity and antagonism mechanisms of *Trichoderma* spp. against turfgrass pathogens." Acta Prataculturae Sinica **30**(9): 137.

Zhong, Y. H., X. L. Wang, T. H. Wang and Q. Jiang (2007). "*Agrobacterium*-mediated transformation (AMT) of *Trichoderma reesei* as an efficient tool for random insertional mutagenesis." Applied Microbiology and Biotechnology **73**(6): 1348-1354.

Zhou, M., B. Zhu, X. Wang and Y. Wang (2017). "Long-term field measurements of annual methane and nitrous oxide emissions from a Chinese subtropical wheat-rice rotation system." Soil Biology and Biochemistry **115**: 21-34.

Zimand, G., Y. Elad and I. Chet (1996). "Effect of *Trichoderma harzianum* on *Botrytis cinerea* pathogenicity." Phytopathol **86**(11): 1255-1260.

Figure

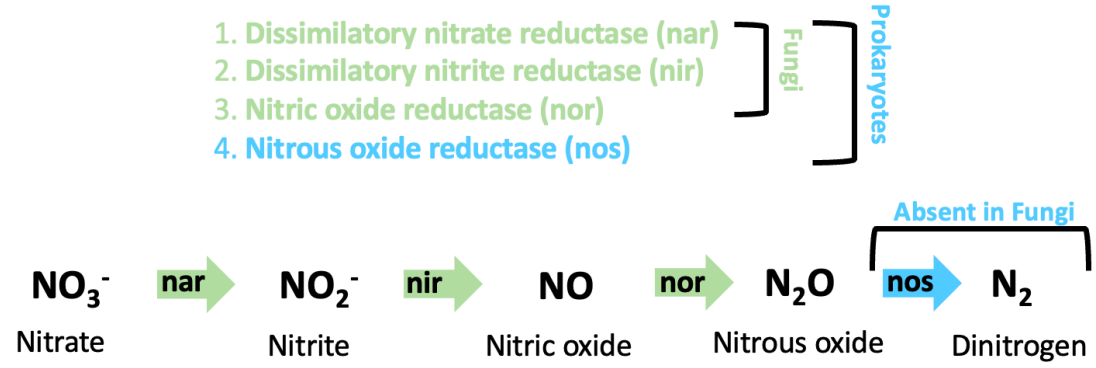

Figure 1.1: Genes and steps in denitrification pathway. Green portions occur in both fungi and prokaryotes, while blue (step four) is absent in fungi.

CHAPTER 2

DEVELOPMENT OF A CO-DOMINANT CLEAVED AMPLIFIED POLYMORPHIC SEQUENCES ASSAY FOR THE RAPID DETECTION AND DIFFERENTIATION OF TWO PATHOGENIC *CLARIREEDIA* SPP. ASSOCIATED WITH DOLLAR SPOT IN TURFGRASS

Stackhouse, T., Martinez-Espinoza, A.D., and Ali, M.E. (2021) Development of a co-dominant cleaved amplified polymorphic sequences assay for the rapid detection and differentiation of two pathogenic *Clarireedia* spp. associated with dollar spot in turfgrass. Agronomy 2021, 11(8), 1489. Reprinted here with permission of the publisher.

Abstract

Dollar spot is one of the most destructive diseases in turfgrass. The causal agents belong to the genus *Clarireedia*, which are known for causing necrotic, sunken spots in turfgrass that coalesce into large, damaged areas. In low tolerance settings like turfgrass, it is of vital importance to rapidly detect and identify the pathogens. A few methods are available to identify the genus *Clarireedia,* but none are rapid enough and characterize down to the species level. This study produced a co-dominant cleaved amplified polymorphic sequences (CAPS) test that differentiates between *C. jacksonii* and *C. monteithiana,* the two species that cause dollar spot within the United States. The calmodulin gene (CaM) was targeted to generate *Clarireedia* spp. specific PCR primers. The CAPS assay was optimized and tested for specificity and sensitivity using DNA extracted from pure cultures of two *Clarireedia* spp. and other closely related fungal species. The results showed that the newly developed primer set could amplify both species and was highly sensitive as it detected DNA concentrations as low as 0.005 ng/μL. The assay was further validated using direct PCR to speed up the diagnosis process. This drastically reduces the time needed to identify the dollar spot pathogens. The resulting assay could be used throughout turfgrass settings for a rapid and precise identification method in the US.

Introduction

Turfgrass is a 40 billon-dollar industry reaching around the world. In the United States alone it is estimated that there are over 62 million acres of turfgrass (Chawla et al. 2018). There is a large number of studies showing greenscapes, including turfgrass, have positive impacts on the surrounding environment, including area temperature reduction, erosion control, and energy use reduction (McPherson 1994, Krenitsky et al. 1998, Dousset and Gourmelon 2003, Kowalczyk et al. 2011, Monteiro 2017).

One of the most economically important turfgrass diseases is dollar spot caused by *Clarireedia* spp. (Vargas 2018). This disease can be caused by at least five species within the genera *Clarireedia*, *C. bennettii*, *C. homoeocarpa*, *C. jacksonii*, *C. monteithiana,* and *C. paspali* (Salgado-Salazar et al. 2018, Hu et al. 2019). Four of these species were reclassified in 2018 into this novel genus (Salgado-Salazar et al. 2018). Previously all dollar spot-causing fungi were classified as *Sclerotinia homoeocarpa*, with various name challenges since the initial naming in 1937 (Bennett 1937, Salgado-Salazar et al. 2018). The newest identified *Clarireedia* species, *C. paspali*, is so far only found in China (Hu et al. 2019). *Clarireedia homoeocarpa* has only been reported within the United Kingdom. *C. bennettii* has been reported in the Netherlands, New York, US, and the United Kingdom. The last two species, *C. jacksonii* and *C. monteithiana*, are found on grasses worldwide, including the United States. Reclassification has rejuvenated research into this pathogen (Crouch et al. 2020, Groben et al. 2020).

Turfgrass used in sports fields and golf courses are often heavily managed to control pests and pathogens and have an extremely low tolerance for damage from dollar spot (Stowell and Gelernter 2001). Symptoms include small white to straw foliar lesions with a brown border (Smiley et al. 2005). These lesions can grow together, coalescing and eventually leading to blighted, sunken spots on the turf, often killing the grass to the soil surface. These spots are often the size of silver dollar coin, giving this disease its name. Mycelium or infected tissues can often be moved by equipment, people, wind, or water, allowing the disease to spread quickly over larger areas (Williams et al. 1996, Horvath et al. 2007). Damage is also often worse on turf facing abiotic stressors, such as low fertility and high moisture (Couch and Bloom 1960, Martínez-Espinoza et al. 2009). Dollar spot damage is unsightly and can reduce the playability of sports fields and golf courses (Baird 2005). Control management can be costly and requires an extremely rapid diagnosis

of problems when they do occur (Little 2019). Control can be achieved with cultural and chemical controls (Goodman and Burpee 1991, Walsh et al. 1999).

Although *C. jacksonii* is typically found on C_3 plants and *C. monteithiana* on C_4 plants (Salgado-Salazar et al. 2018, Sapkota et al. 2020); artificial inoculation studies have found that each of the species can grow on either type of grasses (Aynardi et al. 2019, Hu et al. 2019). These two species are also both found throughout transitional areas in the United States (Aynardi et al. 2019). In areas with both cool and warm season stands near one another both species can be found in close proximity (Aynardi et al. 2019). These pathogens could have varying resistance based on genetic factors, making species differentiation important (Hsiang and Mahuku 1999, Jo et al. 2006, DeVries et al. 2007). These genetic factors for fungicide resistance differences have not yet been studied since the reclassification of the dollar spot causing pathogens. Of the studies that have published since the reclassification, some focus on one species, mainly *C. jacksonii*, while the others simply refer to older nomenclature or the genus (Aynardi et al. 2019, Hu et al. 2020, Marvin et al. 2020).

Pathogen detection of dollar spot has mainly been symptoms, signs, and morphologically based (Salgado-Salazar et al. 2018). Dollar spot can sometimes be confused with other pathogenic diseases or various abiotic factors, making diagnosis by symptoms alone difficult (Vargas 2018). The common dollar spot diagnosis method includes collecting samples, microscopic analysis and culturing, DNA extraction, amplicon sequencing and Blast analysis against GenBank database have been used (Flores and Walker 2014, Salgado-Salazar et al. 2018, Hu et al. 2019). This process is labor intensive and can take several days. Beyond time requirements, determining *Clarireedia* species requires the knowledge to search GenBank for samples under the new nomenclature while all the previously named samples are still present. The three genes being used presently for

Clarireedia spp. identification are ITS, and the calmodulin gene (CaM), and the DNA replication licensing factor (Mcm7); these genes can be used to distinguish *Clarireedia* based on specific SNPs present (Salgado-Salazar et al. 2018). More recently, a new qPCR method was described by Groben et al. (2020) for general diagnosis (Groben et al. 2020). This sensitive method is extremely useful for identifying dollar spot caused by *Clarireedia* spp.; however, this method cannot distinguish between the different species causing dollar spot (Groben et al. 2020). This limits studies of the prevalence of each species and their characterization. Because fungicide resistance can vary by pathogen species, it is important to be able to identify down to species, which is not possible with the current qPCR approach and the PCR method without an additional sequencing step.

Understanding the specific species causing a disease can allow for better chemical treatment and fungicide resistance studies. Species-specific PCR allows for specific identification of a species without sequencing (Oren et al. 2018). This method has been used widely in plant pathology (Palacio-Bielsa et al. 2009, Flores and Walker 2014, Oren et al. 2018). Primers are typically tested in vitro and *in silico* to ensure specificity (Abd-Elsalam 2003). This allows specific species detection within complex samples that often contain other pathogens and plant or soil impurities. This aggregation makes the commonly used universal primers difficult to utilize without pathogen isolation and can take weeks to sort them out (Vincelli and Tisserat 2008, Oren et al. 2018). Using species-specific primers can reduce pathogen identification to a few hours, depending on the protocol. Co-dominant cleaved amplified polymorphic sequences (CAPS) allows for secondary testing of a PCR reaction to identify specific single nucleotide polymorphisms (SNPs) (Michaels and Amasino 1998, Vincelli and Tisserat 2008, Kaundun et al. 2019). In some cases, these specific SNPs can be used to identify specific mutations or differentiate species,

strains, or cultivars (Adachi et al. 1994, Szalanski et al. 1997, Reale et al. 2006, Park et al. 2007, Zhang et al. 2017). The method could be a valuable tool in identifying dollar spot pathogens.

It is critical to identify dollar spot quickly for prompt control measures. This research focuses on creating a novel molecular assay to identify *Clarireedia* species and differentiate between the two dollar spot causing species found in southeastern United States, *C. jacksonii* and *C. monteithiana*, using CAPS approach. This assay would allow for faster response and therefore reduced treatment delay time and reduced chemical control costs to turfgrass professionals.

Materials and Methods

Sample collection

Dollar spot symptomatic samples used in this study were collected within the state of Georgia, U.S. from various cool season and warm season grasses in the years 2019 and 2020 (Table 2.1). All samples were identified using morphological features and sequencing of the calmodulin gene (CaM) and internal transcribed spacer (ITS) (White et al. 1990, Salgado-Salazar et al. 2018). Eleven non-target fungal species samples were taken from various hosts and locations to test the newly designed primers for specificity. These non-target pathogens included *Bipolaris* spp. *Botrytis* sp., *Cladosporium* sp., *Colletotrichum* spp., *Fusarium* sp., *Leptosphaerulina* sp., *Magnaporthe poae Ophiosphaerella korrae*, *Phytophthora sojae*, *Pyricularia grisea*, and *Rhizotonia solani.* These samples were all isolated from of turfgrass samples taken in Georgia. All nontarget species identifications were performed using ITS primers with either ITS1/4 or ITS 4/5.

Fungal pathogens were isolated from plant samples and grown on potato dextrose agar (PDA) plates at 28 °C for 4 to 7 days. Isolates were selected and transferred until pure cultures were obtained. Samples were used for DNA extraction detailed below and placed in glycerol stocks at -80 °C for future experiments.

DNA extraction

For extraction, 100 mg of pure culture samples were taken from plates via scraping with a sterile scalpel and placed in a 1.5 mL tube. DNA extraction was performed using the QIAGEN DNeasy Plant Mini Kit (Qiagen, Valencia, CA) per the manufacturer's instructions. The only modification to the manufacturer's protocol were to elute DNA with prewarmed (65 °C) AE buffer (Waliullah et al. 2019). The DNA samples were quantified using a NanoDrop™ Lite Spectrophotometer (FisherScientific, Waltham, Massachusetts) before storage at -20 °C.

PCR primer design

Previously published gene sequences were used to design novel, specific PCR primers (Salgado-Salazar et al. 2018). Novel PCR primers were designed manually based on partial gene sequences of the ITS, CaM and Mcm7 of *C. jacksonii* and *C. monteithiana.* Twelve primer pairs (Table 2.2), including CaM3_F and CaM3_R primer set (Table 2.2), were created manually in Geneious Prime then checked for quality and content using the Integrated DNA Technologies PrimerQuest Tool software. The melting temperature (T_m) distance between forward and reverse was low and the percent GC content closest to 50% (determined by Geneious Prime). Primer pairs sequences were used to query NCBI GenBank database using BLASTn to provide an in silco assessment of primer binding specificity against turfgrass pathogens. Primers were synthesized by Sigma-Aldrich (St. Louis, Missouri, US), dissolved in DNase/RNase free PCR-grade water to produce 100 µm solutions, and stored at –20 °C.

PCR amplification and optimization

Firstly, PCR testing was performed using GoTaq® Green Master Mix (Promega, Madison, Wisconsin, US) per the manufacturer's instructions. Each 20 µL reaction contained: 10 µL of GoTaq master mix (1X), 1 µL of forward primer (500 nm), 1 µL of reverse primer (500 nm), 1µL

of DNA (5 ng μl^{-1}) sample and rest was filled with PCR grade H_2O. Annealing temperatures tested for optimization were 55 °C to 68 °C, as is common with newly designed primers. The optimal temperature was selected for the highest temperature with strong bands, to encourage specificity. The thermocycler settings for PCR were: initial denaturing of 95 °C for 3m; 35 cycles of 95 °C 30s, 55 to 68 °C for 30s (gradient), 72 °C for 1m; and final extension of 72 °C for 5m. PCR products were run on 1% agarose gels with GelGreen® Nucleic Acid Gel Stain (Biotium, Fremont, California, US) for 25 minutes at 65V before confirming the presence or absence of bands with an Analytik Jena UV transilluminator (Upland, California, US). Secondly, the PCR primers were preliminarily tested, at the optimal temperature selected, with 15 samples of dollar spot to ensure the primers were functional. Thirdly, the PCR primers were next tested for specificity using thirteen samples of nontarget plant pathogens, with eleven different species, all standardized to 5 ng/µl. Finally, the PCR sensitivity was tested using three dollar spot samples starting at 5 ng μL^{-1} and preforming a 10:1 dilution with water to 0.0005 ng μL^{-1}.

CAPS analysis of the PCR product

Co-dominant cleaved amplified polymorphic sequences (CAPS) assay was designed to distinguish between *C. jacksonii* and *C. monteithiana.* Each of the three PCR primer sets (ITS4, CaM2 and CaM3 primers) that did not have nonspecific amplification for other non-*Clarireedia* spp., were examined for single nucleotide polymorphisms between *C. jacksonii* and *C. monteithiana* that would cause unique restriction digest sites. To find unique restriction sites between *C. jacksonii* and *C. monteithiana*, the gene sequences were imported in Geneious v10.1.2 (Biomatters Ltd., Auckland, New Zealand) software for sequence alignment. Utilizing "Find Restriction Sites" with default settings and for enzymes that allowed for one to two cuts, a unique restriction site of *Sca*I enzyme was identified and produced distinguishable bands in a 2% TBE

agarose gel using the CaM3 primers. The selected PCR-RLFP assay were carried out using 15 known dollar spot isolates. The assay was performed by mixing a 30 µL solution comprising of 2 µL of restriction digest enzyme *Sca*I (Sigma-Aldrich, St. Louis, Missouri, US), 2 µL of 10x buffer, 8 µL of DNase/RNase free water, and 20 µL of PCR product. The solution was incubated at 37 °C for 30 minutes. The CAPS reaction products were run on a 2% agarose gel for 30 minutes at 65V.

Direct PCR testing

To speed up the diagnosis process, direct PCR was used on pure cultures from each dollar spot isolate. The direct PCR was performed using the Phire Plant PCR Direct Kit (Thermofisher, Waltham, Massachusetts, US) per the manufacturer's instructions. To proceed the assay, a 10 µL pipette tip was used to collect a small amount (as little as possible) of mycelium which was placed in 20 µL of Phire Direct digestion solution, vortexed, then placed in -20 °C until frozen. This digestion solution contained mycelium that was used in PCR. Each 20 µL reaction incorporates 10 µL of 2x Phire Plant PCR Buffer, 1 µL of CaM3_F primer, 1 µL of CaM3_R primer, 0.4 µL of Phire Hot Start II DNA Polymerase, 6.6 µL of sterile water, and 1 µL of digested mycelium solution. The PCR reaction was performed with initial denaturation at 98 °C for 5 minutes, 40 cycles of 98 °C for 5s, 63 °C for 5s, and 72 °C for 20 seconds, with a final extension of 72 °C for 1m. These are different thermocycler settings based on the Phire Direct Kit specifications. The resulting PCR product was put through the CAPS testing detailed above. These are repeated with each strain four times to ensure consistency with this method.

Results

PCR primer design

Clarireedia spp. isolates were further confirmed via Sanger sequencing using PCR products from the CAL-228F/CAL-737R and ITS4/ITS5 primers using the previously published

sequences for comparison (White et al. 1990, Carbone and Kohn 1999, Salgado-Salazar et al. 2018). Each of the designed primers was systematically tested for single-band amplification, specificity, and CAPS assay targets (Table 2.2). From these results (Supplemental Figure 2.1), the CaM3-F/CaM3-R primers were selected for use.

Optimization of PCR primers

Our newly designed PCR primer set (CaM3-F/CaM3-R) was able to amplify all dollar spot samples successfully and produced a 240 base pair band as expected from *Clarireedia* spp. (Figures 2.2A, C). PCR assay was optimized by using various temperatures (between 55-68 °C) and the reaction with the primer set amplified best at 63 °C annealing temperature, as defined by highest temperature with a consistent, bright band with a standardized sample (Figure 2.2B). Therefore, 63 °C was selected as the optimal temperature. The newly designed CaM3 primer set amplified all the *Clarireedia* spp. samples, without amplifying the nontarget pathogen samples which demonstrated correct and definitive specificity of this marker (Figures 2.2C, D). The sensitivity limit of the PCR reaction was tested using a serial dilution of target DNA started from 5 ng μL−1 down to 0.0005 ng μL−1 and the sensitivity limit was shown to be 0.005 ng μL−1 (Figure 2.2E).

CAPS analysis of PCR fragment

The CAPS assay was able to distinguish between *C. jacksonii* and *C. monteithiana* via product band size. The *Sca*I restriction enzyme was used to cut the 240 base pair (bp) band at the 95th base of *C. jacksonii* isolates. This gave *C. jacksonii* two digested products, 145 and 95 bps long; while *C. monteithiana* remain uncut and only produced the original 240 bp PCR product band (Figures 2.3A, 3C). There were 15 *Clarireedia* spp. isolates tested with the novel PCR-CAPS method, 11 was *C. monteithiana* and 4 was *C. jacksonii* isolates. All the *C. jacksonii* isolates

produced two bands of 145 and 95 bps and all of the *C. monteithiana* produced a single band of 240 bp (Figure 2.3C).

Direct PCR Testing

The 15 *Clarireedia* spp. isolates were tested with the modified CAPS assay method described in the method section 2.6 following direct PCR (Figure 2.4). This was repeated with all strains four times as technical replications. Of the total of 60 runs, all runs produced a band denoting *Clarireedia* spp. and only one run had too light of a band for species differentiation. The 11 *C. monteithiana* and 4 *C. jacksonii* isolates all yielded the same results seen in the CAPS assay seen above. All the *C. jacksonii* samples produced two bands (145 and 95 bp) and all the *C. monteithiana* produced one band (240 bp).

Discussion

Rapid identification of *Clarireedia* spp. is necessary for better and accurate management of dollar spot. This disease causes extensive damage each year to turfgrass and requires heavy, expensive control measures. The two species of *Clarireedia, C. jacksonii* and *C. monteithiana,* observed throughout the United States, need to be differentiated in order to better understand the spread and affected hosts for each of the pathogens (Salgado-Salazar et al. 2018). This requires a fast, accessible method to identify and differentiate between the two species. The diagnosis of dollar spot is currently accomplished by morphological and microscopic techniques, which requires symptoms and expertise that can limit timely disease management decisions (Walsh et al. 1999, Stowell and Gelernter 2001, Vargas 2018, Stackhouse et al. 2020). Additionally, species differentiation cannot be obtained with morphological identification alone. This severely restricts studies on species characterization, fungicide resistance, and species prevalence.

Molecular diagnosis based on PCR and qPCR methods also exist for this pathogen; however, these methods of diagnosis won't ascertain what species we are dealing with (Salgado-Salazar et al. 2018). While originally it was thought that species identifying was possible via knowledge of the host, there is now data showing the host may not always coincide to a specific pathogen species (Aynardi et al. 2019, Hu et al. 2019). Additionally, DNA sequencing approach can take several days and is particularly difficult with *Clarireedia* spp., as the reclassification provides inadequate labeling of most of the dollar spot sequences in GenBank.

In this study, we have developed a quick, reliable and specific PCR identification of *Clarireedia* spp. PCR primers were produced from the calmodulin (CaM) gene region that had preestablished sequences in GenBank for various *Clarireedia* spp. (Figure 2.2). This universal region is commonly used for species identification and species-specific primer design (Mulè et al. 2004, Susca et al. 2007). The Internal transcribed spacer (ITS) and Mcm7 gene (DNA replication licensing factor) regions were both examined for this purpose, but the CaM gene yielded better species-specific primers (Table 2.2). Primers were tested for temperature optimization, selecting the highest temperature to have a strong and neat band (63 °C) (Figure 2.2B). This metric was used because higher temperatures often confer higher specificity (Roux 2009). Specificity was tested against various nontarget species to ensure no nontarget amplification (Figure 2D). Sensitivity was tested to determine the lower limits of DNA concentration of the assay. The novel CaM3 primer set had a detection limit of 0.005 ng/μL^{-1} (Figure 2.2E), which is comparable to other CaM region primer sets reported with a detection limit of 0.01-0.012 ng μL^{-1} on other pathogenic species (Mulè et al. 2004, Susca et al. 2007).

Next, a CAPS method was designed and tested for differentiating the two species. The CaM3 primer set was selected from the three primer sets that amplified only target samples, due

to a unique *Sca*I restriction digest site at the 95th base of the PCR product. With CaM3 primers, PCR amplified both *C. jacksonii* and *C. monteithiana.* Adding the CAPS assay allowed for differentiation (Figure 2.3 & 2.4). There is a long history of using CAPS markers for species differentiation, but to the best of our knowledge the method has not been used in turfgrass pathosystems. (Szalanski et al. 1997, Sialer et al. 1999). This CAPS assay allows for rapid species differentiation without sequencing (about three hours).

The CAPS method was also examined *in silico* against the *Clarireedia* spp. sequences from Salgado-Salazar et al. (2018) study and found that of the sixteen sequences in GenBank, all but one sample of *C. jacksonii* is expected to produce two bands. That one sample had a point mutation within the restriction digest region. That sample was from the Netherlands and had several SNPs that were not present in any other *C. jacksonii* sequences. No U.S. isolates from that study had that SNPs, and none of the U.S. samples were found to have the point mutation that would limit the CAPS method from species differentiation.

Direct PCR allows for plant pathogen identification with a rapid sample processing time. This method has been used previously in plant pathogens and on various fungi samples (Jumpponen et al. 2003, Ben-Amar et al. 2017, Chaffin et al. 2020). It removes the need for DNA extraction and typically halves the time required in a thermocycler. In our study, it cuts the sampling processing time by 40% compared to the same method with a DNA extraction step (Figure 4). Additionally, this reduces labor and material costs in addition to training required.

Overall, the potential benefit of the CAPS assay will allow for faster and accurate pathogen diagnosis for dollar spot. We hope that having a rapid species differentiation protocol will allow for more studies on pathogen distribution and hosts affected by each pathogen. We expect this method to be used by diagnostic clinics for rapid disease detection. This method is simple and

requires only basic molecular tools, making it easily accessible to all diagnosticians. Allowing growers to rapidly know the species of *Clarireedia* present will allow for swift disease response and species targeted fungicide applications, reducing fungicide use and potential for new resistances to form.

Author Contributions

TLS – Investigation, methodology, validation, visualization, writing of original draft preparation, reviewing and editing. AME – conceptualization, project administration, review, and editing. MEA –conceptualization, project administration, resources, supervision, and review.

References

Abd-Elsalam, K. A. (2003). "Bioinformatic tools and guideline for PCR primer design." African Journal of Biotechnology **2**(5): 91-95.

Adachi, M., Y. Sako and Y. Ishida (1994). "Restriction fragment length polymorphism of ribosomal DNA internal transcribed spacer and 5.8s regions in Japanese *Alexandrium* species (dinophyceae)." Journal of Phycology **30**(5): 857-863.

Aynardi, B. A., M. Jiménez-Gasco and W. Uddin (2019). "Effects of isolates of *Clarireedia jacksonii* and *Clarireedia monteithiana* on severity of dollar spot in turfgrasses by host type." European Journal of Plant Pathology **155**: 817 - 829.

Baird, P. R. (2005). "Determining dollar spot fungicide resistance in Tennessee and northern Mississippi."

Ben-Amar, A., S. Oueslati and A. Mliki (2017). "Universal direct PCR amplification system: a time-and cost-effective tool for high-throughput applications." 3 Biotech **7**(4): 1-7.

Bennett, F. (1937). "Dollar spot disease of turf and its causal organism *Sclerotinia homoeocarpa* n. sp." Ann. Appl. Biol. **24**(2).

Carbone, I. and L. M. Kohn (1999). "A method for designing primer sets for speciation studies in filamentous ascomycetes." Mycologia **91**(3): 553-556.

Chaffin, A., M. Dee, S. Boggess, R. Trigiano, E. Bernard and K. Gwinn (2020). "First report of *Chaetomium globosum* causing a leaf spot of hemp (*Cannabis sativa*) in Tennessee." Plant Disease **104**(5): 1540.

Chawla, S., A. Roshni, M. Patel, S. Patil and H. Shah (2018). Turfgrass: A billion dollar industry. National Conference on Floriculture for Rural and Urban Prosperity in the Scenerio of Climate Change-2018.

Couch, H. B. and J. R. Bloom (1960). "Influence of environment on diseases of turf-grasses. II. Influence of nutrition, pH and soil moisture on Sclerotinia dollar spot." Phytopathology **50**: 761-763.

Crouch, J. A., L. Beirn, M. Boehm, I. Carbone, B. B. Clarke, J. P. Kerns, M. Malapi, T. Mitchell, R. Venu and L. Tredway (2020). "Genome resources for seven fungal isolates that cause dollar spot disease in turfgrass, including *Clarireedia jacksonii* and *C. monteithiana*." Plant Dis.(ja): 1-7.

DeVries, R. E., R. N. Trigiano, M. T. Windham, A. S. Windham, J. C. Sorochan, T. A. Rinehart and J. M. Vargas (2007). "Genetic analysis of fungicide-resistant *Sclerotinia homoeocarpa* isolates from Tennessee and Northern Mississippi." Plant Dis. **92**(1): 83-90.

Dousset, B. and F. Gourmelon (2003). Surface temperatures of the Paris Basin during summertime, using satellite remote sensing data. 5th International Conference on Urban Climate, Lodz, Poland.

Flores, F. and N. Walker (2014). "First Report of dollar spot of sandbur caused by *Sclerotinia homoeocarpa* in Oklahoma." Plant Dis. **98**(8): 1160-1160.

Goodman, D. and L. Burpee (1991). "Biological control of dollar spot disease of creeping bentgrass." Phytopathology **81**(11): 1438-1446.

Groben, G., B. B. Clarke, J. A. Murphy, P. L. Koch, J. A. Crouch, S. Lee and N. Zhang (2020). "Real-time PCR detection of *Clarireedia* spp., the causal agents of dollar spot in turfgrasses." Plant Dis.(ja): 1-6.

Horvath, B., A. Kravchenko, G. Robertson and J. Vargas Jr (2007). "Geostatistical analysis of dollar spot epidemics occurring on a mixed sward of creeping bentgrass and annual bluegrass." Crop Sci. **47**(3): 1206-1216.

Hsiang and Mahuku (1999). "Genetic variation within and between southern Ontario populations of *Sclerotinia homoeocarpa*." Plant Pathol. **48**(1): 83-94.

Hu, J., J. Wu, M. Gu, J. Geng, C. Guo, Z. Yang and K. Lamour (2020). "Baseline sensitivity and control efficacy of fluazinam against *Clarireedia homoeocarpa*." J. Crop Prot. **137**: 105290.

Hu, J., Y. Zhou, J. Geng, Y. Dai, H. Ren and K. Lamour (2019). "A new dollar spot disease of turfgrass caused by *Clarireedia paspali*." Mycol. Prog. **18**(12): 1423-1435.

Jo, Y.-K., A. L. Niver, J. W. Rimelspach and M. J. Boehm (2006). "Fungicide sensitivity of *Sclerotinia homoeocarpa* from golf courses in Ohio." Plant Dis. **90**(6): 807-813.

Jumpponen, A., K. K. Newsham and D. J. Neises (2003). "Filamentous ascomycetes inhabiting the rhizoid environment of the liverwort *Cephaloziella varians* in Antarctica are assessed by direct PCR and cloning." Mycologia **95**(3): 457-466.

Kaundun, S. S., E. Marchegiani, S.-J. Hutchings and K. Baker (2019). "Derived polymorphic amplified cleaved sequence (dPACS): A novel PCR-RFLP procedure for detecting known single nucleotide and deletion–insertion polymorphisms." Int. J. Mol. Sci. **20**(13): 3193.

Kowalczyk, A., S. Twardy and A. Kuźniar (2011). "Permanent turf grass as the factor alleviating water erosion in the Carpathian Mountains." J. Water Land Dev. **15**(1): 41-51.

Krenitsky, E., M. Carroll, R. Hill and J. Krouse (1998). "Runoff and sediment losses from natural and man-made erosion control materials." Crop Sci. **38**(4): 1042-1046.

Little, E. L. (2019). 2017 Georgia plant disease loss estimates. University of Georgia. U. o. Georgia. **Annual Publication 102-10:** 1-21.

Martínez-Espinoza, A. D., L. L. Burpee and C. Waltz (2009). Abiotic injuries and disorders of turfgrasses in Georgia. University of Georgia. U. o. Georgia. University of Georgia. **Bulletin 1258**.

Marvin, J. W., R. A. Kerr, L. B. McCarty, W. Bridges, S. B. Martin and C. E. Wells (2020). "Curative evaluation of biological control agents and synthetic fungicides for *Clarireedia jacksonii*." HortScience **55**(10): 1622-1625.

McPherson, E. G. (1994). Cooling urban heat islands with sustainable landscapes. The ecological city: preserving and restoring urban biodiversity. R. H. R. Platt, Rowan A.; Muick, Pamela C. Amherst, MA, University of Massachusetts Press**:** 151-171.

Michaels, S. D. and R. M. Amasino (1998). "A robust method for detecting single-nucleotide changes as polymorphic markers by PCR." Plant J **14**(3): 381-385.

Monteiro, J. A. (2017). "Ecosystem services from turfgrass landscapes." Urban For. Urban Green. **26**: 151-157.

Mulè, G., A. Susca, G. Stea and A. Moretti (2004). "A species-specific PCR assay based on the calmodulin partial gene for identification of *Fusarium verticillioides*, *F. proliferatum* and *F. subglutinans*." Eur. J. Plant Pathol. **110**(5): 495-502.

Oren, E., W. Klingeman, R. Gazis, J. Moulton, P. Lambdin, M. Coggeshall, J. Hulcr, S. J. Seybold and D. Hadziabdic (2018). "A novel molecular toolkit for rapid detection of the pathogen and primary vector of thousand cankers disease." Plos one **13**(1): e0185087.

Palacio-Bielsa, A., M. A. Cambra and M. M. López (2009). "PCR detection and identification of plant-pathogenic bacteria: updated review of protocols (1989-2007)." J. Plant Pathol.: 249-297.

Park, E.-J., S. Fukuda, H. Endo, Y. Kitade and N. Saga (2007). "Genetic polymorphism within *Porphyra yezoensis* (Bangiales, Rhodophyta) and related species from Japan and Korea detected by cleaved amplified polymorphic sequence analysis." Eur. J. Phycol. **42**(1): 29-40.

Reale, S., S. Doveri, A. Díaz, A. Angiolillo, L. Lucentini, F. Pilla, A. Martín, P. Donini and D. Lee (2006). "SNP-based markers for discriminating olive (*Olea europaea* L.) cultivars." Genome **49**(9): 1193-1205.

Roux, K. H. (2009). "Optimization and troubleshooting in PCR." Cold Spring Harbor Protocols **2009**(4): pdb. ip66.

Salgado-Salazar, C., L. A. Beirn, A. Ismaiel, M. J. Boehm, I. Carbone, A. I. Putman, L. P. Tredway, B. B. Clarke and J. A. Crouch (2018). "Clarireedia: a new fungal genus comprising four pathogenic species responsible for dollar spot disease of turfgrass." Fungal Biol. **122**(8): 761-773.

Sapkota, S., A. Martinez Espinoza, E. Ali, B. Vermeer and B. Bahri (2020). "Taxonomical identification of *Clarireedia* species causing dollar spot disease of turfgrass in Georgia." Plant Dis.

Sialer, M. F., F. Cillo, L. Barbarossa and D. Gallitelli (1999). "Differentiation of cucumber mosaic virus subgroups by RT-PCR RFLP." J. Plant Path.: 145-148.

Smiley, R., P. Dernoeden and B. Clarke (2005). Compendium of Turfgrass Diseases. St. Paul, Minnesota, American Phytopathological Society.

Stackhouse, T., A. D. Martinez-Espinoza and M. E. Ali (2020). "Turfgrass disease diagnosis: Past, present, and future." Plants **9**(11): 1544.

Stowell, L. and W. Gelernter (2001). "Diagnosis of turfgrass diseases." Annu. Rev. Phytopathol. **39**(1): 135-155.

Susca, A., G. Stea, G. Mulé and G. Perrone (2007). "Polymerase chain reaction (PCR) identification of *Aspergillus niger* and *Aspergillus tubingensis* based on the calmodulin gene." Food Addit. Contam. **24**(10): 1154-1160.

Szalanski, A. L., D. D. Sui, T. S. Harris and T. O. Powers (1997). "Identification of cyst nematodes of agronomic and regulatory concern with PCR-RFLP of ITS1." J. Nematol. **29**(3): 255-267.

Vargas, J. M. (2018). Management of turfgrass diseases, CRC Press.

Vincelli, P. and N. Tisserat (2008). "Nucleic acid-based pathogen detection in applied plant pathology." Plant Dis. **92**(5): 660-669.

Waliullah, S., O. Hudson, J. E. Oliver, P. M. Brannen, P. Ji and M. E. Ali (2019). "Comparative analysis of different molecular and serological methods for detection of *Xylella fastidiosa* in blueberry." PloS one **14**(9): e0221903.

Walsh, B., S. S. Ikeda and G. J. Boland (1999). "Biology and management of dollar spot (*Sclerotinia homoeocarpa*); an important disease of turfgrass." HortScience **34**(1): 13-21.

White, T. J., T. Bruns, S. Lee and J. Taylor (1990). "Amplification and direct sequencing of fungal ribosomal RNA genes for phylogenetics." PCR protocols: a guide to methods and applications **18**(1): 315-322.

Williams, D. W., A. J. Powell, P. Vincelli and C. T. Dougherty (1996). "Dollar Spot on bentgrass influenced by displacement of leaf surface moisture, nitrogen, and clipping removal." Crop Sci. **36**(5): cropsci1996.0011183X003600050039x.

Zhang, Y., B. J. Iaffaldano, X. Zhuang, J. Cardina and K. Cornish (2017). "Chloroplast genome resources and molecular markers differentiate rubber dandelion species from weedy relatives." BMC plant bio. **17**(1): 1-14.

Figures

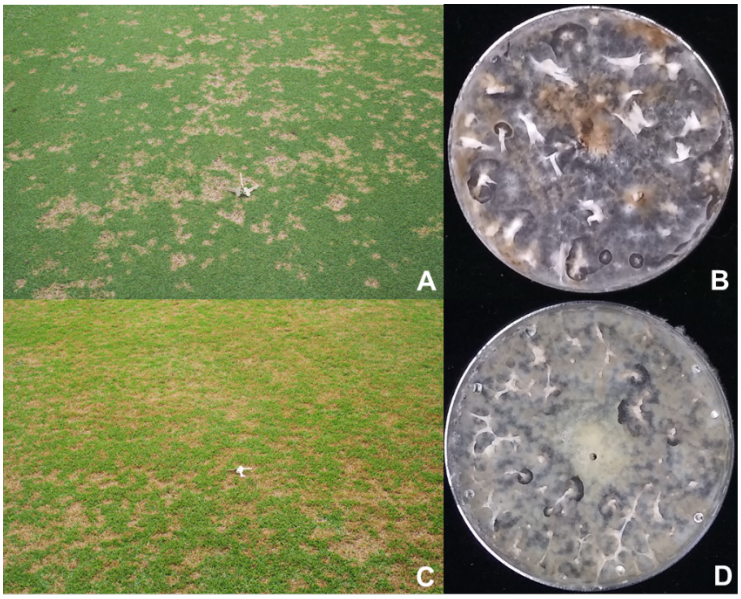

Figure 2.1. Signs and cultures of *Clarireedia jacksonii* and *C. monteithiana.* A) Symptoms of dollar spot caused by *C. jacksonii* on *Agrostis stolonifera* (bentgrass). B) Culture of *C. jacksonii* grown on potato dextrose agar (PDA) for 14 days. C) Symptoms of dollar spot caused by *C. monteithiana* on *Paspalum vaginatum* (seashore paspalum). D) Culture of *C. monteithiana* grown on potato dextrose agar (PDA) for 14 days.

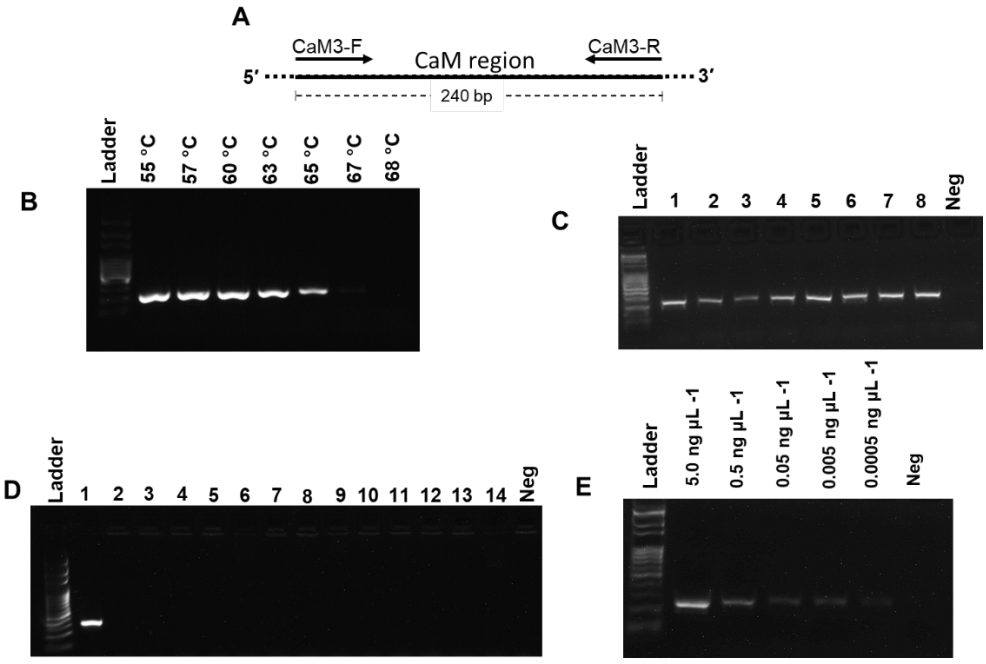

Figure 2.2. CaM PCR primer design and optimization. A) New primer design for CaM3 PCR primers amplifying *Clarireedia* spp. B) Temperature optimization of CaM3 primers from 55-68 °C using 2020-DS2 dollar spot sample. C) Testing CaM3 PCR primers, at the optimal annealing temperature of 63 °C, with eight *Clarireedia* spp. samples (1: 2020-DS2, 2: 2020-DS3, 3: 2020-DS4, 4: 2020-DS5, 5: 2020-DS6, 6: 2020-DS8, 7: 2020-DS10, 8: 2020-DS15). D) Specificity test against one *Clarireedia* spp. isolate (1: 2020-DS2) and 11 nontarget species (2: *Phytophthora sojae*, 3: *Fusarium* sp., 4: *Colletotrichum* spp., 5: *Bipolaris* spp. 6: *Botrytis* sp., 7: *Cladosporium* sp., 8: *Rhizotonia solani*, 9: *Leptosphaerulina* sp., 10: *Fusarium* sp., 11: *Pyricularia grisea*, 12: *Rhizotonia solani*, 13: *Ophiosphaerella korrae*, and 14: *Magnaporthe poae*). E) Sensitivity test of CaM3 primers using a serial dilution of targeted DNA from 5ng μL^{-1} to 0.0005 ng μL^{-1} using 2020-DS2 dollar spot sample. Here, Ladder: 100bp as ladder marker, Neg: dH_20 as negative control.

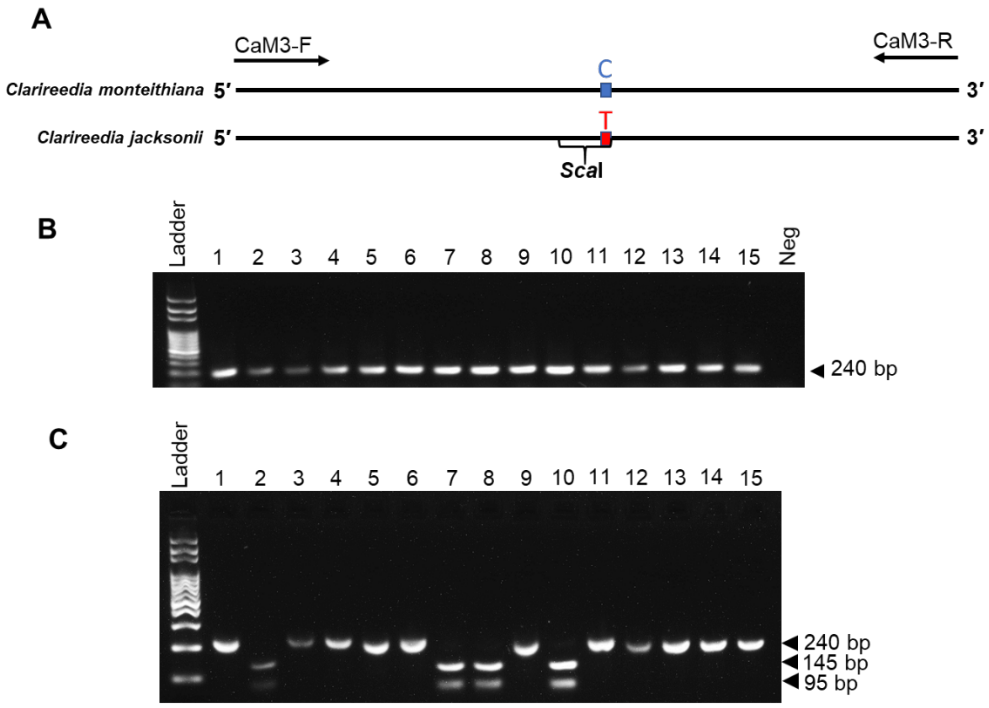

Figure 2.3. CAPS assay on CaM3 amplification products using ScaI. A) ScaI restriction site (AGT^ACT) was only identified in *C. jacksonii* at the 95th base pair. B) 240 bp amplification products using CaM3 primer set of fifteen Clarireedia spp. samples. C) CAPS assay results targeting a SNP in *C. jacksonii* at the 95th base pair. The result was a (240 bp) band in *C. monteithiana* isolates (samples 1, 3-6, 9, 11-15) and two (95 and 145 bp) bands in *C. jacksonii* isolates (samples 2, 7-8, 10). B) and C) were performed on 11 isolates of *C. monteithiana* (1:2020-DS2, 3: 2020-DS4, 4: 2020-DS5, 5: 2020-DS6, 6: 2020-DS7, 9: 2020-DS11, 11: 2020-DS16, 12: 2020-DS17, 13: 2020-DS18, 14: 2020-DS19, 15: 2020-DS21) and 4 *C. jacksonii* (2: 2020-DS3, 7: 2020-DS8, 8: 2020-DS10, 10: 2020-DS15). 100bp ladder marker was used, Neg: dH20.

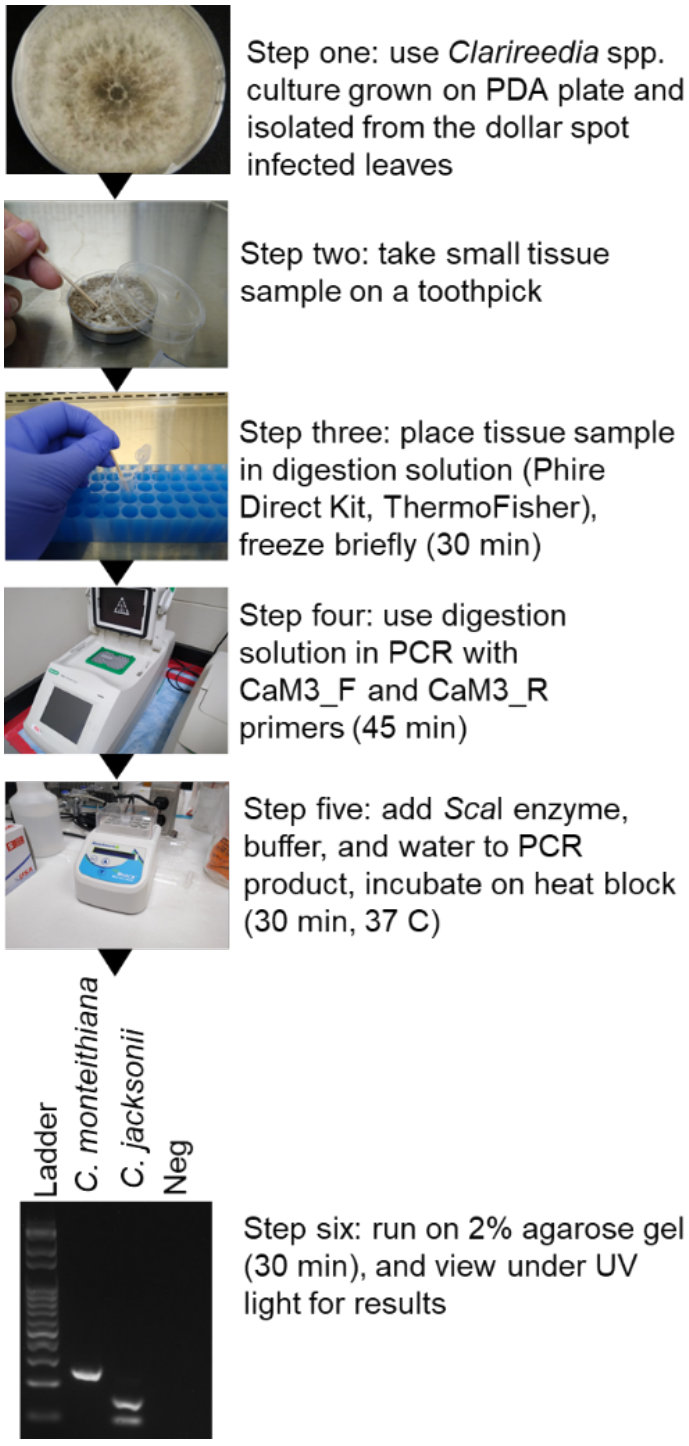

Figure 2.4. Step by step protocol of CAPS assay. Modified CAPS assay using direct PCR to detect specifically *C. jacksonii* and *C. monteithiana*. The estimated time for this protocol was 3 hours.

Tables

Table 2.1. Georgia (GA) 2019-2020 *Clarireedia* spp. samples used in this study.

Pathogen	MDL name	Grass Species	Grass Type	GA, U.S. County
C. monteithiana	2020-DS2	*Zoysia* sp.	Warm	Spalding
C. jacksonii	2020-DS3	*Agrostis stolonifera*	Cool	Spalding
C. monteithiana	2020-DS4	*Zoysia* sp.	Warm	Fulton
C. monteithiana	2020-DS5	*Cynodon dactylon*	Warm	Cook
C. monteithiana	2020-DS6	*Paspalum vaginatum*	Warm	Cook
C. monteithiana	2020-DS7	*Cynodon dactylon*	Warm	Spalding
C. jacksonii	2020-DS8	*Digitaria* sp.	Warm	Spalding
C. jacksonii	2020-DS10	*Festuca arundinacea*	Cool	Spalding
C. monteithiana	2020-DS11	*Zoysia* sp.	Warm	Fulton
C. jacksonii	2020-DS15	*Agrostis stolonifera*	Cool	Spalding
C. monteithiana	2020-DS16	*Cynodon dactylon*	Warm	Spalding
C. monteithiana	2020-DS17	*Paspalum vaginatum*	Warm	Spalding
C. monteithiana	2020-DS18	*Zoysia* sp.	Warm	Spalding
C. monteithiana	2020-DS19	*Cynodon dactylon*	Warm	Coweta
C. monteithiana	2020-DS21	*Zoysia* sp.	Warm	Upson

Table 2.2. All primers designed for this study.

Primer Set Name	Gene Target	Forward Primer Sequence (F)	Reverse Primer Sequence (R)	Recommended Annealing Temperatures F/R (°C)	Produced bands at recommended temperatures?	Only one, correctly sized band?	Amplified only target samples? (Specificity)	Had a good CAPS assay target?
MCM1	Mcm7	GCTGGAATTTCGATGCCCTAG	AGCCGACCGTTGAAGTTAATG	66.7/65	No	-	-	-
MCM3	Mcm7	CTGTTCAATCCGTCTAAACACG	ACCAGTTGGTCATATTCCGAG	63.3/62.7	No	-	-	-
ITS1	ITS	TTTGGCAGGCTGCTGCC	ACCCTGTAACGAGAGGTATGT	69/59	No	-	-	-
CaM4	CaM	CTATTTCAGCCCTATGTGAAC	CAGCATGATATTCAAGATCGC	57.8/62.1	No	-	-	-
MCM2	Mcm7	CATCGAGATGGCCGTAGATC	GATGTCGTAGATGTCGCCG	64.5/64.4	Yes	No	-	-
MCM4	Mcm7	GCAAGAATATGCCGGCGAC	CGCCAGACTGCAAGGTCA	67.7/66.6	Yes	No	-	-
ITS2	ITS	TTTGGCCGGCTGCTCGA	ACCCTGTAACGAGAGGTATGTGT	71.8/62.5	Yes	Yes	No	-
ITS3	ITS	GCTTTGGCAGGCTGCTGGA	GCCCTGTAACGAGGTGTATGT	71.2/62.3	Yes	Yes	No	-
CaM1	CaM	AGTCCTCCGCTACCATCC	CAGCATGATATTCAAGATCGC	61.7/62.1	Yes	Yes	No	-
ITS4	ITS	CTTTGGCCGGCTGCTCGA	ACCCTGTAACGAGAGGTATGTGT	72.2/62.5	Yes	Yes	Yes	No
CaM2	CaM	CTTGGACCACTATCGCGACC	TGCAAACGTCAGTCTACAGC	66.8/61.7	Yes	Yes	Yes	No
CaM3	CaM	CTATTTCAGCCCTTTGCGAAG	CAGCATGATATTCAAGGTCGC	64.7/64.4	Yes	Yes	Yes	Yes

CHAPTER 3

PROBE-BASED LOOP-MEDIATED ISOTHERMAL AMPLIFICATION ASSAY FOR RAPID DETECTION OF TWO CLARIREEDIA SPP., THE CAUSAL AGENT OF DOLLAR SPOT OF TURFGRASS

Stackhouse, T., Bass, A., Waliullah, S., Martinez-Espinoza, A.D., & Ali, M.E. (2024) Probe-based loop mediated isothermal amplification assay for rapid detection of two Clarireedia spp., the causal agent of dollar spot of turfgrass. Plant Disease, 108(10). Reprinted here with permission of publisher.

Abstract

Dollar spot is a major fungal disease affecting turfgrass worldwide and can quickly destroy turfgrass swards. An assimilating probe-based loop-mediated amplification (LAMP) assay was developed to detect *Clarireedia monteithiana* and *C. jacksonii*, the causal agents of dollar spot within the continental US. Five LAMP primers were designed to target the calmodulin gene with the addition of a 6-carboxyl-fluorescein florescent assimilating probe and the temperature amplification was optimized for *C. jacksonii* and *C. monteithiana* identification. The minimum amount purified DNA needed for detection was 0.05 ng μL^{-1}. Specificity assays against host DNA and other turfgrass pathogens were negative. Successful LAMP amplification was also observed for dollar spot infected turfgrass field samples. Further, a DNA extraction technique via rapid heat-chill cycles and visualization of LAMP results via a florescent flashlight was developed and adapted for fast, simple and reliable detection in 1.25 hours. This assimilating probe-based LAMP assay has proved successful as a rapid, sensitive, and specific detection of *C. monteithiana* and *C. jacksonii* in pure cultures and from symptomatic turfgrass leaf blades. The assay represents a promising technology to be used in the field for on-site, point-of-care pathogen detection.

Introduction

Turfgrass comprises a multi-billion-dollar worldwide industry. In 2018, the growth, development, and use of more than 62 million acres of turfgrass was responsible for over 820,000 jobs in the United States (Chawla et al. 2018). Dollar spot is one of the most important and prevalent fungal diseases affecting turfgrass worldwide. The most relevant *Clarireedia* species in North America are *C. jacksonii* and *C. monteithiana*; these are both globally distributed (Salgado-Salazar et al. 2018). It has been recently demonstrated that dollar spot can be caused by at least seven species in the *Clarireedia* genera, formerly *Sclerotinia homeocarpa* (Bennett 1937, Salgado-Salazar et al. 2018, Hu et al. 2019). The known distribution of the other *Clarireedia* species is

more restricted with *C. bennettii* in the Netherlands, United Kingdom, and New York, United States (Salgado-Salazar et al. 2018). *C. homeocarpa* is found in the United Kingdom, and the most novel species, *C. paspali* and *C. hainanense* are currently found in China, while *C. aff. Paspali* has been described in China and Hawaii (Salgado-Salazar et al. 2018, Hu et al. 2019, Zhang et al. 2022, Bahri et al. 2023). It was previously thought *C. jacksonii* only infected cool season grasses and *C. monteithiana* only infected warm season grasses, but recent studies have found that both species infect both types of grasses and can co-exist in the transitional zone of the United States, with *C. jacksonii* being the more virulent of the two species (Aynardi et al. 2019). Based on these species distributions and the ability to infect similar hosts, *C. jacksonii* and *C. monteithiana* are the most prevalent and important species in the United States.

Traditionally the detection of *Clarireedia* spp. has relied on identification based on signs, symptomology, and morphology (Bennett 1937, Salgado-Salazar et al. 2018). When looking at signs and symptoms of disease, one must be able to rule out abiotic factors such as nutrient deficiencies and the quality and amount of light and water (Stowell and Gelernter 2001). Dollar spot symptoms include leaves with a yellow-brown discoloration surrounded by a dark brown border and a water-soaked appearance (Mori et al. 2002; Lucchi et al. 2010; Niessen 2015). The infected leaves form necrotic patches that are circular and straw colored, and the patches are typically up to 5.0 cm in diameter but can be larger (Mori et al. 2002; Lucchi et al. 2010; Niessen 2015). Patches can coalesce, forming larger areas of affected grass. A prominent sign of dollar spot pathogen is mycelial growth which is noticeable in high humidity or when dew is present (Mori et al. 2002; Lucchi et al. 2010; Niessen 2015). However, initial symptoms of several turfgrass diseases are similar and can be misidentified, emphasizing the importance of efficient, accurate, and rapid detection (Roux 2009, Notomi et al. 2015, Salgado-Salazar et al. 2018, Sapkota

et al. 2021). Microscopy can be used to identify *Clarireedia* spp. morphologically using mycelial features and colony morphology on growing media (Salgado-Salazar et al. 2018). However, microscopic identification by non-experts is difficult because *Clarireedia* spp. do not readily sporulate (Smiley et al. 2005, Salgado-Salazar et al. 2018, Sapkota et al. 2021). Therefore, molecular identification of *Clarireedia* spp. is helpful for diagnosis. DNA extraction, polymerase chain reaction (PCR) amplification, and DNA sequencing can be performed using known conserved genes that can be used as molecular markers including the internal transcribed spacer (ITS) region of the ribosomal DNA, calmodulin (CaM) gene, and DNA replication licensing factor Mcm7 gene (Salgado-Salazar et al. 2018). By cross-referencing the BLAST analysis with GenBank, a diagnosis to the species level can be made. However, getting the results from sequencing and performing a thorough analysis can take several days and well-trained personnel. Rapid detection of dollar spot is vital as it can destroy turfgrass swards within days. Therefore, as the time needed to make a diagnosis increases, and the time used to develop and implement effective disease management strategies decreases (Mori et al. 2002; Si Ammour et al. 2017).

Recent advances in the molecular detection of *Clarireedia* spp. focus on speed and reliability. In 2020, a quantitative PCR (qPCR) detection assay using genus-specific ITS primers was developed for dollar spot (Groben et al. 2020). This method takes significantly less time to yield results than the standard PCR and sequencing process. More recently, a co-dominant cleaved amplified polymorphic sequences (CAPS) assay has been developed for the species identification and differentiation of *C. jacksonii* and *C. monteithiana* (Stackhouse et al. 2021). This assay is relatively less time consuming and provides species differentiation without sending PCR products for sequencing (Stackhouse et al. 2021). Rapid species differentiation allows for a more specialized response to disease management.

Loop-mediated isothermal amplification (LAMP) is a gene amplification assay recognized for its high specificity and rapid detection time (Notomi et al. 2015). LAMP utilizes four to six primers to amplify six to eight specific DNA regions in the target sequence yielding an exponential number of stem-loop DNA products (Notomi et al. 2000, Nagamine et al. 2002, Notomi et al. 2015). LAMP DNA amplification occurs at a constant temperature and takes fifteen minutes to an hour to complete. The addition of loop primers often reduces the reaction time. (Notomi et al. 2000, Nagamine et al. 2002, Notomi et al. 2015). LAMP also can be conducted in the field, allowing for real-time detection and point-of-care testing. The results from LAMP can be analyzed using gel electrophoresis, turbidity measures, or intercalating fluorescent dyes (Notomi et al. 2000, Mori et al. 2001, Lucchi et al. 2010, Niessen 2015, Notomi et al. 2015). Instruments like the Genie® III (OptiGene, West Sussex, UK) can provide real-time quantitative fluorescence measurements. This equipment is portable and lightweight and provides rapid and accurate LAMP results. LAMP has successfully detected filamentous fungi that cause various plant diseases (Niessen 2015, Si Ammour et al. 2017, Hamilton et al. 2021). In addition, real-time quantification of the LAMP reaction has been utilized for rapid, early, and on-site detection of several pathogens (Si Ammour et al. 2017; Hamilton et al. 2020). This method consists of assimilating probes comprised of labeled oligonucleotide probes pair, a florescent (F) strand and a quencher (Q) strand, that are partially complementary. The F strand contains a fluorescence label on the 3' end, a sequence complementary to Q strand, and the target loop sequence. The Q strand contains a sequence complementary to the F strand and a compatible quencher molecule on the 5' end. During LAMP reactions, the overhang of the F strand attaches to the loop sequence and the Q strand is displaced as the F strand is assimilated into the product. This allows for fluorescence and real-time

quantification of the LAMP reaction. Simplicity, speed, and high specificity make LAMP, coupled with real-time quantification, an ideal candidate for *Clarireedia* spp. detection.

The objectives of study were to develop an assimilating probe-based loop-mediated amplification assay that could detect *C. monteithiana* and *C. jacksonii* in pure cultures and from symptomatic turfgrass blades. As well as to develop an assay that could potentially be used in laboratory and field.

Materials and Methods

Dollar spot fungal isolates and DNA extraction

Nine isolates of *C. monteithiana* (DS29, DS180-DS183, DS185-DS188) and one of *C. jacksonii* (DS3) were used in this study. These isolates are part of a dollar spot collection stored on oat/barley/wheat grain mixture at -20 °C at the UGA Griffin campus. Host species, isolate location, and isolate ID were detailed in Ghimire et al. 2023. Briefly, these isolates were 1) collected from turfgrass showing symptomatic dollar spot symptoms from cool and warm season grasses throughout the state of Georgia from 2019 to 2021 2) isolated and purified on Potato Dextrose Agar (PDA) media and 3) identified at the species level using both morphological features and Sanger sequencing the ITS region of the ribosomal DNA.

Clarireedia mycelium grown as pure cultures of the isolates used, were scraped from the PDA plates using a sterile scalpel and 50-100 mg of tissue was were placed in 1.5 mL SafeLock tubes containing 3-5 4mm diameter stainless steel beads. The SafeLock tubes containing the mycelium and the beads were run on FastPrep FP120 homogenizer, run twice at setting 6 for 30 seconds at a time (Thermo Electron Corporation). DNA extraction was completed using the QIAGEN DNeasy Plant Mini Kit (Qiagen, Valencia, CA) using the manufacturer's protocol, except the AE buffer (10 mM Tris-Cl; 0.5 mM EDTA; pH 9.0) was preheated to 65 °C before

elution. DNA integrity and quality were checked on agarose gel 1% and NanoDrop™ Lite Spectrophotometer (FisherScientific, Waltham, MA, USA), and stored at -20 °C.

LAMP primer and probe design specific to Clarireedia spp.

Sequences from Salgado-Salazar et al. 2018 of three regions, CaM, ITS, and Mcm7, were examined to identify areas with high variation between the two *Clarireedia* species present throughout North America and potential LAMP primer locations. The sequences of *C. jacksonii* and *C. monteithiana* samples and closely related species (*C. bennettii* and *C. homeocarpa)* were compared within Geneious Prime (Biomatters Ltd., Auckland, NZ) using consensus alignment (alignment type: global alignment, cost matrix: 93% similarity). A region of about 200bp on the CaM was selected based on SNPs that both target species contained when compared to other closely related species, and LAMP primers were designed as detailed by Notomi et al. (Notomi et al. 2000) and Nagamine et al. (Nagamine et al. 2002). The LAMP primer set used in this study contained two outer (F3 and B3) primers, two inner (FIP and BIP) primers, and a loop primer forward (LF). A 6-carboxyl-flurescein (FAM) florescent assimilating probe with an associated quencher strand was design against the loop backward primer (LB) (Fig. 3.1; Table 3.1) (Kubota et al. 2011, Hamilton et al. 2020). Primers were synthesized by Sigma Aldrich (Millipore Sigma, St. Louis, MO), and the probe was synthesized by Integrated DNA Technologies Inc. (IDT, Coralville, IA, USA).

Optimization of LAMP conditions for *Clarireedia* spp. detection in pure cultures

The optimal temperature of the LAMP reaction was determined for both *C. jacksonii* and *C. monteithiana* isolates. Each 25-µL LAMP reaction contained 12.5 µL of LavaLAMP™ DNA Master Mix (Lucigen, Middleton, WI, USA), 1.6 µM of FIP and BIP primers, 0.2 µM of F3/B3 primers, 0.8 µM of LF primer, 0.1 µM of LB partial F strand, and 0.2 µM of Q strand, 1 µL of

DNA at 5 ng μL^{-1}, and filled up to 25 µL. These amplification reactions were first performed as a temperature gradient from 69-76 °C for 60 min with a final step from 95-80 °C at -0.5 °C/sec in a Genie III instrument. The FAM fluorescence was measured as a sequence-specific graphical quantification of LAMP amplification. This temperature gradient assay was first tested on DS180 and DS3 isolates of *C. monteithiana* and *C. jacksonii,* respectively. Next, five *C. monteithiana* isolates (DS181, DS182, DS185, DS186, and DS188) at 5 ng μL^{-1} were run at the target temperature of 72 °C for 60 minutes to ensure consistent results and an adequate length of time to complete the reaction. This test at 72 °C for 60 minutes was also repeated for DS180 and DS3 isolates of *C. monteithiana* and *C. jacksonii,* respectively.

Sensitivity and specificity analysis of LAMP assay

The sensitivity of the LAMP assay was tested with serially diluted DNA of *C. jacksonii* (isolate DS3) and *C. monteithiana* (isolate DS180) (Ghimire et al. 2023). DNA of each species was diluted in ten-fold serial dilutions from 5-0.0005 ng μL^{-1} of DNA. Diluted DNA was run at the target temperature of 72 °C for 60 minutes and LAMP amplification was detected by the FAM fluorescence, as described above. These tests were used to determine the minimum quantity of DNA required to detect the presence of dollar spot.

To determine the specificity of the LAMP assay against *Clarireedia* species. Several fungi that are pathogenic in turfgrass, as well as other that are non-pathogenic in turfgrass, were tested. Therefore, DNA from six non-target turfgrass pathogens (Bip: *Bipolaris* sp., Col: *Colletotrichum* sp., Mg: *Magnaporthe grisea,* Mp: *Magnaporthe poae,* Ok: *Ophiosphaerella korrae,* and Rs: *Rhizoctonia solani*) were tested along with isolate DS180 of *C. monteithiana* as positive control and one sample of sterile water as a negative control. Pure cultures of these pathogens were obtained by fungal tip and/or single spore transfer to new media. In addition, six asymptomatic

host samples from greenhouse-grown turfgrass (Pv1: *Paspalum vaginatum* 'sea isle supreme', Pv2: *Paspalum vaginatum* 'sea dwarf', Cd1: *Cynodon dactylon* 'TifGrand', Cd2: *Cynodon dactylon* 'TifDwarf', Z1: *Zoysia japonica* 'Meyer', Z2: *Zoysia japonica* 'Empire') were also tested along with isolate DS3 of *C. jacksonii* as positive control and one sample of sterile water as a negative control. These tests were performed to confirm the non-cross reaction of the *Clarireedia* LAMP assay with other turfgrass pathogens or with host DNA. All DNAs were run at 72 °C for 60 minutes, and the FAM fluorescence was measured, as described above.

Optimization of the LAMP assay for facilitating point-of-care utilization

To optimize the LAMP assay developed in this study for detecting *C. jacksonii* and *C. monteithiana* on-site and facilitate its utilization at the point-of-care, we tested it directly in field samples and developed a rapid DNA extraction for LAMP assay and a simple visualization of LAMP results via florescent flashlight.

LAMP assay for Clarireedia *spp. detection in field samples*

The LAMP assay was used to test direct field samples that were visually diagnosed with dollar spot. For direct detection, leaves of four turfgrass field samples (21_DS1, 21_DS3, 21_DS5, and 21_DS6; Supplemental Table 3.1) presenting dollar spot symptoms were tested with LAMP amplification at the target temperature of 72 °C for 60 minutes. 21_DS1 and 21_DS3 were collected from seashore paspalum (*Paspalum vaginatum)* and zoysiagrass (*Zoysia japonica*) in August 2021 at UGA Griffin Campus, Spalding County, GA; 21_DS5 and 21_DS6 were collected from bermudagrass (*Cynodon dactylon*) 'TifSport' and bermudagrass 'TifEagle' in August 2021 at UGA Tifton Campus, Tift County, GA. For this test, 100 mg of fresh leaves for each sample were disrupted at room temperature with a FastPrep FP 120 homogenizer until thoroughly homogenized. DNA extraction, quantification, and LAMP amplification were performed on pure fungal cultures

as described above. A negative water control was also used in this test. This assay was performed to assess the success of the LAMP assay method without media isolation.

Rapid DNA extraction for LAMP assay

A rapid DNA extraction method was examined to make the assay field-ready. For this method, a 1mm square of mycelium grown on PDA media from isolate DS3 of *C. jacksonii* and six isolates (DS180, DS181, DS183, DS186, DS188) of *C. monteithiana* were used. Each sample was placed in 20 µL of Phire Direct digestion solution (ThermoFisher, Waltham, MA, USA), inverted vigorously, put on a heat block at 90 °C for 2 min, inverted vigorously, then placed in liquid nitrogen to flash freeze. This was repeated once and then thawed in the 90 °C heat bath. Additionally, this method was tested using ice water instead of liquid nitrogen and repeated twice. This adjustment was made to make the technique more field-accessible. LAMP was performed using the previously detailed protocol, except 2 µL of the DNA solution instead of 1 µL of pure DNA (Griffiths et al. 2006, Stackhouse et al. 2021). Water was used as a negative control.

Simple visualization of LAMP results via florescent flashlight

The LAMP assay was replicated under the optimized settings, but with the addition of ROX Passive Reference Dye (1X concentration) to visually distinguish the negative and positive results outside of the Genie III system using previously described fluorescent quantification systems (Stackhouse et al. 2021). Samples used were C. *jacksonii* (isolate DS3)*, C. monteithiana* (isolate DS29), *Rhizoctonia solani* (Rs)*, Bipolaris* spp. (Bip)*,* and H_2O. The assay used the Genie Isothermal Amplification instrument, a thermocycler, and a dry water bath with optimized reaction settings. These sample results were visualized using a NightSea Xite Fluorescence Royal Blue Flashlight System (NightSea, Hatfield, PA, USA). The expected results are green-colored as positive samples and red-colored as negative samples.

The LAMP assay with NightSea visualization was tested with an addition of ROX at different concentrations (1X, 0.5X, 0.25X, 0.13X, 0.06X, 0.03X, and 0.016X). These concentrations were selected based on the amount of ROX found in qPCR systems, and the final optimized ROX concentration used was determined based on the inability to view any red signal in the positive samples after amplification that could give unclear results.

A viewing apparatus was 3D printed to allow for more targeted light distribution and visualization of the results. This was important to make photographing results more accessible in bright settings, such as in field assay running.

Point-of-care utilization of the LAMP assay

The LAMP assay was replicated using three field samples under the optimized settings for rapid DNA extraction. These samples were first disrupted using a polypropylene pellet pestle (Grainder industrial supply) at room temperature followed by two heat and chill cycles using ice water, and a simple visualization of LAMP results via florescent flashlight using ROX at a concentration of 0.25X and the target temperature of 72 °C for 60 minutes (see description above). The three field samples were collected at the UGA Griffin campus, Griffin, GA in March 2023 (Supplemental Table 3.1). They consisted of a dollar spot infected seashore paspalum 'Seastar' (23_DS1), a bentgrass 'Pure Eclipse' field sample presenting dollar spot and *Microdochium* Patch infections (23_DS3), and a disease-free seashore paspalum 'Seastar' (23_DS2). A pure culture of C. *jacksonii* (isolate DS3) and *Bipolaris* spp. (Bip) were also added as positive and negative controls. The samples were incubated isothermally in a Bio-Rad CFX96 qPCR Real-Time PCR Module to quantitate fluorescence.

Results

Optimization of LAMP conditions for detecting Clarireedia spp. in pure culture

The LAMP primer set (including F3, B3, FIP (F1c-F2), BIP (B1c-B2), and LF primers) were designed within the CaM gene to amplify both *C. jacksonii* and *C. monteithiana*. The areas of the gene with the most SNPs between the two *Clarireedia* species were targeted at the 3' end of primer binding sites to help promote specificity. An assimilating probe was designed in the area commonly used for an LB primer to increase the assay's specificity further. The resulting primer set was able to amplify *C. jacksonii* and *C. monteithiana* DNA.

The LAMP reactions were performed with a gradient from 69-76 °C to determine the optimal temperature for *C. jacksonii* and *C. monteithiana* detection. The reactions were run using the Genie III Isothermal Amplification instrument with the blue channel used to identify the assimilation of the probe. Samples had near identical amplification curves from 69-72 °C. The optimal temperature was determined to be 72 °C (Fig. 3.2). This temperature was selected because temperatures often lead to better specificity in PCR or LAMP assays, and that was the highest temperature that didn't affect assay effectiveness (Roux 2009). LAMP reactions were then performed at this optimal temperature with seven *Clarireedia* spp. isolates (one *C. jacksonii* isolate and six *C. monteithiana* isolates (Fig. 3.3). All samples were standardized to 5 ng μL^{-1} and had completed their amplification by 25 minutes. The amplification results showed that the LAMP method optimized here is rapid and efficacious in amplifying pure cultures of *C. jacksonii* and *C. monteithiana* isolates.

Specificity and sensitivity of LAMP Clarireedia spp. detection

Nontarget turfgrass pathogens and non-infected host DNA were tested using the LAMP assay to determine specificity. None of the six non-target turfgrass pathogens, *Bipolaris* sp.,

Colletotrichum sp., *Magnaporthe grisea, Magnaporthe poae, Ophiosphaerella korrae,* and *Rhizoctonia solani*, amplified using the LAMP assay (Fig. 3.4A). Additionally, none of the six non-infected host samples amplified using the LAMP assay (Fig. 3.4B). In addition, a series of ten-fold dilutions of *C. jacksonii* and *C. monteithiana* DNA extracted from pure cultures was used to determine the sensitivity of the LAMP assay. Our results showed that 0.05 ng μL^{-1} is the detection limit for this assay (Fig. 3.5), as samples with less DNA were falsely negative.

Optimization of the LAMP assay

The LAMP assay was first tested on dollar spot-infected turfgrass field samples. All four samples tested positive for the presence of *Clarireedia* spp. (Fig. 3.6). This LAMP test showed that field samples can be tested without requiring culturing and isolation of *Clarireedia* samples before testing, providing a point-of-care detection.

In addition, the LAMP assay was tested using a rapid heat-chill extraction method with ice water to make the assay more field-friendly and point-of-care ready. All the *Clarireedia* spp. samples were determined to be positive using this method (Fig. 3.7). This DNA crude extraction protocol is rapid, sensitive, specific, and reliable, and it takes 5-10 minutes to complete before LAMP preparation. The LAMP assay was shown to be highly efficient, providing results in an hour from sampling to results (~75 min), but positives can be seen as soon as 30 min.

Furthermore, the LAMP assays testing probe visualization using blue light filtering found that the positive *Clarireedia* spp. samples visualized yielded a green color when viewed with the NighSea (Hatfield, PA) Xcite fluorescence flashlight and blue light filtering glasses combination (Royal blue 440-460nm excitation; emission long pass over 500nm while the negative samples such as *Rhizoctonia solani, Bipolaris* sp., and H_2O samples yielded visually a red color under the same conditions (Fig. 3.8). Polypropylene tubes, like PCR and Genie LAMP tubes appear slightly

green under the royal blue NightSea light by themselves, hampering a clear view of the reactions. Therefore, a passive reference dye (ROX) was added. This addition allows users to look for the red visual signal to denote a negative result. Upon testing for the ideal ROX concentration, 0.25X concentration was selected based on the inability to view any red signal in the positive samples after amplification. Using higher concentrations yielded a slight orange color (data not shown). Additionally, a viewing apparatus was 3D printed to allow for more targeted light distribution and visualization of the results. Samples were viewed and photographed by placing the BlueSea filter glasses between the sample view port and the phone to allow filtering of the blue light or directly worn.

Point-of-care utilization of the LAMP assay

To provide a point-of-care detection, the LAMP assay was further tested on dollar spot-free and dollar spot-infected turfgrass field samples using the rapid heat-chill extraction method and probe visualization using blue light filtering. The LAMP assay results were positive (green color) for the seashore paspalum with symptoms (23_DS1) as well as for the bentgrass sample presenting dollar spot and *Microdochium* Patch co-infections (23_DS3) and the pure culture of C. *jacksonii* (isolate DS3). However, the disease-free seashore paspalum field sample (23_DS2) and the pure culture of *Bipolaris* spp. (Bip) tested negative and yielded a red color visually under the same conditions.

Discussion

Dollar spot is one of the most important and damaging fungal diseases affecting a broad range of both warm- and cool-season turfgrasses. In the US, dollar spot is mainly caused by two species, *C. jacksonii* and *C. monteithiana*. Turfgrass managers rely on a rapid, sensitive, and correct diagnosis for dollar spot management (Stackhouse et al. 2020). Currently dollar spot can

be detected with symptomology, qPCR, or a CAPS PCR assay (Groben et al. 2020, Stackhouse et al. 2021). Dollar spot symptoms are typically distinct, but can be misdiagnosed, especially at the onset of the disease. The qPCR and CAPS assays require a well-equipped laboratory, highly skilled personnel, and considerable time, rendering the assays with little potential for field-read, point-of-care applications. It is essential to rapidly and reliably detect dollar spot to implement control measures to prevent the rapid spread and damage.

The LAMP assimilating-probe assay developed in this study proved to be rapid, sensitive, and specific for *C. jacksonii* and *C. monteithiana* detection. Pure cultures were used to optimize the protocol; then, field samples were tested for in-situ, direct field sampling, point-of-care use detection. LAMP primers were designed to target the calmodulin gene (CaM) and the temperature amplification of 72 °C and an incubation time of 60 min were selected for an optimized specificity and sensitivity detection towards *Clarireedia jacksonii* and *C. monteithiana*. Ten *Clarireedia* spp. isolates were standardized at a DNA amount of 5 ng μL^{-1} and tested with the LAMP assay at 72 °C to ensure replicability of the assay. Successful LAMP amplification reactions were completed within 25 minutes, indicating the rapid speed of the test, except in cases of very low DNA concentrations, which took up to 45 minutes. Specificity was tested using various turfgrass and non-turfgrass pathogens and non-infected host tissue. This LAMP assay did not amplify any of the non-target samples. This is vital for assays because co-infections are not uncommon in turfgrass pathogens and can make diagnosis more difficult. Additionally, a sensitivity test was performed, using ten-fold dilutions from 5-0.0005 ng μL^{-1}, to determine the detection limit and the optimal run time for the assay. The results demonstrated that 0.05 ng μL^{-1} is the detection limit for this LAMP assay.

The LAMP assay was further tested using turfgrass samples with visual symptoms of *Clarireedia* spp. Four *Clarireedia* spp. field samples were tested using the optimized LAMP assay and were all found to be positive. Additionally, *Clarireedia* spp. mycelia was placed through a heat and chill cycling to obtain crude exacts. The freezing portion of the protocol was tested at various temperatures and freezing substrates, with similar results throughout. Ice water was selected, as it is easiest to use in a field setting. This was repeated with seven *Clarireedia* spp. isolates and all were able to amplify using this LAMP assay. This method demonstrates a rapid protocol that could excludes a time-consuming, commonly used extraction method for obtaining DNA (Griffin et al. 2002, Griffiths et al. 2006). Instead, there is a rapid, under ten-minute crude extract protocol that, with the LAMP assay can make point-of-care take just over an hour, with most of the time being non-labor time and many positive results seen in the first 30 minutes. This is drastically faster than many other protocols and can allow for faster detection results.

While this LAMP assay can be performed using portable equipment such as the Genie III, the equipment is unique, costly, has a low throughput, and requires trained personnel. Therefore, visualizing the probe fluorescence after running in a dry bath and then using a NightSea blue light was evaluated. This method has been used previously to visualize PCR results with the intent to avoid requiring additional expensive equipment. To make these results most user-friendly, a ROX passive reference dye was added to the samples during the mixing step to make the samples appear red when negative. This did not affect the ability of the Genie III to read results and allows for an easy visualization, with the positive samples appearing green and negative samples appearing red. This method is just as rapid as using costly highly specialized equipment by simply visualizing the fluorescence. The assay was performed in highly lighted areas providing reliable, reproducible, conclusive results. Adding this as an alternative method of viewing LAMP results using

intercalating dyes can allow this assay to be more widely used without requiring fluorescence quantifying equipment. The technique developed in this study can be applied to other difficult to for other hard to diagnose turfgrass pathogens.

To our knowledge, this study is the first report of an assimilating probe-based LAMP assay for *Clarireedia* spp. detection. Additionally, this is the first study using probe visualization via blue light within a LAMP assay setting allowing for rapid, onsite, point-of-care detection of the causal agents of dollar spot of turfgrass. This method can potentially be utilized by plant disease diagnosticians, practitioners, and turfgrass managers alike.

Author Contributions

Conceptualization, A.D.M.E & M.E.A.; Data curation, T.S., B.B, Funding acquisition, & A.D.ME. & M.E.A.; Investigation, T.S., A.D.M.E. & M.E.A.; Project administration, A.D.M.E, M.E.A., & B.B.; Resources, A.D.M.E., B.B. & M.E.A.; Supervision, M.E.A.; Writing–original draft, T.S., A.B., S. W., M.E.A., A.D.M.E & B.B.; Writing–review & editing, T. S., A.B., S.W., M.E.A, A.D.M.E & B.B.

Acknowledgements

The authors wish to thank all the UGA Plant Pathology Molecular Diagnostic Laboratory members for their assistance and guidance in writing this article. Thanks to Dr. Suraj Sapkota, Mr. Brian Vermeer, Mr. Turner Spratling, Mr. Gary Clayton, and Dr. Karen Harris for assistance in sample collections. We want to thank Mr. Brock Taylor for his aid in 3D printing the probe viewing apparatus.

Supplemental Information

The STL file for the 3D printed tube viewer can be freely accessed and downloaded at the NIH 3D print exchange at https://3d.nih.gov/entries/3DPX-020866.

References

Aynardi, B. A., M. M. Jiménez-Gasco and W. Uddin (2019). "Effects of isolates of *Clarireedia jacksonii* and *Clarireedia monteithiana* on severity of dollar spot in turfgrasses by host type." European Journal of Plant Pathology **155**(3): 817-829.

Bahri, B. A., R. K. Parvathaneni, W. T. Spratling, H. Saxena, S. Sapkota, P. L. Raymer and A. D. Martinez-Espinoza (2023). "Whole genome sequencing of Clarireedia aff. paspali reveals potential pathogenesis factors in Clarireedia species, causal agents of dollar spot in turfgrass." Front Genet **13**: 1033437.

Bennett, F. T. (1937). "Dollarspot disease of turf and its causal organism, *Sclerotinia homoeocarpa* n.sp." Annals of Applied Biology **24**(2): 236-257.

Chawla, S., A. Roshni, M. Patel, S. Patil and H. Shah (2018). Turfgrass: A billion dollar industry. National Conference on Floriculture for Rural and Urban Prosperity in the Scenerio of Climate Change-2018.

Ghimire, B., M. Aktaruzzaman, S. R. Chowdhury, W. T. Spratling, C. B. Vermeer, J. W. Buck, A. D. Martinez-Espinoza and B. A. Bahri (2023). "Sensitivity of *Clarireedia* spp. to benzimidazoles and dimethyl inhibitors fungicides and efficacy of biofungicides on dollar spot of warm season turfgrass." Frontiers in Plant Science **14**: 1155670.

Griffin, D. W., C. Kellogg, K. Peak and E. Shinn (2002). "A rapid and efficient assay for extracting DNA from fungi." Letters in Applied Microbiology **34**(3): 210-214.

Griffiths, L. J., M. Anyim, S. R. Doffman, M. Wilks, M. R. Millar and S. G. Agrawal (2006). "Comparison of DNA extraction methods for *Aspergillus fumigatus* using real-time PCR." Journal of Medical Microbiology **55**(9): 1187-1191.

Groben, G., B. B. Clarke, J. Murphy, P. Koch, J. A. Crouch, S. Lee and N. Zhang (2020). "Real-time PCR detection of *Clarireedia* spp., the causal agents of dollar spot in turfgrasses." Plant Disease **104**(12): 3118-3123.

Hamilton, J., S. Fraedrich, C. Nairn, A. Mayfield and C. Villari (2021). "A field-portable diagnostic approach confirms Laurel Wilt Disease diagnosis in minutes instead of days." Arboriculture & Urban Forestry **47**(3): 98-109.

Hamilton, J. L., J. N. Workman, C. J. Nairn, S. W. Fraedrich and C. Villari (2020). "Rapid detection of *Raffaelea lauricola* directly from host plant and beetle vector tissues using loop-mediated isothermal amplification." Plant Disease **104**(12): 3151-3158.

Hu, J., Y. Zhou, J. Geng, Y. Dai, H. Ren and K. Lamour (2019). "A new dollar spot disease of turfgrass caused by Clarireedia paspali." Mycological progress **18**: 1423-1435.

Kubota, R., A. Alvarez, W. Su and D. Jenkins (2011). "FRET-based assimilating probe for sequence-specific real-time monitoring of loop-mediated isothermal amplification (LAMP)." Biological Engineering Transactions **4**(2): 81-100.

Lucchi, N. W., A. Demas, J. Narayanan, D. Sumari, A. Kabanywanyi, S. P. Kachur, J. W. Barnwell and V. Udhayakumar (2010). "Real-time fluorescence loop mediated isothermal amplification for the diagnosis of malaria." PLoS ONE **5**(10): e13733.

Mori, Y., K. Nagamine, N. Tomita and T. Notomi (2001). "Detection of loop-mediated isothermal amplification reaction by turbidity derived from magnesium pyrophosphate formation." Biochemical and Biophysical Research Communications **289**(1): 150-154.

Nagamine, K., T. Hase and T. Notomi (2002). "Accelerated reaction by loop-mediated isothermal amplification using loop primers." Molecular & Cellular Proteomics **16**(3): 223-229.

Niessen, L. (2015). "Current state and future perspectives of loop-mediated isothermal amplification (LAMP)-based diagnosis of filamentous fungi and yeasts." Applied microbiology biotechnology **99**(2): 553-574.

Notomi, T., Y. Mori, N. Tomita and H. Kanda (2015). "Loop-mediated isothermal amplification (LAMP): principle, features, and future prospects." Journal of Microbiology **53**(1): 1-5.

Notomi, T., H. Okayama, H. Masubuchi, T. Yonekawa, K. Watanabe, N. Amino and T. Hase (2000). "Loop-mediated isothermal amplification of DNA." Nucleic Acids Research **28**(12): e63-e63.

Roux, K. H. (2009). "Optimization and troubleshooting in PCR." Cold Spring Harb Protoc **2009**(4): pdb.ip66.

Salgado-Salazar, C., L. A. Beirn, A. Ismaiel, M. J. Boehm, I. Carbone, A. I. Putman, L. P. Tredway, B. B. Clarke and J. A. Crouch (2018). "Clarireedia: A new fungal genus comprising four pathogenic species responsible for dollar spot disease of turfgrass." Fungal Biology **122**(8): 761-773.

Sapkota, S., K. E. Catching, P. L. Raymer, A. D. Martinez-Espinoza and B. Bahri (2021). "New approaches to an old problem: Dollar spot of turfgrass." Phytopathology®.

Si Ammour, M., G. J. Bilodeau, D. M. Tremblay, H. Van der Heyden, T. Yaseen, L. Varvaro and O. Carisse (2017). "Development of real-time isothermal amplification assays for on-site detection of *Phytophthora infestans* in potato leaves." Plant Disease **101**(7): 1269-1277.

Smiley, R., P. Dernoeden and B. Clarke (2005). Compendium of Turfgrass Diseases, APS Press.

Stackhouse, T., S. L. Boggess, D. Hadziabdic, R. N. Trigiano, M. D. Ginzel and W. E. Klingeman (2021). "Conventional gel electrophoresis and TaqMan probes enable rapid

confirmation of Thousand Cankers Disease from diagnostic samples." Plant Disease **105**(10): 3171-3180.

Stackhouse, T., A. D. Martinez-Espinoza and M. E. Ali (2020). "Turfgrass disease diagnosis: Past, present, and future." Plants **9**(11): 1544.

Stackhouse, T., S. Waliullah, A. D. Martinez-Espinoza, B. Bahri and E. Ali (2021). "Development of a co-dominant cleaved amplified polymorphic sequences assay for the rapid detection and differentiation of two pathogenic *Clarireedia* spp. associated with dollar spot in turfgrass." Agronomy **11**(8): 1489.

Stowell, L. and W. Gelernter (2001). "Diagnosis of turfgrass diseases." Annual Review of Phytopathology **39**(1): 135-155.

Zhang, H., Y. Dong, Y. Zhou, J. Hu, K. Lamour and Z. Yang (2022). "Clarireedia hainanense: a new species is associated with dollar spot of turfgrass in Hainan, China." Plant Disease **106**(3): 996-1002.

Table

Table 3.1: Primers and assimilating probe set for Clarireedia spp. LAMP assay designed in the calmodulin (CaM) gene.

Primer or Probe	Sequence (5'-3')
LAMP primer set	
F3	CCTTGAATATCATGCTGATGG
B3	TCTACAGCCCGAACCATC
FIP	ATTTTGGCCAAGGGATCGCAT*TTTT*GCTTCAAGGACAAATTACTAG C
BIP	CCTCAGAGTCTGAGCTTCAGG*TTTT*TCATACCCGGGAAGTCAAT
LF	ACGGTGCCCAGCTCCTT
Assimilating Probe[a]	
FAM, florescent strand	/FAM/ACGCTGAGGACCCGGATGCGAATGCGGATGCGGATGCCGAA TATGATCAACGAGGTTGACGC
Q, quench strand	TCGGCATCCGCATCCGCATTCGCATCCGGGTCCTCAGCGT /BHQ/

[a]Assimilating probe was designed as per Kubota et al. (2011). The underlined fragment acts as a loop primer backward (LB). FAM is 6-carboxyl-fluorescein, and BHQ is Black Hole Quencher.

Figures

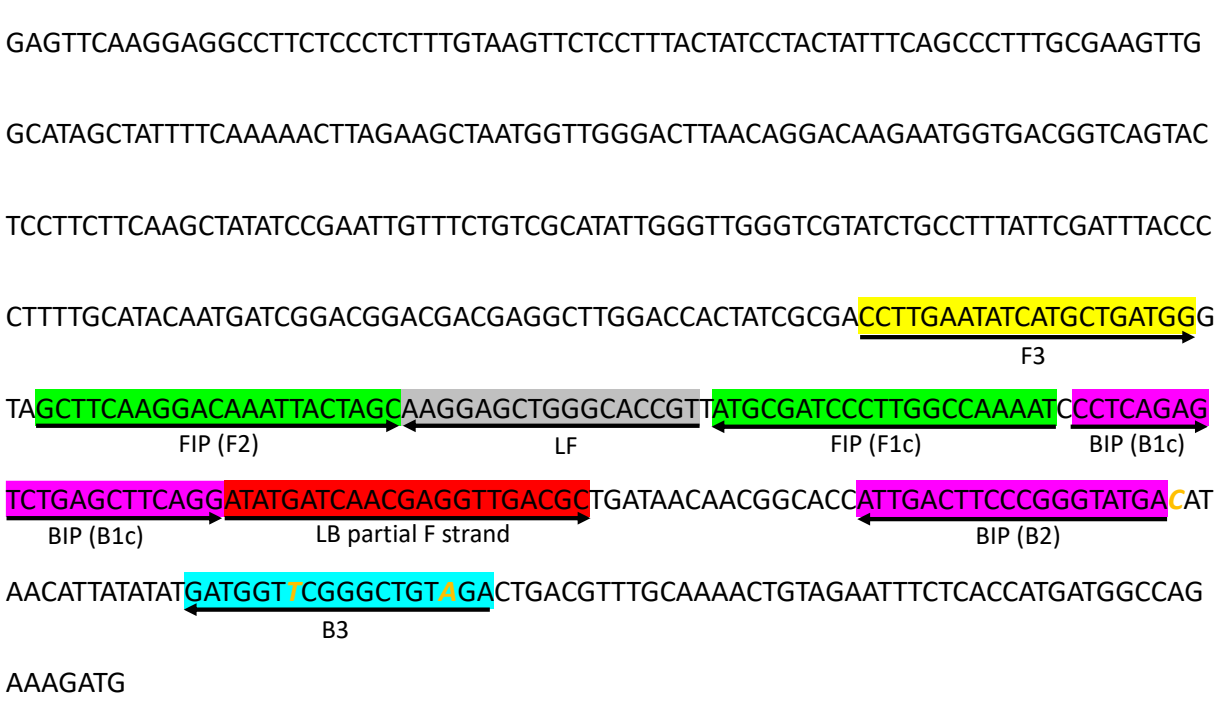

Figure 3.1: Location and sequences of loop-mediated isothermal amplification (LAMP) primer and probe sets targeting *Clarireedia jacksonii* and *C. monteithiana.* LAMP assay designed in the *calmodulin* (CaM) gene. Locations of the LB probe target, two outer (F3 and B3), inner (FIP [F1c-F2], and BIP [B1c-B2]), and looping primer (LF) are marked with colors. The FIP primer is comprised of the F1c and F2 sequences with 4 thymine nucleotides between them. Arrows indicate the extension direction. Polymorphic single nucleotide positions between *Clarireedia* species are noted in italics.

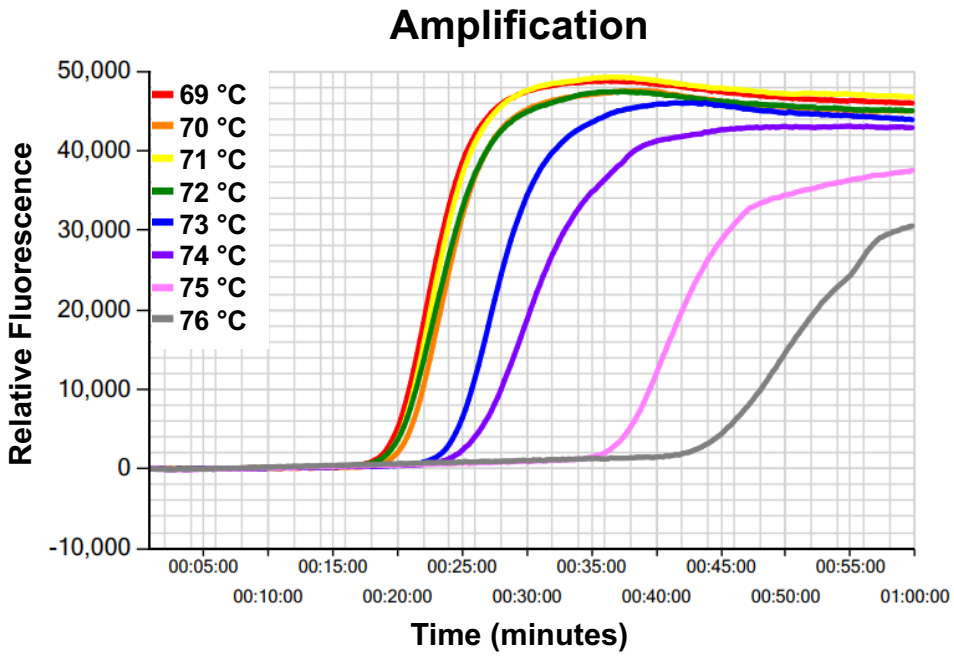

Figure 3.2: Temperature optimization with *Clarireedia jacksonii* DNA. Probe-based loop mediated amplification was performed from 69-76 °C for 60 min. All wells contained 5 ng μL^{-1} of *C. jacksonii* DNA of isolate DS3. Successful real-time amplification is denoted by the amplification curve using the Genie® III.

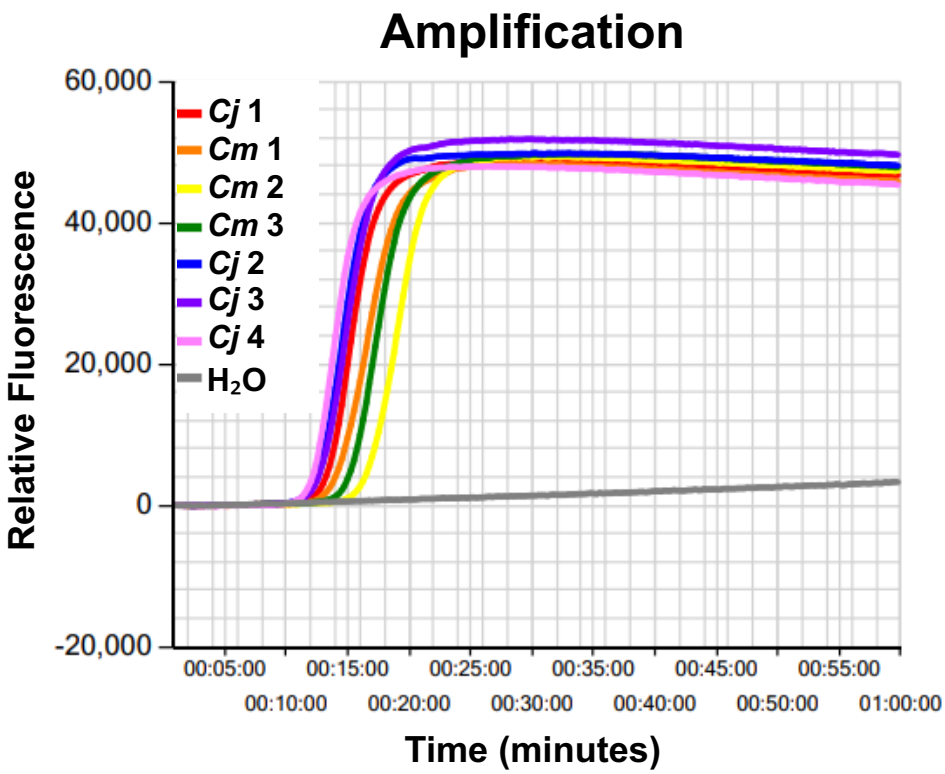

Figure 3.3: Primer/probe assay with seven *Clarireedia* spp. DNA samples. Probe-based loop-mediated amplification was performed for 60 min at 72 °C. Samples tested included one DNA sample of *Clarireedia jacksonii* (DS3, red), six DNA samples of *Clarireedia monteithiana* (DS180, orange; DS181, yellow; DS182, green; DS185, Blue; DS186, purple and DS188, pink), and H_2O negative control (gray). Successful real-time amplification is denoted by the amplification curve using the Genie® III.

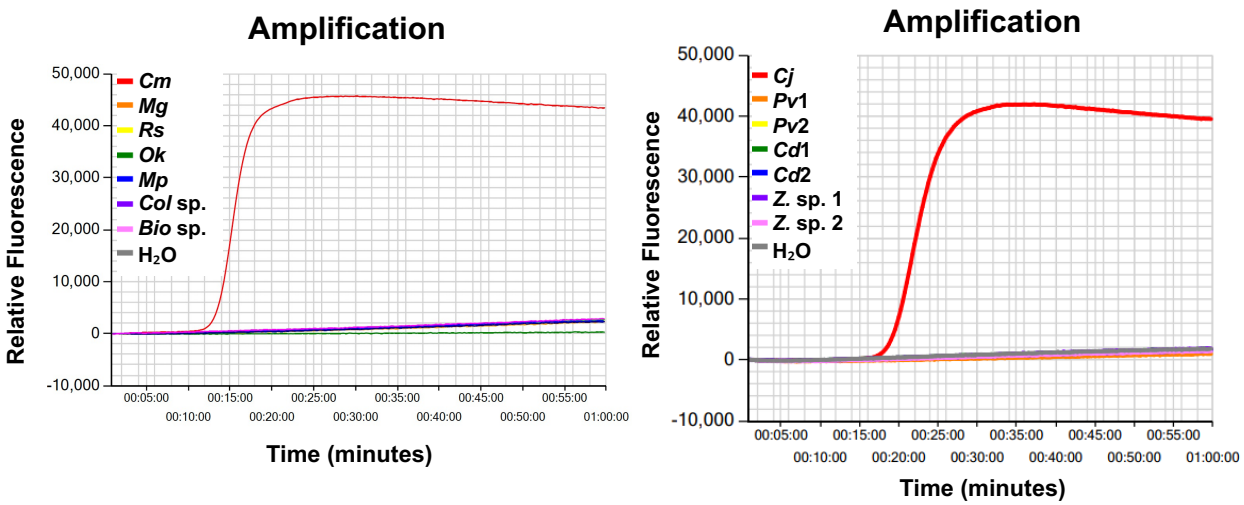

Figure 3.4: Primer/probe specificity assay with other plant pathogens and host DNA. Probe-based loop-mediated amplification was performed for 60 min at 72 °C. Successful real-time amplification is denoted by the amplification curve using the Genie® III. A) Samples included *Clarireedia monteithiana* (DS180, red), *Magnaporthe grisea* (Mg, orange), *Rhizoctonia solani* (Rs, yellow), *Ophiosphaerella korrae (*Ok*,* green), *Magnaporthe poae* (Mp*,* blue), *Colletotrichum* sp (Col, purple), *Bipolaris* sp. (Bip, pink), and H_2O negative control (gray). B) Samples included *Clarireedia jacksonii* (Ds3, red), *Paspalum vaginatum* 'sea isle supreme' (Pv1, orange), *Paspalum vaginatum* 'sea dwarf' (Pv2, yellow), *Cynodon dactylon* 'TifGrand' (Cd1, green), *Cynodon dactylon* 'TifDwarf' (Cd2, blue), *Zoysia japonica* 'Meyer' (Z1, purple), *Zoysia japonica* 'Empire' (*Z*2, pink), and H_2O negative control (gray).

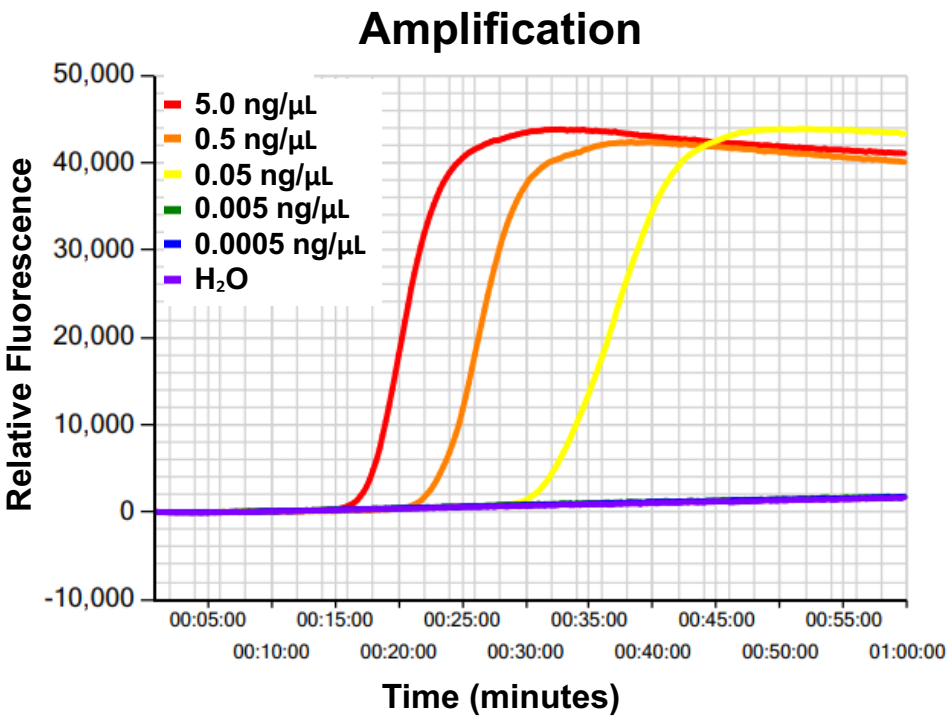

Figure 3.5: Primer/probe sensitivity assay with *Clarireedia jacksonii* DNA. Probe-based loop mediated amplification was performed for 60 min at 72 °C. Samples included DNA of *Clarireedia jacksonii* (DS3) at various concentrations; 5.0 ng/µL (red), 0.5 ng/µL (orange), 0.05 ng/µL (yellow), 0.005 ng/µL (green), 0.0005 ng/µL (blue), and H_2O negative control (purple). Successful real-time amplification is denoted by the amplification curve using the Genie® III.

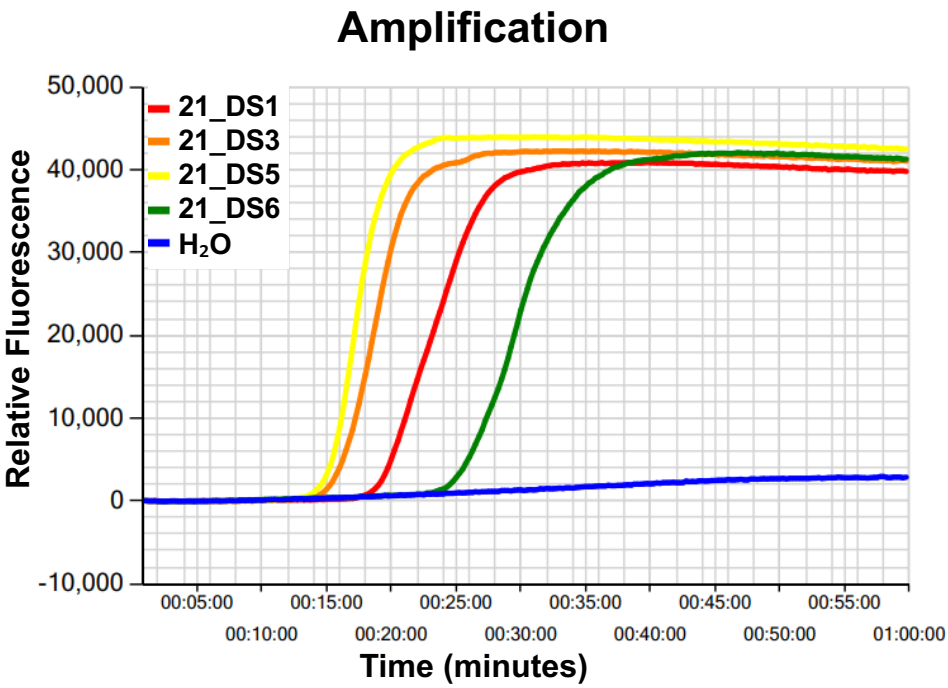

Figure 3.6: Primer/probe assay with four field samples suspected of *Clarireedia* spp. infection. Probe-based loop mediated amplification was performed for 60 min at 72 °C. Samples included four field samples (21_DS1, red; 21_DS3, orange; 21_DS5, yellow; 21_DS6, green) and H_2O negative control (blue). Successful real-time amplification is denoted by the amplification curve using the Genie® III. 21_DS1 and 21_DS3 were collected from seashore paspalum and zoysiagrass in August 2021 at UGA Griffin Griffin Campus, Spalding County, GA; 21_DS5 and 21_DS6 were collected from *Cynodon dactylon* 'TifSport' and *Cynodon dactylon* 'TifEagle' in August 2021 at UGA Tifton Campus, Tift county, GA.

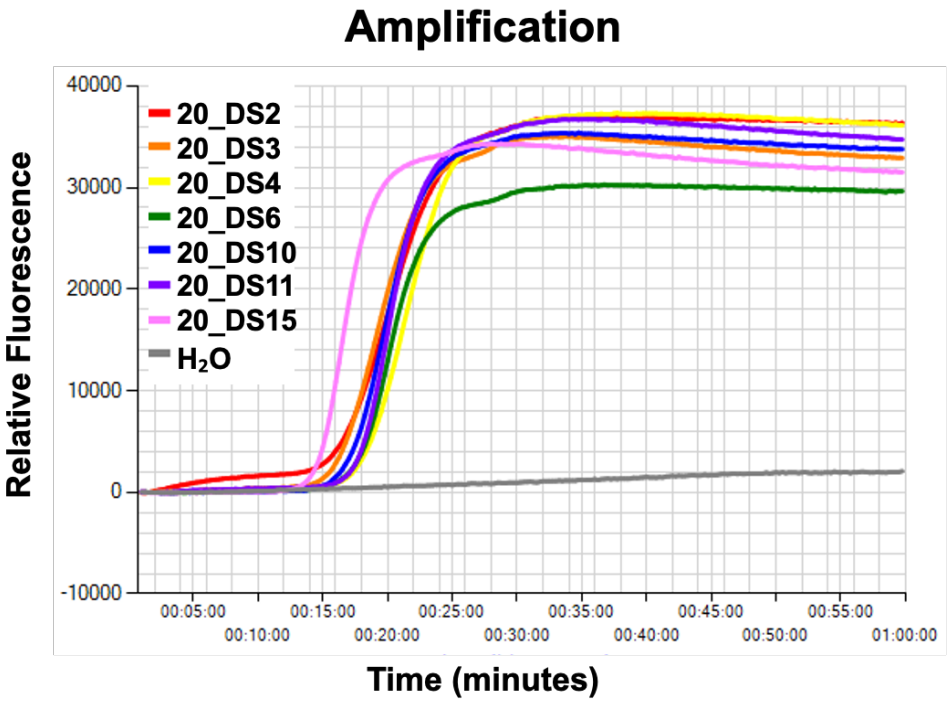

Figure 3.7: Primer/probe assay with quick extraction of *Clarireedia* spp. mycelia. Probe-based loop-mediated amplification was performed for 60 min at 72 °C. Samples included isolate DS3 (orange) of *C. jacksonii*, six isolates (DS180, red; DS181, yellow; DS183, green; DS186, blue; DS187, purple; DS188, pink) of *C. monteithiana*, and a H_2O negative control (gray). Successful real-time amplification is denoted by the amplification curve using the Genie® III.

The master mix is red like negative samples before the DNA is added and the samples incubated

The results are viewed by shining the blue light on the tubes and viewing the samples through the blue light filtering glasses

A closeup image of the results of a *Clarireedia jacksonii* sample (left) and a *Rhizoctonia soloni* sample (right)

Figure 3.8: Visualization of LAMP results via florescent flashlight for point-of-care utilization. Negative samples appear red, and the positive samples appear green. This step takes seconds after the incubation step.

CHAPTER 4

IMPOSTER SYNDROME: ELUCIDATING THE GENOMIC CONTRIBUTIONS OF PROTOPLAST FUSION PARTICIPANTS USED TO GENERATE THE COMMERCIAL BIOLOGICAL CONTROL FUNGUS, *TRICHODERMA AFROHARZIANUM* T22

Oleander, K.A., Olson, D.E., Brown, D.W., Satterlee, T.R., Martinez-Espinoza, A.D., and Gold, S.E. (2025) Imposter syndrome: Elucidating the genomic contributions of protoplast fusion participants used to generate the commercial biological control fungus, Trichoderma afroharzianum T22. In preparation for submission to Fungal Genetics.

Abstract

The fungal strain *Trichoderma* T22 has been used commercially as a biological control agent and biofertilizer to protect plants from five key fungal genera of root pathogens. T22 was initially patented (Chaverri et al. 2015) in 1990 as a protoplast fusion product of two auxotrophic mutants T12 and T95. The fusion participant strain of T12 was an effective biocontrol agent against plant pathogenic soil-borne fungi, while the fusion participant strain of T95 had elevated capacity to colonize the plant rhizosphere. The resulting fusion product, *Trichoderma* strain T22, has been used globally to control root pathogens and promote root health. Specific information on the genetic contributions of the participant or parent strains to the T22 genome were unavailable. Here, we performed whole genome comparisons of T12, T95 and T22 to determine the contributions of fusion participants T12 and T95 to T22. While we expected that T22 would have roughly evenly divided genomic contributions from the two fusion participant strains, we found few SNPs in T22 compared to T12 (38 total), whereas T22 had approximately $2x10^5$ SNPs when compared to T95. None of the 38 SNPs between T12 and T22 appear to have originated from T95. Structural variants were also explored within the genomes, but the structural variation results found no evidence that T95 contributed to T22. We conclude that T22 is essentially a mutant of T12, with only minor T95 contributions to the T22 genome. With T12 and T22 being nearly identical, the few SNPs present in the T22 genome compared to T12 may contribute to the reported enhanced rhizosphere colonization capacity of T22 over T12.

Introduction

Trichoderma species represent one of the most frequently isolated soil fungi, with 10^1-10^3 colony-forming units (CFU) per gram in most temperate and tropical soils (Abbas et al. 2022). The presence of the genus in soil is often considered an indicator of good soil health, with many strains

forming plant symbiotic relationships (Harman et al. 2004, Contreras-Cornejo et al. 2009, Lange 2014). *Trichoderma* was first characterized from soil and plant debris in 1794 (Persoon 1794). As of 2019, over 300 species of *Trichoderma* have been identified (Marik et al. 2019). Some species of *Trichoderma* do not have sexual phases, while others have the previously named teleomorph genus *Hypocreales* (Druzhinina and Kubicek 2005, Druzhinina et al. 2010). While some strains form plant symbiotic relationships, others thrive primarily as saprotrophs (Contreras-Cornejo et al. 2009).

Trichoderma species are frequently endophytic and will colonize in and around the roots of many host plants (Harman et al. 2004, Bailey and Melnick 2013). *Trichoderma* and the plant interact through physical contact or release of chemicals like volatile organic compounds (VOCs) and key plant metabolites, including phytoalexins and phytohormones (Contreras-Cornejo et al. 2009, Manganiello et al. 2018, Villalobos-Escobedo et al. 2020). Root colonization of *Trichoderma* spp. induce both local and systemic resistance that helps the plants defend against future pathogen attacks (Djonovic et al. 2006). *Trichoderma* spp. produce many degradative enzymes for mycoparasitism, including chitinases, proteases, and glucanases (Zimand et al. 1996, Harman et al. 2004). Many *Trichoderma* species are non-pathogenic opportunistic plant symbionts that can be used as low-cost, effective biocontrol and biofertilizer agents. They can lead to plant resistance to a range of plant pathogens, increase nutrient absorption, stress tolerance to salt, heat, and drought, and stimulate biosynthesis of various metabolites, including plant growth regulators, siderophores, and antibiotics (Kuć 2001, Van Wees et al. 2008, Fu et al. 2021).

While some species of fungi are relatively easy to modify through sexual crosses, this is not available in all *Trichoderma* species. An alternative method to improve those species is protoplast fusion. This method combines two strains or related species of fungi, and the resulting

products demonstrate recombination of the progenitor strains. *Trichoderma* strain T22 was reportedly generated from a protoplast fusion of two complementary auxotrophic mutant strains T12 and T95 (Stasz et al. 1988). Strain T12 was selected for its biocontrol efficacy while T95 was chosen for its rhizosphere competency (Stasz et al. 1988, Sivan and Harman 1991). The goal was to produce a protoplast fusion product with both traits. Auxotrophy in the fusion participant strains was meant to ensure that the resulting prototrophic fusion product recombined the genomes of the two starting strains. The selected progeny strain, T22, was a prototroph that outcompeted the parental strains in several key characteristics, including biocontrol efficacy, rhizosphere competency, and growth rate (Harman et al. 1993). T22 has been a commercial success worldwide and is a key ingredient in multiple products (i.e., RootShield) providing biological control and soil fertilization (Harman et al. 1993). RootShield is labeled for managing various fungi including *Pythium, Rhizoctonia, Fusarium, Thielaviopsis*, and *Cylindrocladium* as well as species of Oomycota and is recommended for use on many plants including corn, turf, and ornamentals. Prior to the current study, there was little genomic sequence information available for strains T95 and T12. In contrast, strain T22 was sequenced by the Joint Genome Institute (JGI) (https://mycocosm.jgi.doe.gov/mycocosm/home/releases?flt=t22).

This study aimed to understand the genetic qualities of T22 that make it an effective biocontrol strain by characterizing the genomic contributions of the fusion participant strains. Our strategy was to compare the genomic sequence of the parent strains T12 and T95 to its protoplast progeny strain T22, to determine the origin of T22's genes and possible their link to T22's favorable phenotypic and biological control traits.

Materials and Methods

Strain acquisition

Trichoderma strains T22 (ATCC 20847), T95 (ATCC 60850), and T12 (ATCC 20737) were obtained from the American Type Culture Collection (ATCC). The strains were grown at 25 °C on potato dextrose agar for 5 to 7 days prior to collection of mycelia.

Illumina sequencing

DNA was extracted from freshly collected mycelia with the ZR Fungal/Bacterial DNA MiniPrep kit (Zymo Research, Irvine, CA). DNA libraries were prepared with the Illumina Nextera XT DNA Library Preparation Kit (Illumina, San Diego, CA). Sequencing was performed with the MiSeq Reagent Kit Version 3 using the MiSeq sequencing platform (Illumina). Sequence reads were imported into the QIAGEN CLC Genomics Workbench (QIAGEN, Redwood City, CA) and screened against genome sequences of 84 bacterial species to remove reads generated from trace bacterial DNA. Adapters were removed, and low-quality reads were trimmed using default parameters.

Oxford nanopore sequencing and genome assembly

Long-read sequence reads of T12, T95 and T22 genomic DNA were generated using Nanopore technology by CD Genomics (Shirley, New York). The Nanopore and Illumina sequence data was processed using MaSuRCA (4.1.0) (Zimin et al. 2013) as a hybrid assembly using the default parameters. The resulting genomes were quality-checked using QUAST (5.2.0) and BUSCO (5.5.0) using the hypocreales_odb10 dataset. Draft genome sequences were generated using Canu (2.2) (Koren et al. 2017) with the default parameters. T12 and T22 Canu generated assemblies were subsequently polished essentially as described. First, minimap2 (v2.26) created

SAM files by aligning ONT reads to respective genome assemblies. The SAM files were then used as input for downstream polishing using Racon (v1.5.0)(Vaser et al. 2017), Medaka (v1.11.3) (Medaka 2018), and Pilon (v1.24) (Walker et al. 2014).

Fusion participant strain species identification

A species phylogeny for strains T12, T95, T22, and 36 other *Trichoderma* sequences for both TEF1 and ITS (Pfordt et. al., (2020) was inferred from the housekeeping genes *TEF1* and *ITS*. Of note, one of the other strains used in the phylogeny is also named T12 but differs from the strain T12 used to create T22. The evolutionary history of the 39 TEF1 and ITS sequences was inferred using the Maximum Likelihood (ML) method in MEGA 10.0.5 using default settings with 1000 bootstrap replications. Nucleotide sequences were aligned with ClustalW as implemented in MEGA. T22 was initially reported as *Trichoderma harzianum* but was later identified as *Trichoderma afroharzianum* (Harman et al. 1993, Chaverri et al. 2015). The identification of T12 and T95 was not publicly available to our knowledge prior to this work.

SNP and indel comparison

Burrows-Wheeler Aligner (BWA) (0.7.17) (Li 2013) was used to index the reference genome T12. T12 was chosen as the reference genome because it the assembled genome had the fewest number of contigs of the studied three strains. Next, the Illumina reads for T95 and T22 were mapped to the reference using default settings in SAMtools (v1.16.1) (Li et al. 2009, Danecek et al. 2021) for conversion and indexing. Variant data was generated using BCFtools, mpileup, and BCFtools call, and further filtered using BCFtools filter (QUAL<40 || DP<10) (Danecek et al. 2014, Danecek et al. 2021). Once low-quality variants were removed, two separate datasets were generated for biallelic SNPs and indels only. VCF files were then visualized and verified in Integrated Genome Viewer (IGV; v2.17.3) (Robinson et al. 2011).

Structural variation identification

Sniffles2 (2.0.7) (Smolka et al. 2024) was used to identify structural variations within the genomes by comparing the genome assembly to the raw Nanopore reads. This program can identify larger than indel (short insertion/deletion) differences between the genomes caused by additions or subtractions within genome recombination events that would not be apparent from the SNP/Indel data. Strain T22 (protoplast fusion product) was used as the reference genome for this step. Sniffles2 analysis was performed on all three genomes to compare where structural variation was present. BCFtools was used to filter out variant reads with <40 quality score and <3 Nanopore read coverage support. Minigraph-Cactus (2.6.7) was used with default settings on the T12 and T22 genomes to validate Sniffles2 results.

Genome annotation

The T12 and T22 genomes were annotated using the Funannotate pipeline (Palmer 2023). First, genomes were prepared for gene prediction using the clean, sort, and mask commands. The genome sequences were then used as input for 'funannotate predict' to generate gene models using various genome prediction model programs including Eggnog (5.0) (Huerta-Cepas et al. 2019). The Busco seed species used was "*Fusarium*," as that was the closest related genera available. Once gene models were generated, Interproscan and antiSMASH were run locally. Finally, InterProScan, anti-SMASH, and Funannotate predict results were input in 'Funannotate annotate' to create and compile genome annotations. Identified SNPs were then compared to genome annotations to determine the functional relevance of the SNPs. Using the default settings, 'Funannotate compare' was performed between T12 and T22 to compare the genome annotations.

Results

Sequencing and genome assembly

Illumina sequencing of T12 and T95 generated reads estimated to provide 20X and 26X coverage, respectively (Table 4.1). Illumina sequence data for T22 was downloaded from JGI (https://mycocosm.jgi.doe.gov/TriharT22_1/TriharT22_1.home.html) and estimated to provide 129X coverage. Nanopore sequencing of T12, T95 and T22 generated over 50X additional coverage for each genome.

Both MaSuRCA (4.1.0) and Canu were used for genome assembly. The genomes were drafted several times throughout the data acquisition timeframe, and each genome's best drafts were used for the subsequent analysis (Supplemental Table 4.1). The “Best” parameter was selected based on scaffold count, closeness to the expected genome size, QUAST, and BUSCO (Simão et al. 2015) scores. From our data, the Canu assemblies were the best-quality genome assemblies. Problems in the MaSuRCA runs included extremely high duplicate BUSCO scores and lower than expected genome size. The T95 assembly had, by far, the most scaffolds at 551, while the T12 and T22 assemblies had 17 and 9 scaffolds, respectively. The BUSCO scores for all three genome were around 97-98%, with 2.6% duplicates in the T95 assemble as compared to 0.3% in both T12 and T22 assemblies (Table 4.2). The three genomes also all had similar fragmented (0.6-0.8%) and missing (1.7-2.0%) Busco scores. This means they are comparable even though T12 and T22 are more complete, and T95 might have small duplication in the genome (Simão et al. 2015).

Phylogenetic analysis of TEF1 and ITS sequence from T12, T95, T22 and 36 select *Trichoderma* strains in MEGA10 revealed that strains T12, T95, T22 are likely *Trichoderma*

afroharzianum. All three strains were in well supported clades that included multiple *T. afroharzianum* strains (Figure 4.3).

SNP and Indel comparison

SNPs and indels were identified with Burrows-Wheeler Aligner (BWA) and extracted with BCFtools before visualization in IGV. Unexpectedly, only a handful of SNPs (38 total) were found between the T12 and T22 genomes (Table 4.3). In contrast, comparison of T12 and T95 identified over 197,900 SNPs scattered across the genome comparison. A closer examination of the indels found that most were in simple sequence repeat regions (SSRs) in single nucleotide repeat regions. Additionally, if the reference genome (T12 Canu genome) is run against itself (T12 Illumina reads), many of these "indels" exist throughout the reference genome, further supporting that these indels are inaccurate. Comparing the reference to itself should have few, if any, differences. These differences were downloaded and visualized using IGV (Figure 4.1).

Structural variation identification

Sniffles2 was used to identify larger DNA variations between the genomes. One variant was identical within all three genomes and was removed as a likely sequencing error (Supplemental Figure 4.1). Sniffles2 found many variations between T22 and T95 but none between T22 and T12 (Figure 4.2). Cactus also identified a handful of variations between the genomes. However, a comparison of the structural variant calls to the raw Nanopore reads in Geneious Prime with BLAST, suggested that these variations were sequencing errors rather than genuine DNA additions or deletions in genomic sequence.

Impact of SNPs on predicted gene function

The T12 and T22 genomes were annotated using the Funannotate gene prediction pipeline, and then the genomic differences between T12 and T22 from the SNP analysis were used assess

any impact on gene function. Of the 38 SNPs identified in T22 as compared to T12, 14 were intragenic. Seven were found in introns and may affect the transcript splicing, while the other seven are found in exons (Table 4.4). Two of the SNPs in exons are silent, while the other five would lead to missense mutations in any translated protein (Table 4.4). For these five genes, one predicted function relates to secondary metabolites biosynthesis, transport, and catabolism, two could function in chromatin structure, one function may involve post-translational modification, protein turnover, and chaperones, while the final gene function is unknown (Table 4.4 and Supplemental Table 4.3). SNPs located in intergenic regions can be viewed in Supplemental Table 4.2. Because of the significant number of SNPs identified between T12 and T95 (>197k), we did not assess their individual impact on gene function.

Discussion

Here we generated high quality genomic sequence data for *Trichoderma* strains T12 and T95 and *Trichoderma afroharzianum* strain T22 to ensure accurate and representative genomic comparisons (Table 4.1). All three genomes were assembled from the collected sequence reads with Canu-2.2 and MaSuRCA. Although MaSuRCA had been reported to produce higher quality genome assemblies than Canu-2.2, as measured by lower Scaffold numbers per genome and higher Busco Scores (Gorman et al. 2023, Mochizuki et al. 2023), we found that Canu-2-2 yielded better results for our fungal genomes.

The SNP analysis found an overwhelming difference in number of SNPs identified in the T12 to T22 genome comparison relative to the T12 to T95 comparison. Based on the identification of only 39 SNPs between T12 and T22, they are extremely similar. These few differences were not clustered and thus were most likely accumulated during serial transfers of T22 on lab growth media, which is consistent with typical mutation rates seen in fungi (Le Crom et al. 2009).

The genome of T95 appears to not have contributed significantly to the genome of T22. The very minimal to no homology observed to T95 near the SNPs in T22 support out hypothesis that T22 is not the product a fusion of T12 and T95 but rather T12 serially transferred for a few generations on media.

Indels were also examined, but the indels identified were almost exclusively in simple sequence repeat regions (SSRs), with most identified as single or double nucleotide repeats. These are likely sequencing errors, and even if not, high repeat regions are unlikely to be found within intragenic areas. Those repeats are unlikely to account for the difference in phenotype. These errors are not entirely surprising, considering that BWA analysis uses Illumina data to compare to the complete genomes. Illumina is a "sequencing by synthesis" based sequencing technology and struggles with repeat regions (Fuller et al. 2009). These errors are supported by calls of "indels" throughout the reference genome if the genome is compared to its Illumina reads (data not shown). Even if some of these indels are present, given that they are primarily single nucleotide repeats, they are unlikely to be in coding regions and effect phenotype. Because of this, the indels were not used in further analysis. Sniffles2 was used to identify structural variations and protoplast fusion is expected to have some structural variation in the protoplast progeny. Still, we did not see this in our data comparing T12 and T22. This means the key differences found between the two genomes were the SNPs.

Fusion participant strains T12 and T22 were identified as the same species, *Trichoderma afroharzianum*. This was checked because T22 had been reclassified, and protoplast fusion can combine two species of the same genera (Harman et al. 1993, Hassan 2014). This data can inform what traits are found within *Trichoderma afroharzianum.* Additionally, this research makes the genomes of two more strains available for further study after the genomes are submitted to

Genbank. As mentioned previously, T22 is still sold under the trade name “RootShield” and is labeled as *Trichoderma harzianum* despite being identified as *Trichoderma afroharzianum* (Chaverri et al. 2015). Retaining the old nomenclature in the product packaging material is likely for marketing purposes, a practice previously noted for other biologically derived products (Yeung et al. 2002, Marrone 2007).

The T12 and T22 genomes were annotated using the Funannotate pipeline to assist in identifying how genomic differences might be responsible for their phenotype differences. This process determined whether the 38 SNPs between the two strains were in genes and if a mutation effect was expected. Of the 38 SNPs, five hold the highest potential to affect phenotype as they are missense mutations that may change gene function. These genes could be further studied for the phenotypic difference between T12 and T22. Again, having so few differences is unusual, as there is expected to be 10^{-9} substitutions per base per generation plus whatever genome reshuffling the protoplast fusion would have likely made (Le Crom et al. 2009).

Our data support the hypothesis that strain T22 is entirely derived from T12 rather than a protoplast fusion of T12 and T95. There are a few mutations, much less than expected, that make the genomes different from one another. Initially, both T95 and T12 were UV mutagenized into auxotrophs for the fusion experiments (Harman et al. 1993). These auxotrophic markers are absent in the genomes analyzed here, as the mutagenesis was performed after the strains were deposited in AATC. While the T12 used in the fusion was an auxotroph, that auxotrophy was lost in T22 after the fusion treatment. This could have been a reversion event. There is no evidence that the auxotrophy was resolved by homologous recombination from T95. It is possible that T95 and T12 fused, and the fusion resolved, with almost no T95 incorporation into the genome. We hypothesize that the fusion performed in polyethylene glycol (PEG) solution could have allowed T12 to pick

up any free-floating DNA within the solution, allowing for small fragments to be incorporated into T22, but no such T95 fragments were found either (Lichius et al. 2020). It is extremely unlikely that T95 contributed to the phenotype of T22, and instead, it is likely differences caused by naturally occurring SNPs. There could be other genotypic architecture we cannot see in the current nanopore, and Illumina reads, such as methylations that affect gene regulation (Liu et al. 2021, Li et al. 2023). Testing for the presence of methylations would require new nanopore sequencing with different settings and a new flow cell, which is beyond this project's scope. Additionally, more information could be obtained about these genomes with transcriptomics, which is beyond this project's scope.

Conclusions

Our comparison of the genome sequence of strains T12 and T95 to strain T22 indicate that T22 is essentially the same as T12 and not a fusion product of the T12 and T95 genomes. We found no sequence in T22 originated from T95. The phenotypes associated with T22 success as a biocontrol are likely due to either the few genetic differences identified here between T12 and T22 or epigenetic changes brought on by protoplasting of the T12 derived auxotrophic strain prior to isolation of T22. Moving forward, one could study the genes with point mutations to better understand the phenotypic differences between T12 and T22.

Funding

This project was funded by U.S. Department of Agriculture, Agricultural Research Service and the University of Georgia Plant Pathology Department scholarship to KO. USDA is an equal opportunity provider and employer. Mention of trade names or commercial products in this publication is solely for the purpose of providing specific information and does not imply recommendation or endorsement by the U.S. Department of Agriculture.

Author Contributions

KAO – Conceptualization, data curation, formal analysis, investigation, methodology, validation, visualization, original draft preparation, review, and editing. DEO – Data curation, formal analysis, review, and editing. DWB – Investigation, review, and editing. TRS – Methodology, validation, review, and editing. ADME – Supervision, review, and editing. SEG – Conceptualization, funding acquisition, methodology, project administration, resources, supervision, review, and editing.

References

Abbas, A., M. Mubeen, H. Zheng, M. A. Sohail, Q. Shakeel, M. K. Solanki, Y. Iftikhar, S. Sharma, B. K. Kashyap, S. Hussain, M. Del Carmen Zuñiga Romano, E. A. Moya-Elizondo and L. Zhou (2022). "*Trichoderma* spp. genes involved in the biocontrol activity against *Rhizoctonia solani*." Front Microbiol **13**: 884469.

Bailey, B. A. and R. L. Melnick (2013). The endophytic *Trichoderma*. *Trichoderma*: Biology and applications, CABI Wallingford UK**:** 152-172.

Chaverri, P., F. Branco-Rocha, W. Jaklitsch, R. Gazis, T. Degenkolb and G. J. Samuels (2015). "Systematics of the *Trichoderma harzianum* species complex and the re-identification of commercial biocontrol strains." Mycologia **107**(3): 558-590.

Contreras-Cornejo, H. A., L. Macías-Rodríguez, C. Cortés-Penagos and J. López-Bucio (2009). "*Trichoderma virens*, a plant beneficial fungus, enhances biomass production and promotes lateral root growth through an auxin-dependent mechanism in *Arabidopsis*." Plant Physiol **149**(3): 1579-1592.

Danecek, P., J. K. Bonfield, J. Liddle, J. Marshall, V. Ohan, M. O. Pollard, A. Whitwham, T. Keane, S. A. McCarthy, R. M. Davies and H. Li (2021). "Twelve years of SAMtools and BCFtools." Gigascience **10**(2).

Danecek, P., S. Schiffels and R. Durbin (2014). Multiallelic calling model in bcftools (-m), June.

Djonovic, S., C. Howell and C. Kenerley (2006). "Sm1, a proteinaceous elicitor secreted by the biocontrol fungus *Trichoderma virens* induces plant defense responses and systemic resistance." Mol Plant Microbe Interact **19**: 838-853.

Druzhinina, I. and C. P. Kubicek (2005). "Species concepts and biodiversity in *Trichoderma* and *Hypocrea:* From aggregate species to species clusters?" J Zhejiang Univ Sci B **6**(2): 100-112.

Druzhinina, I. S., C. P. Kubicek, M. Komoń-Zelazowska, T. B. Mulaw and J. Bissett (2010). "The *Trichoderma harzianum* demon: Complex speciation history resulting in coexistence of hypothetical biological species, recent agamospecies and numerous relict lineages." BMC Evol Biol **10**(1): 1-14.

Fu, J., Y. Xiao, Y. F. Wang, Z. H. Liu, Y. F. Zhang and K. J. Yang (2021). "*Trichoderma asperellum* alters fungal community composition in saline–alkaline soil maize rhizospheres." Soil Sci Soc Am J **85**(4): 1091-1104.

Fuller, C. W., L. R. Middendorf, S. A. Benner, G. M. Church, T. Harris, X. Huang, S. B. Jovanovich, J. R. Nelson, J. A. Schloss and D. C. Schwartz (2009). "The challenges of sequencing by synthesis." Nat Biotechnol **27**(11): 1013-1023.

Gorman, Z., J. Chen, A. A. P. de Leon and C. M. Wallis (2023). "Comparison of assembly platforms for the assembly of the nuclear genome of *Trichoderma harzianum* strain PAR3." BMC genet **24**(1): 454.

Harman, G. E., C. R. Howell, A. Viterbo, I. Chet and M. Lorito (2004). "*Trichoderma* species—opportunistic, avirulent plant symbionts." Nature Rev Microbiol **2**(1): 43-56.

Harman, G. E., T. E. Stasz and N. F. Weeden (1993). Fused biocontrol agents. United States, Cornell Research Foundation Inc. **US5260213A**.

Hassan, M. M. (2014). "Influence of protoplast fusion between two *Trichoderma* spp. on extracellular enzymes production and antagonistic activity." Biotechnol Biotechnol Equip **28**(6): 1014-1023.

Huerta-Cepas, J., D. Szklarczyk, D. Heller, A. Hernández-Plaza, S. K. Forslund, H. Cook, D. R. Mende, I. Letunic, T. Rattei and L. J. Jensen (2019). "eggNOG 5.0: a hierarchical, functionally and phylogenetically annotated orthology resource based on 5090 organisms and 2502 viruses." Nucleic acids research **47**(D1): D309-D314.

Koren, S., B. P. Walenz, K. Berlin, J. R. Miller, N. H. Bergman and A. M. Phillippy (2017). "Canu: Scalable and accurate long-read assembly via adaptive k-mer weighting and repeat separation." Genome Res **27**(5): 722-736.

Kuć, J. (2001). "Concepts and direction of induced systemic resistance in plants and its application." Eur J Plant Pathol **107**: 7-12.

Lange, L. (2014). "The importance of fungi and mycology for addressing major global challenges." IMA Fungus **5**(2): 463-471.

Le Crom, S., W. Schackwitz, L. Pennacchio, J. K. Magnuson, D. E. Culley, J. R. Collett, J. Martin, I. S. Druzhinina, H. Mathis, F. Monot, B. Seiboth, B. Cherry, M. Rey, R. Berka, C. P. Kubicek, S. E. Baker and A. Margeot (2009). "Tracking the roots of cellulase hyperproduction by the fungus *Trichoderma* reesei using massively parallel DNA sequencing." Proc Natl Acad Sci U S A **106**(38): 16151-16156.

Li, H. (2013). "Aligning sequence reads, clone sequences and assembly contigs with BWA-MEM." arXiv preprint arXiv:1303.3997.

Li, H., B. Handsaker, A. Wysoker, T. Fennell, J. Ruan, N. Homer, G. Marth, G. Abecasis and R. Durbin (2009). "The sequence alignment/map format and SAMtools." Bioinform **25**(16): 2078-2079.

Li, Y.-H., J.-C. Chang, M.-R. Yen, Y.-F. Huang, T.-H. Chen, L.-H. Chen and Y.-S. Nai (2023). "Whole-genome DNA methylome analysis of different developmental stages of the entomopathogenic fungus *Beauveria bassiana* NCHU-157 by nanopore sequencing." Front Genet **14**: 1085631.

Lichius, A., D. M. Ruiz and S. Zeilinger (2020). Genetic transformation of filamentous fungi: Achievements and challenges. Grand Challenges in Fungal Biotechnology. H. Nevalainen. Cham, Springer International Publishing**:** 123-164.

Liu, Y., W. Rosikiewicz, Z. Pan, N. Jillette, P. Wang, A. Taghbalout, J. Foox, C. Mason, M. Carroll, A. Cheng and S. Li (2021). "DNA methylation-calling tools for Oxford Nanopore sequencing: A survey and human epigenome-wide evaluation." Genome Biol **22**(1): 295.

Manganiello, G., A. Sacco, M. R. Ercolano, F. Vinale, S. Lanzuise, A. Pascale, M. Napolitano, N. Lombardi, M. Lorito and S. L. Woo (2018). "Modulation of tomato response to *Rhizoctonia solani* by *Trichoderma harzianum* and its secondary metabolite harzianic acid." Front Microbiol **9**: 1966.

Marik, T., C. Tyagi, D. Balázs, P. Urbán, Á. Szepesi, L. Bakacsy, G. Endre, D. Rakk, A. Szekeres and M. A. Andersson (2019). "Structural diversity and bioactivities of peptaibol compounds from the *Longibrachiatum* clade of the filamentous fungal genus *Trichoderma*." Front Microbiol **10**: 1434.

Marrone, P. G. (2007). "Barriers to adoption of biological control agents and biological pesticides." CABI Reviews(2007): 12 pp.

Medaka, O. (2018). "Sequence correction provided by ONT research." Github. Available from: https://github. com/nanoporetech/medaka.

Mochizuki, T., M. Sakamoto, Y. Tanizawa, T. Nakayama, G. Tanifuji, R. Kamikawa and Y. Nakamura (2023). "A practical assembly guideline for genomes with various levels of heterozygosity." Brief Bioinform **24**(6): bbad337.

Palmer, J. M., & Stajich, J. E. (2023). Funannotate.

Persoon, C. H. (1794). "Disposita methodical fungorum." Romers Neues Mag Bot **1**: 81-128.

Pfordt, A., S. Schiwek, P. Karlovsky and A. von Tiedemann (2020). "*Trichoderma Afroharzianum* ear rot–a new disease on maize in Europe." Front Agron **2**.

Robinson, J. T., H. Thorvaldsdóttir, W. Winckler, M. Guttman, E. S. Lander, G. Getz and J. P. Mesirov (2011). "Integrative genomics viewer." Nature Biotechnol **29**(1): 24-26.

Simão, F. A., R. M. Waterhouse, P. Ioannidis, E. V. Kriventseva and E. M. Zdobnov (2015). "BUSCO: Assessing genome assembly and annotation completeness with single-copy orthologs." Bioinform **31**(19): 3210-3212.

Sivan, A. and G. Harman (1991). "Improved rhizosphere competence in a protoplast fusion progeny of *Trichoderma harzianum*." Microbiol **137**(1): 23-29.

Smolka, M., L. F. Paulin, C. M. Grochowski, D. W. Horner, M. Mahmoud, S. Behera, E. Kalef-Ezra, M. Gandhi, K. Hong, D. Pehlivan, S. W. Scholz, C. M. B. Carvalho, C. Proukakis and F. J. Sedlazeck (2024). "Detection of mosaic and population-level structural variants with Sniffles2." Nature Biotechnol.

Stasz, T., G. Harman and N. Weeden (1988). "Protoplast preparation and fusion in two biocontrol strains of *Trichoderma harzianum*." Mycologia **80**(2): 141-150.

Van Wees, S. C., S. Van der Ent and C. M. Pieterse (2008). "Plant immune responses triggered by beneficial microbes." Curr Opin Plant Biol **11**(4): 443-448.

Vaser, R., I. Sović, N. Nagarajan and M. Šikić (2017). "Fast and accurate de novo genome assembly from long uncorrected reads." Genome Res **27**(5): 737-746.

Villalobos-Escobedo, J. M., S. Esparza-Reynoso, R. Pelagio-Flores, F. López-Ramírez, L. F. Ruiz-Herrera, J. López-Bucio and A. Herrera-Estrella (2020). "The fungal NADPH oxidase is an essential element for the molecular dialog between *Trichoderma* and *Arabidopsis*." Plant J **103**(6): 2178-2192.

Walker, B. J., T. Abeel, T. Shea, M. Priest, A. Abouelliel, S. Sakthikumar, C. A. Cuomo, Q. Zeng, J. Wortman, S. K. Young and A. M. Earl (2014). "Pilon: an integrated tool for comprehensive microbial variant detection and genome assembly improvement." PLOS ONE **9**(11): e112963.

Yeung, P., M. Sanders, C. L. Kitts, R. Cano and P. S. Tong (2002). "Species-specific identification of commercial probiotic strains." J Dairy Sci **85**(5): 1039-1051.

Zimand, G., Y. Elad and I. Chet (1996). "Effect of *Trichoderma harzianum* on *Botrytis cinerea* pathogenicity." Phytopathol **86**(11): 1255-1260.

Zimin, A. V., G. Marçais, D. Puiu, M. Roberts, S. L. Salzberg and J. A. Yorke (2013). "The MaSuRCA genome assembler." Bioinform **29**(21): 2669-2677.

Tables

Table 4.1: Sequencing coverage.

Strain	Illumina coverage	Nanopore coverage
T22	**129X***	**53X**
T12	**20X**	**54X**
T95	**26X**	**53X**

*T22 Illumina sequence is downloaded from JGI.

Table 4.2: Genome summaries of genomes after Canu assembly.

Genome	Program used	Size	Scaffold #	Busco Score
T22	Canu-2.2	40.74	17	C:97.5%[S:97.2%,D:0.3%],F:0.6%,M:1.9%,n:4494
T12	Canu-2.2	40.63	9	C:97.2%[S:96.9%,D:0.3%],F:0.8%,M:2.0%,n:4494
T95	Canu-2.2	44.86	551	C:97.7%[S:95.1%,D:2.6%],F:0.6%,M:1.7%,n:4494

Table 4.3: Total SNP counts in each genome compared to T12.

Strain Name	SNPs
T12	21
T95	197992
T22	39

Table 4.4: Intragenic SNPs found between T22 and T12. Impact of SNP differences between T12 and T22 on predicted genes and the Eggnog mapper information available for each gene.

Scaffold	Scaffold Location	T22	T12	Location	If in exon, effect and AA variant group	Eggnog-mapper Function
scaffold_1	2979489	G	A	Intron	-	Function unknown - G-beta repeat protein
scaffold_1	4058532	G	A	Exon	Ser>Leu Polar uncharged to nonpolar aliphatic	Secondary metabolites biosynthesis, transport, and catabolism P-loop containing nucleoside triphosphate hydrolase protein
scaffold_1	4132688	T	G	Intron	-	Function unknown - methyltransferase
scaffold_2	552573	A	T	Exon	His>Gln Positively charged to polar uncharged	Chromatin structure and dynamics SET (Su(var)3-9, Enhancer-of-zeste, Trithorax) domain
scaffold_2	3916753	A	G	Exon	Phe>Lue Nonpolar, aromatic to nonpolar aliphatic	Function unknown - JmjC domain protein
scaffold_2	4799024	C	A	Intron	-	Function unknown fg-gap repeat domain-containing protein
scaffold_2	6011698	T	C	Intron	-	Amino acid transport and metabolism Belongs to the D-isomer specific 2-hydroxyacid dehydrogenase family
scaffold_3	1573997	T	C	Intron	-	Function unknown - Ankyrin repeat protein
scaffold_5	2721804	C	T	Exon	Pro>Ser Both polar uncharged	Post-translational modification, protein turnover, and chaperones pentatricopeptide repeat domain-containing protein
scaffold_5	2919565	T	A	Intron	-	Nucleotide transport and metabolism GMP synthase
scaffold_6	4182443	C	T	Exon	Silent mutation	Function unknown
scaffold_7	2628075	A	C	Exon	Asn>Thr Both polar uncharged	Function unknown
scaffold_7	2944585	A	G	Intron	-	Transcription - Component of the velvet transcription factor complex that controls sexual asexual developmental ratio in response to light, promoting sexual development in the darkness while stimulating asexual sporulation under illumination
scaffold_7	3827993	G	A	Exon	Silent mutation	Function unknown - domain-containing protein

Figures

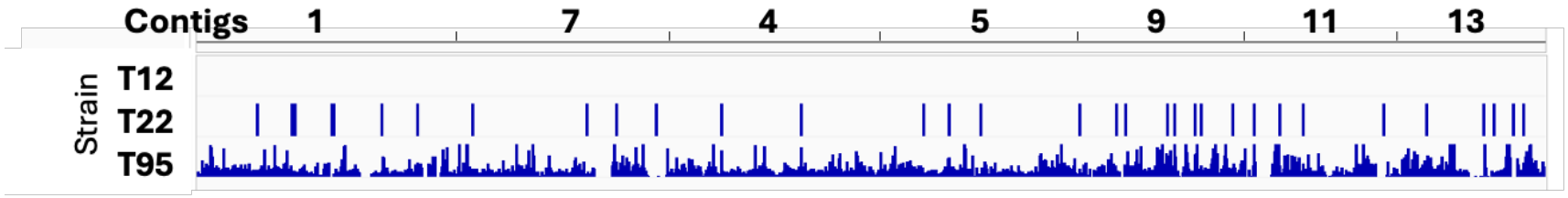

Figure 4.1: Whole genome visualization of SNPs using IGV after polishing the reference genomes. The order in this figure is T12 (top), T22 (middle), and T95 (bottom). The blue lines denote where an SNP is present when comparing that genome with T12.

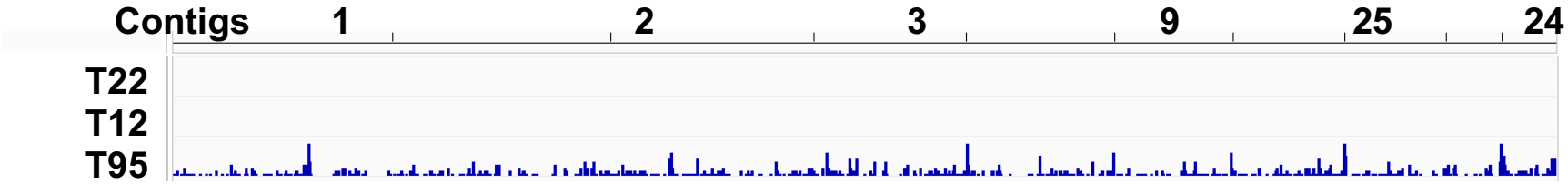

Figure 4.2: Whole genome visualization of structural variations visualized using IGV. The order in this figure is T22 (top), T12 (middle), and T95 (bottom). The blue lines denote where a structural variation is present when comparing that genome with T22.

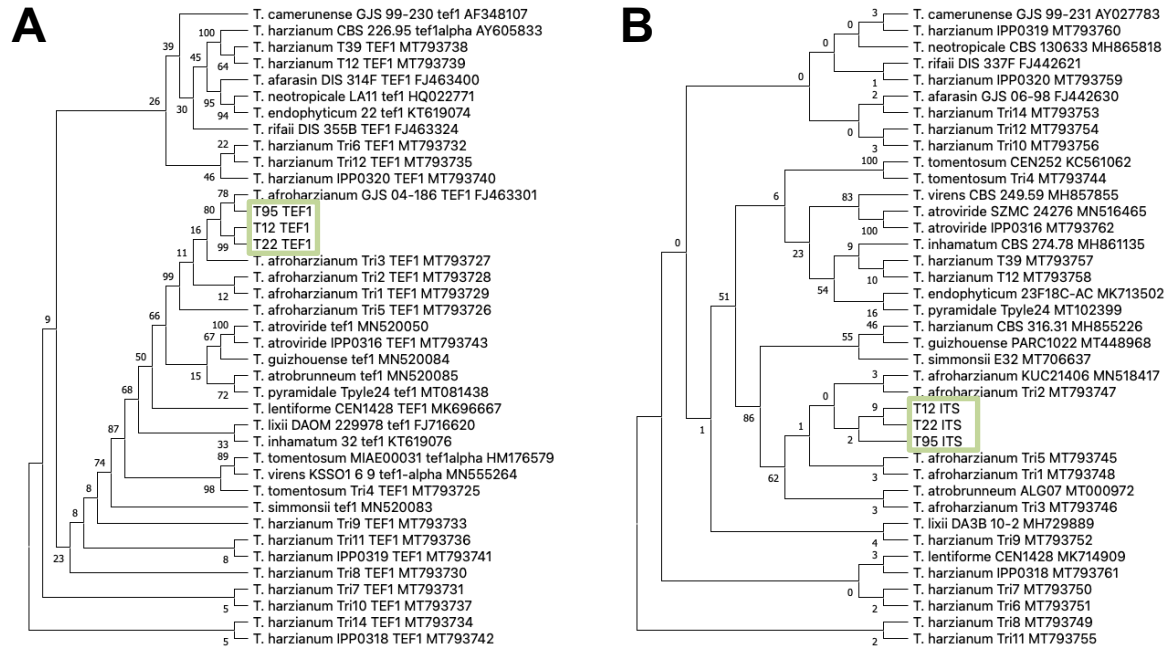

Figure 4.3: Phylogenic analysis of TEF1 (A) and ITS (B) using the Maximum Likelihood method as implemented in MEGA 10. Strains T12, T95 and T22 all group with *Trichoderma afroharzianum* with high bootstrap support.

Supplemental Figures and Tables

Supplemental Table 4.1: Busco scores, scaffold count, and size of this project's main genome assembly runs.

Genome	Program used	Data used for process	Size	Scaffold #	BUSCO Score
T22	Velvet*	JGI_Illumina	40.38	478*	C:97.4% [S:97.1%, D:0.3%], F:0.6%, M:2.0%, n:4494
T22	MaSuRCA-4.1.0	JGI_Illumina	40.45	285	C:97.5% [S:97.1%, D:0.4%], F:0.6%, M:1.9%, n:4494
T12	MaSuRCA-4.1.0	Peoria_Illumina	32.43	3463	C:57.3% [S:56.9%, D:0.4%], F:7.3%, M:35.4%, n:4494
T95	MaSuRCA-4.1.0	Peoria_Illumina	37.48	5898	C:56.9% [S:56.1%, D:0.8%], F:11.3%, M:31.8%, n:4494
T22	MaSuRCA-4.1.0	JGI_Illumina+Nanopore1	40.21	58	C:98.2% [S:12.0%, D:86.2%], F:0.6%, M:1.2%, n:4494
T12	MaSuRCA-4.1.0	Peoria_Illumina+Nanopore1	38.51	72	C:98.8% [S:8.9%, D:89.9%], F:0.3%, M:0.9%, n:4494
T95	MaSuRCA-4.1.0	Peoria_Illumina+Nanopore1	41.45	161	C:97.6% [S:12.8%, D:84.8%], F:1.3%, M:1.1%, n:4494
T22	MaSuRCA-4.1.0	JGI_Illumina+Nanopore1+Nanopore2	37.2	77	C:93.2% [S:92.3%, D:0.9%], F:1.4%, M:5.4%, n:4494
T12	MaSuRCA-4.1.0	Peoria_Illumina+Nanopore1+Nanopore2	37.2	104	C:88.8% [S:88.1%, D:0.7%], F:1.9%, M:9.3%, n:4494
T95	MaSuRCA-4.1.0	Peoria_Illumina+Nanopore1	40.9	192	C:95.6% [S:94.9%, D:0.7%], F:0.9%, M:3.5%, n:4494
T22	Canu-2.2	Nanopore1+Nanopore2	40.74	17	C:97.5% [S:97.2%, D:0.3%], F:0.6%, M:1.9%, n:4494
T12	Canu-2.2	Nanopore1+Nanopore2	40.63	9	C:97.2% [S:96.9%, D:0.3%], F:0.8%, M:2.0%, n:4494
T95	Canu-2.2	Nanopore1	44.86	551	C:97.7% [S:95.1%, D:2.6%], F:0.6%, M:1.7%, n:4494

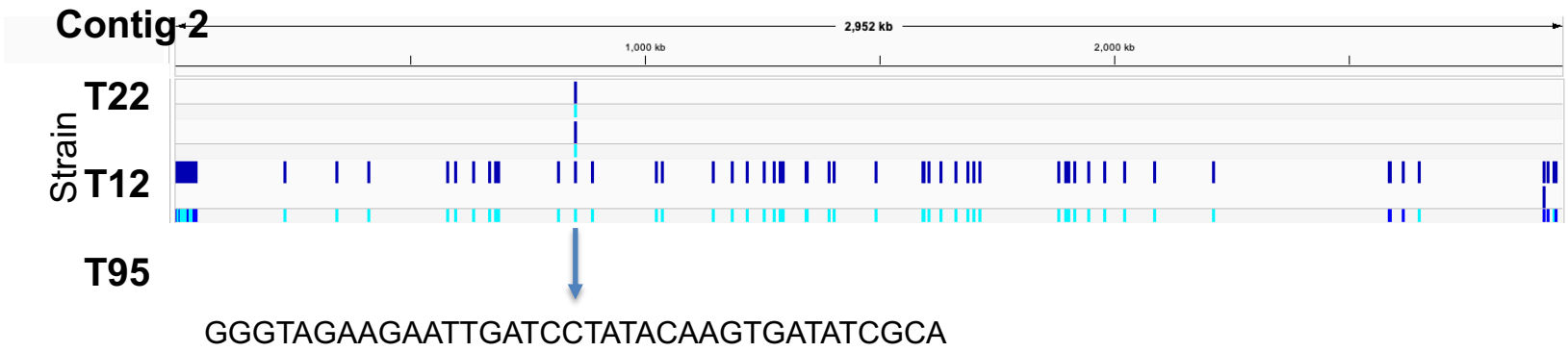

Supplemental Figure 4.1: Structural variant was removed as an error because it is present in all three genomes.

Supplemental Table 4.2: SNPs in intergenic regions between T22 and T12.

Scaffold #	Scaffold Location	T22	T12	Location
scaffold_1	1840890	C	T	Intergenic
scaffold_1	2875497	C	T	Intergenic
scaffold_1	5560711	C	T	Intergenic
scaffold_1	6628143	A	G	Intergenic
scaffold_3	3955840	C	T	Intergenic
scaffold_4	1346719	C	T	Intergenic
scaffold_4	2096788	A	T	Intergenic
scaffold_4	3052297	T	C	Intergenic
scaffold_5	94351	A	G	Intergenic
scaffold_5	1195880	T	C	Intergenic
scaffold_5	1467630	T	A	Intergenic
scaffold_5	3548353	C	T	Intergenic
scaffold_5	3746979	A	C	Intergenic
scaffold_5	4643962	C	T	Intergenic
scaffold_6	301566	C	T	Intergenic
scaffold_6	310697	G	A	Intergenic
scaffold_6	310701	G	A	Intergenic
scaffold_6	310710	A	G	Intergenic
scaffold_6	323654	T	C	Intergenic
scaffold_6	328752	G	A	Intergenic
scaffold_6	330861	T	C	Intergenic
scaffold_6	1095952	T	C	Intergenic
scaffold_6	1769282	C	G	Intergenic
scaffold_7	928159	T	A	Intergenic
scaffold_7	3512680	A	G	Intergenic

Supplemental Table 4.3: Intragenic SNPs found between T22 and T12. Impact of SNP differences between T12 and T22 on predicted genes and the funnannotate information available for each gene.

Scaffold #	Scaffold Location	T22	T12	Location	Funannotate information
scaffold_1	2979489	G	A	Intron	**ID:** FUN_000863-T1 **product:** hypothetical protein **note:** COG:S **EggNog:** ENOG503P0H7
scaffold_1	4058532	G	A	Exon	**ID:** FUN_001157-T1 **product:** hypothetical protein **Dbxref:** PFAM:PF00005, InterPro:IPR003593, InterPro:IPR027417, InterPro:IPR017871, InterPro:IPR011527, InterPro:IPR036640, PFAM:PF00664, InterPro:IPR003439 **note:** TransMembrane:14 (o53-71i92-112o118-137i149-167o179-200i295-314o334-356i431-449o455-474i912-935o955-980i1033-1051o1057-1076i1153-1178o) **EggNog:** ENOG503NYQW, COG:Q **Ontology_term:** GO:0015440, GO:0016887, GO:0005524, GO:0042626, GO:0140359, GO:0000324, GO:0016020, GO:0055085
scaffold_1	4132688	T	G	Intron	**ID:** FUN_001174-T1 **product:** hypothetical protein **Dbxref:** PFAM:PF13649, PFAM:PF13489, PFAM:PF08242, InterPro:IPR029063, PFAM:PF08241 **EggNog:** ENOG503NZFC, COG:S **Ontology_term:** GO:0008757, GO:0008168
scaffold_2	552573	A	T	Exon	**ID:** FUN_002298-T1 **product:** hypothetical protein Dbxref: PFAM:PF00856 note: EggNog:ENOG503P4IX, COG:B
scaffold_2	3916753	A	G	Exon	**ID:** FUN_003258-T1 **product:** hypothetical protein **Dbxref:** PFAM:PF02373, PFAM:PF10497 **EggNog:** ENOG503NXHM, COG:S
scaffold_2	4799024	C	A	Intron	**ID:** FUN_003494-T1 **product:** hypothetical protein **Dbxref:** PFAM:PF13517, PFAM:PF13472, PFAM:PF00657 **note:** SECRETED:SignalP(1-19), CAZy:CE3, COG:S **EggNog:** ENOG503PAS4
scaffold_2	6011698	T	C	Intron	**ID:** FUN_003830-T1 **product:** glyoxylate reductase **Dbxref:** PFAM:PF02826, PFAM:PF00389 **note:** COG:E, antiSMASH:Cluster_11, SMCOG1072:dehydrogenase **EggNog:** ENOG503NW94 **EC_number:** 1.1.1.26
scaffold_3	1573997	T	C	Intron	**ID:** FUN_004340-T1 **product:** hypothetical protein **Dbxref:** PFAM:PF13637, InterPro:IPR036770, InterPro:IPR002110, PFAM:PF13606, PFAM:PF12796, PFAM:PF00023

					EggNog: ENOG503PHTC, COG:S,TransMembrane:1 (i213-234o) **Ontology_term:** GO:0005515, GO:0005737
scaffold_5	2721804	C	T	Exon	**ID:** FUN_008034-T1 **product:** hypothetical protein **Dbxref:** PFAM:PF13041, PFAM:PF01535 **note:** COG:S, **EggNog:** ENOG503NW1K
scaffold_5	2919565	T	A	Intron	**ID:** FUN_008092-T1 **product:** GMP synthase (glutamine-hydrolyzing) **Dbxref:** PFAM:PF00958 **EggNog:** ENOG503NUUQ, COG:F **EC_number:** 6.3.5.2
scaffold_6	4182443	C	T	Exon	**ID:** FUN_009709-T1 **product:** hypothetical protein **EggNog:** ENOG503P4QF **Ontology_term:** GO:0000981, GO:0000976, GO:0005634, GO:0006355
scaffold_7	2628075	A	C	Exon	**ID:** FUN_010476-T1 **product:** hypothetical protein **Dbxref:** PFAM:PF20684 **EggNog:**ENOG503PC1U **TransMembrane:** 7 (o6-26i38-62o82-109i121-141o161-182i194-212o232-253i) **antiSMASH:** Cluster_7
scaffold_7	2944585	A	G	Intron	**ID:** FUN_010561-T1 **product:** velum formation-related protein **Dbxref:** InterPro:IPR038491, InterPro:IPR037525, PFAM:PF11754, InterPro:IPR021740 **note:** COG:K **EggNog:**ENOG503Q3V0
scaffold_7	3827993	G	A	Exon	**ID:** FUN_010756-T1 **product:** hypothetical protein **Dbxref:** PFAM:PF04424, InterPro:IPR033979, InterPro:IPR007518 **note:** MEROPS:MER0902165, COG:S **EggNog:** ENOG503NU2A, **antiSMASH:** Cluster_10 **Ontology_term:** GO:1990380, GO:0004843, GO:0016807, GO:0005829, GO:0071944, GO:0071108

CHAPTER 5

EXPLORING THE USE OF THE BIOCONTROL AGENT *TRICHODERMA* T22 TO REDUCE FUNGAL NITROUS OXIDE EMISSIONS AND NITROGEN LOSS

Oleander, K.A., Satterlee, T.R., Mitchell, T., Read, Q., Gold, S., Oakley, B., Martinez-Espinoza, A.D., and Glenn, A. (2025) Exploring the use of the biocontrol agent *Trichoderma* T22 to reduce fungal nitrous oxide emissions and nitrogen loss,. In preparation for submission to Frontiers in Plant Pathology.

Abstract

Nitrous oxide (N_2O) is a potent greenhouse gas attributed to agricultural soil emissions from fungal denitrification. Various fungi are denitrifiers and produce N_2O, with identified species concentrated in the order *Hypocreales*. The fungal strain *Trichoderma* T22 has been used commercially since the 1990s as a biological control agent and biofertilizer to protect many host plants from several fungal genera of root pathogens, including *Fusarium*, a known N_2O producer. This work aims to evaluate the potential of T22 to mitigate N_2O emissions of *F. verticillioides* (*Fv*). We demonstrated that T22 can drastically reduce *Fv* N_2O emissions in minimal medium plus (15 mM) + L-lysine (1 mM) (15 mM) + L-lysine (1 mM) (15 mM) + L-lysine (1 mM) flasks. We also observed that T22 can be an N_2O producer itself and the N_2O producing potential of T22 depends on the medium in which it is grown in in vitro experiments. In experimental soil settings, T22 was found to be an N_2O emitter.

Introduction

About 50% of the food that the world's population depends on is nitrogen fertilizer dependent, and the agricultural need for nitrogen fertilizers and atmospheric N_2O concentration are expected to increase as populations rise (Galloway et al. 2008, Walling and Vaneeckhaute 2020). Fourteen million metric tons of ammonia are utilized annually in the U.S., with 88% of that attributed to fertilizer application as urea, ammonium nitrate, ammonium phosphate, and other nitrogen compounds derived from atmospheric nitrogen (Survey 2023). Additionally, 50-70% of applied nitrogen is lost to the environment through denitrification, runoff, and other environmental factors (Coskun et al. 2017). With a vast majority of N_2O emissions directly derived from

agricultural soil management, there is a need to mitigate agricultural soil nitrogen emissions (EPA 2023).

Denitrification is the biological process of redox reactions from nitrate (NO_3^-) and nitrite (NO_2^-) to atmospheric nitrogen (N_2) or nitrous oxide (N_2O). The enzymes responsible for denitrification include dissimilatory nitrate reductase (*dNAR*), dissimilatory nitrite reductase (*dNIR*), nitric oxide reductase (*NOR*; *p450nor*), and nitrous oxide reductase (*NOS*) (Figure 5.1) (Shoun et al. 1992). This process occurs in both prokaryotes and eukaryotes, with bacteria, archaea, and fungi being the most relevant soil denitrifiers. Nitrous oxide reductase (*NOS*) is only present in prokaryotes. Fungi lack *NOS*, so they produce N_2O as a final product without further reduction in dinitrogen. To be considered a fungal denitrifier, a strain must have the genomic presence and function of *dNIR* and *NOR* to convert NO_2^- to N_2O (Shoun et al. 2012, Oakley 2023). N_2O has about 300 times the warming potential of CO_2 (pound for pound) and an atmospheric lifetime of 116 ± 9 years (Prather et al. 2015, EPA 2023). N_2O concentration in the atmosphere has increased from 270 ppb before the Industrial Revolution to 334 ppb in 2021 (Pachauri and Reisinger 2007, Galloway et al. 2008, Signor and Cerri 2013, Wuebbles 2017).

N_2O-emitting fungal species were primarily in the order *Hypocreales (Maeda et al. 2015)*. Most isolates produced more N_2O at a neutral pH with $\leq$ 10% atmospheric O_2 (Lavrent'ev et al. 2008, Maeda et al. 2015). Oakley (2023) examined the genus *Fusarium* for the pathway genes, and among the 73 strains used from GenBank, approximately 85% had at least a portion of the denitrification pathway (Oakley 2023). There were various pathway combinations, but all strains with any portion of the denitrification pathway contained NOR (Oakley 2023). Most of the strains with NOR also contained dNIR, while dNAR was present in about 31% of the strains examined

(Oakley 2023). While not all genera within Hypocreales exhibit this characteristic, it suggests that many species of *Fusarium* are denitrifiers. Additionally, fungi with high N_2O emissions were primarily associated with intensively managed soil systems. *Fv*, along with other species in Hypocreales, produces N_2O in agricultural soils (Shoun et al. 1992, Lavrent'ev et al. 2008, Mothapo et al. 2013, Maeda et al. 2015, Mothapo et al. 2015). Many of these species are saprotrophs distributed throughout the soil, an environment that can often be hypoxic, therefore triggering denitrification.

Fusarium verticillioides (Fv) was found to produce N_2O in malt medium and sterile soil supplemented with sodium nitrite (Maeda et al. 2015). Oakley (2023) found that *Nor1* deletion mutants produced 50-fold less N_2O than the wild-type on minimal medium plus sodium nitrite (15 mM) + L-lysine (1 mM) (Oakley 2023). That study asserts that *NOR1* could be a valuable target for eliminating fungal-derived agricultural N_2O emissions. Since 50% of applied fertilizer is lost due to soil processes and environmental conditions, inhibiting fungal N_2O emissions could reduce nitrogen fertilizer loss, thus having economic and ecological benefits (Hirel et al. 2011).

Trichoderma was first characterized from soil and plant debris in 1794 (Persoon 1794). As of 2019, over 300 species of *Trichoderma* have been identified (Marik et al. 2019). *Trichoderma* is one of the most frequently isolated soil fungi, with 10^1 - 10^3 colony forming units (CFU) per gram in most temperate and tropical soils, and is often considered an indicator of soil health (Harman et al. 2004, Lange 2014). *Trichoderma* is endophytic and will colonize in and around the roots of many host plants (Harman et al. 2004, Bailey and Melnick 2013). Root colonization of *Trichoderma* induces both local and systemic resistance that helps the plants defend against future pathogen attacks (Djonovic et al. 2006).

Many *Trichoderma* species are non-pathogenic opportunistic plant symbionts that can be used as low-cost, effective biocontrol and biofertilizer agents. Yield improvements from *Trichoderma* applied as a biofertilizer can be dramatic; for example, an $8 treatment of *Trichoderma* led to yield improvements of over $400 per hectare (Harman 2011). Trichoderma biological control treatments contribute to plant resistance to various pathogens, increase nutrient absorption, increase abiotic stress tolerance, and stimulate biosynthesis of various metabolites, including plant growth regulators, siderophores, and antibiotics (Kuć 2001, Van Wees et al. 2008, Fu et al. 2021). Several hundred strains of *Trichoderma* have been used commercially as biocontrol agents worldwide (Singh et al. 2009).

Trichoderma afroharzianum strain T22 (shortened to T22) is a biocontrol and biofertilizer strain that has been sold worldwide as RootShield and several other names to manage various fungi and Oomycota since the early 1990s (Harman et al. 1993). T22 is labeled for control of *Pythium, Rhizoctonia, Fusarium, Thielaviopsis,* and *Cylindrocladium* and is used on a range of plant hosts, including corn, turfgrass, and ornamentals. T22 was generated using protoplast fusion of two complementary auxotrophic mutants of T12 and T95 (Stasz et al. 1988). *Trichoderma* has been transformed using various methods to study the organism and produce better biological control strains. These methods include polyethylene glycol (PEG) mediated protoplast transformation, *Agrobacterium tumefaciens*-mediated transformation (ATMT), electroporation, and biolistic bombardment (Te'o et al. 2002, Elena et al. 2006, Kim and Miasnikov 2013, Cai et al. 2021, Wang et al. 2022).

Trichoderma is a potential N_2O producer, but some strains have been used to reduce overall N_2O emissions when applied as a biofertilizer in some cropping systems. Generally, *Trichoderma*

is considered a potential N_2O producer or denitrifier, with some strains capable of producing high amounts of N_2O, while others are non-producers (Maeda et al. 2015). Many reports on mitigating N_2O emissions describe *Trichoderma* as a biofertilizer along with other nitrogen inputs, such as agricultural wastewater or biochar, instead of conventional fertilizer sources (Kashyap et al. 2017, Xu et al. 2018, Sani et al. 2020, Geng et al. 2021, Wang et al. 2021). Tea plants are often used as models for N_2O-mitigation research in the field and greenhouse settings. Tea fields have a much higher (9.4 ± 6.2 times) N_2O flux when compared to woodlands, and these N_2O emissions can be mitigated with *Trichoderma* biofertilizer applications (Xu et al. 2014, Xu et al. 2017), specifically using T22 as the strain of interest they found a decrease in N_2O emissions (Haque et al. 2010, Sani et al. 2020). Most emission reduction is attributed to the difference in nitrogen source from conventional nitrogen fertilizers to biofertilizers, compost, biochar, etc. Still, it shows promise in the use of *Trichoderma* as a biofertilizer plus other tools to mitigate agricultural N_2O emissions.

The objective of this investigation was to mitigate *Fv*' N_2O emissions, a common fungal soil denitrifier, through application of *T. afroharzianum* T22. This research uses *Fv* as a model organism to determine whether T22 can reduce N_2O emissions by managing *Fv.* This research details a series of experiments on different media, including malt, minimal, and soil, to identify if T22 can reduce *Fv* N_2O emissions.

Materials and Methods

Fungal material acquisition

Trichoderma strain T22 (ATCC 20847) was obtained from the American Type Culture Collection (ATCC). Nine *Trichoderma* strains and three *Fusarium* strains were obtained from the National Research Institute for Agriculture, Food, and Environment (INRAE) collection in France

for testing (Table 5.1). These strains were selected to allow for a range of high-, medium-, and low-producing strains within this study's two genera of interest (Maeda et al. (2015). Table 5.1 details more information about these strains, including names, sources, and reasons for study inclusion. The strains were grown at 25 °C on potato dextrose agar (PDA; Neogene, Lexington, KY, USA) for 5 to 7 days for spore collection. Previous studies made available *Fv* WT M3125, and *FvNOR1* mutants (Oakley 2023).

Spore collection protocol

Cultures were grown on PDA at 27 °C until sporulation occurred (3-5 days). A volume of 20 ml of sterile water was added to the plate, and a sterile L-shaped cell spreader was used to dislodge conidia. The spore suspension was filtered through sterile gauze into a 50 mL tube to remove mycelia, agar, and other debris. Using a hemacytometer, the flow through suspension was diluted in water to adjust the concentration of 10^6 conidia/mL or other concentrations as needed. In all cases, 1 mL of spore solution was added to the final experimental flask.

BLAST analysis of the Trichoderma T22 genome

The T22 genome, publicly available through the Joint Genome Institute (JGI), was analyzed using tBLASTn in Geneious Prime (Prime) for orthologs of the three critical canonical fungal denitrification-associated genes (NAR1, DNI1, and NOR1) (Altschul et al. 1990, Grigoriev et al. 2012).

N_2O emissions in vitro studies using minimal medium

Media containing 25 mL of minimal medium + sodium nitrite (15 mM) + L-lysine (1 mM) was added to sterile 50 mL flasks before inoculating with 1 mL of 10^6 conidia/mL spore suspension. The flasks were closed using a cotton ball and aluminum foil with stationary dark

incubation for three days at 27 °C. The flasks were then sealed with a rubber septum, and samples were subjected to stationary incubation at 27 °C for 24 hours before a 3 mL headspace air sample was taken using a syringe and needle fitted with a stopcock. The syringe was flushed three times between samples by filling it with atmospheric air. The air samples were assessed for N_2O emissions using a Shimadzu GC-2010 gas chromatograph (GC) equipped with electron capture detector (ECD) (Shimadzu Scientific Instruments, Inc., Durham, NC, USA) and an AOC-6000 autosampler (PAL System, Distribution by Archer Science, Lake Elmo, MN, USA). Standards containing 1, 10, 100, 1,000, and 10,000 ppm N_2O in nitrogen gas were used as controls for quantification.

PDA plate competition assay of T22 and Fv

T22 was tested to manage *Fusarium*, one of the most significant fungal N_2O producers (Maeda et al. 2015). T22 and *Fv* were grown on PDA plates for six days at 27 °C to evaluate T22's ability to outcompete or inhibit *Fv* under these conditions. Each plate was inoculated with 20 μL of 10^6 spores/mL suspension at 2.5 cm from the edge of the plate. For the competition plates, the other strain was inoculated on the opposite side of the plate 2.5 cm from the edge, leaving 5 cm between the two inoculation points. Four biological replications were used. Photographs were taken daily on days 2-6.

Competition and growth advantage assays N_2O production measurements on minimal medium

Flask competition experiments with T22 and *Fv* WT were performed in minimal medium plus sodium nitrite (15 mM) + L-lysine (1 mM) using the conditions detailed above in the initial flask experiments. The flasks were either inoculated with both organisms at the same starting concentrations (10^6), or one organism was given a time advantage over the other (12, 24, 48, or 72

hours). N_2O concentrations of the assay mixtures were measured. Two biological replications were used for each treatment tested.

In vitro-flask emission measurements for reportedly high N_2O producing samples

An assay was performed using minimal medium + sodium nitrite (15 mM) + L-lysine (1 mM) and four reportedly high N_2O-producing strains from Maeda et al. (2015). Wild-type *Fv* and T22 were used for N_2O emission comparison. Non-inoculated flasks were used as a negative control. Three biological replicates were used for each strain.

Results from the reportedly high-producing strains on minimal media necessitated the addition of an assay following the protocol in Maeda et al. 2015 on malt + sodium nitrite. Cultures were grown, and spores were collected as described previously. One mL of 10^6 spore solution was added to 12.5 mL of malt medium (Neogene, Lexington, KY, USA). The flasks were sealed and incubated at 25 °C at 125 rpm shaking in darkness. After three days of incubation, 12.5 mL of malt medium + sodium nitrite (10mM, pH 7.5) were added to each flask and sealed with a rubber septum before being placed back in shaking incubation. At 24 hours post amendment and sealing, a 3 mL headspace air sample was taken as described above, and the flask was placed back in shaking incubation. After six additional days, a 3 mL headspace air sample was collected, and the culture material was dried on filter paper as described above. Three biological replications were used for each strain tested.

Competition assays emission measurements on minimal medium over 7 days

A final minimal medium + sodium nitrite (15 mM) + L-lysine (1 mM) experiment of flask N_2O production was performed, and measurements were taken on days 1, 3, 5, and 7. The setup was performed as previously described. Samples used in this assay included *Fv* WT, T22, non-

inoculated (control), T22 and *Fv* combined, T22 and *Fv* with T22 given a 72-hour time advantage, and *Fv* with a 72-hour time delay as a control for the "advantage" assay. Additional atmospheric air (4 mL) was added to the flasks on day 5 to prevent the flasks from being under pressure after the previous air sample removals. Three biological replicates were used for each treatment tested.

Soil Nitrous Oxide Production Assays

Fungal samples were tested to evaluate their N_2O production and emission in soil (Maeda et al. 2015). For this purpose, three different soil types were used. The soil types were selected based on their utilitarian use. One soil type was collected from a corn field at the end of a growing season (Tifton, GA, USA). This sample was selected because *Fv* is a common endophyte and pathogen of corn. Additionally, two turfgrass samples were selected because the N_2O emissions of turfgrass have been studied a great deal in the past (Horgan et al. 2002, Braun 2017, Braun and Bremer 2018). One of the areas where turfgrass soil samples were taken had a history of being intensively managed (Griffin, GA, USA) with the routine use of fertilizers, herbicides, growth regulators, fungicides, core aeration, and other cultural practices. The second turfgrass soil was minimally managed (Athens, GA, USA), where no agronomic inputs were used. We hypothesized that given the high nitrogen fertilizer use in grass systems, there was an expectation that these areas would produce high amounts of N_2O. Soil testing was performed by the University of Georgia Agricultural & Environmental Services Laboratories to obtain the general soil characteristics of each soil sample. For the assay, sterile water was added to the soil to reach 60% holding capacity. Five grams of soil were placed in 125 mL flasks and inoculated with 1 mL of 10^6/mL spore suspension of one of the following treatments: T22, *Fv*, T22 and *Fv*, MIAE 00042, *Fv* WT with a delay of 7 days or T22 and *Fv* WT with a time advantage of 7 days given to T22 and incubated for

7 days. In addition, non-inoculated soil was used as a negative control. Three biological replications were used for each treatment. After 7 days, 2mL of sodium nitrite (10mM) was added to the colonized soils and water was added to adjust the water-holding capacity to 90%. This is when samples with a time delay ("advantage") were inoculated. The flasks were sealed, and the N_2O concentration was measured after 2, 4, and 7 days by taking a headspace sample as previously described. If the samples were under vacuum following the collection, 4 ml of atmospheric air were added on day 4 to prevent negative pressure in flasks.

Statistical analyses

Within each dataset and day, a log-log regression was fit to the analytical standard peak areas. We used the parameters of this regression to convert peak areas (a) to concentration (c) in ppm units, using the formula $c = e^{\beta_0} a^{\beta_1}$, where β_0 is the intercept and β_1 the slope. We fit linear mixed-effects models to each dataset, using log-transformed concentration as the response variable. In all cases, treatment was a categorical fixed effect. For datasets measuring concentration on multiple days, day and treatment by day interaction were also included as categorical fixed effects.

The soil assay data had a 2×2 factorial design, with treatment crossed with soil type; treatment, soil, day, and their two-way and three-way interactions were the fixed effects. All models included a random intercept for replicate.

The models for all multiple-day datasets, except the soil assay, also included a compound symmetry error covariance to account for the repeated measures over time points within each combination of treatment and replicate. The model for the soil assay did not support the inclusion

of an error covariance term; therefore, we included a random intercept term for each combination of treatment and replicate.

We estimated marginal means by treatment for each model within each day where applicable. For the soil assay, we also estimated marginal means by soil type within each day, which was averaged over treatments, and marginal means by treatment within each combination of soil type and day. We used the Kenward-Roger method to estimate degrees of freedom for the t-statistics used to calculate the 95% confidence intervals of the means and to test whether the ratio of each pair of means was equal to 1. P-values associated with the pairwise comparisons were adjusted using the Tukey HSD procedure. All means were back-transformed from the log scale for presentation. Statistical analysis was performed using R software v4.4.1 (R Core Team 2024), with the packages emmeans v1.10.6 (Lenth 2024) and glmmTMB v1.1.11 (Brooks et al. 2017).

Results

Analysis of *T22 denitrification pathway*

To identify if the T22 genome contained the full fungal denitrification pathway, a tBLASTn search was performed using homologs of the *Fv* denitrification pathway. A gene homolog with high homology was found in T22 for the gene *FvNOR1* (78% identity) and TRIVIDRAFT_186579 (93% identity) of the *Trichoderma NOR1* gene available in GenBank (AA alignment; Figure 5.2). *FvDNI1* and *FvNAR1* did not have a matching alignment or any significant partial matches to indicate the presence of an ortholog gene in T22. These BLAST results indicate that T22 has portions of the denitrification pathway. Still, since it lacks *DNI1* and *NAR1* genes, it cannot be considered a complete denitrifier; instead, it can be categorized as an N_2O producer (Oakley 2023).

T22 production of N_2O emissions in minimal medium assays

To determine the capacity of T22 to emit N_2O, initial in-vitro flask experiments were performed using the protocol outlined in Oakley (2023) The initial experiment was performed with the *Fusarium* NOR1 mutants, *Fv*, and T22. This assay showed that T22, despite potentially having a NOR1 gene, produced low N_2O amounts (17 ppm) that were similar, but not statistically grouped with the *ΔFvNOR1* mutants (7 and 5 ppm; Figure 5.3). With results demonstrating that T22 produces much less N_2O than *Fv* (154 ppm), we evaluated its capacity as a mitigation tool for N_2O emissions.

T22 suppression of Fv *in PDA plates*

When *Trichoderma* T22 was co-cultured in confrontation assays with *Fv* on PDA agar plates, T22 would grow into direct contact with *Fv* and inhibit its growth by day three (Figure 5.4). By the fourth day, T22 covered the entire plate and surrounded the *Fv* colony (Figure 5.4). *Fv* was present at the end of six days, but its growth was inhibited (Figure 5.4). T22 can suppress the outward growth of *Fv* but does not completely inhibit it, especially if *Fv* has been established first.

Reduction of Fv *N_2O emissions with T22 Treatment*

Flask competition experiments using *Trichoderma* T22 and *Fv* showed that T22 can suppress *Fv*, especially if T22 is given an initial 72 hour advantage (Figure 5.5). These experiments were designed to test T22 and T22 vs *Fv* (TvF) N_2O emissions in flasks, compare them to *Fv* results, and determine if the pathogen is likely being suppressed. T22 and *Fv* co-inoculated and grown together reduced the total N_2O emissions by 2/3rds (TvF 950 ppm, *Fv* alone 2864 ppm) when both strains were inoculated simultaneously (Figure 5.5). If either organism was given a time advantage, the N_2O emissions were similar to that of the organism alone. Therefore, if T22 had a

growth time advantage, the emissions of *Fv* were significantly lower compared to the *Fv* monoculture (Figure 5.5) and vice versa. These results indicate that giving T22 a time advantage over *Fv* would dramatically reduce N_2O emissions (Figure 5.5).

T22 and Fv N_2O production compared to reported high-producing strains

Strains from the Maeda et al. (2015) paper were obtained and grown alongside treatments of T22 and *Fv.* Based on the previous results of Maeda et al. (2015) it was expected that the strains from this study would have a wide range of N_2O emissions; however, little (5-103 ppm) N_2O production was observed in any of the *Trichoderma* strains, including T22 (Figure 5.6) in minimal medium + sodium nitrite (15 mM) + L-lysine (1 mM), despite being extremely high producers in Maeda et al. (2015) (Figure 5.6). Therefore, experiments were reconducted to mimic the exact growing conditions described in Maeda et al. 2015.

Flask experiments were performed using malt medium + sodium nitrite (5mM) and corroborated the N_2O production potential of the *Trichoderma* strains, including T22. The one-day samples were compared to the previous results with minimal medium + sodium nitrite (15 mM) + L-lysine (1 mM). These results were not as high producing as on the minimal media for *Fv*, but all the tested MIAE strains produced N_2O (317-2178 ppm; Figure 5.7). Notably, T22 significantly increased N_2O production at the 7-day reading (from 204 to 2022 ppm), rivaling *Fv* emissions and the highest producers from Maeda et al. (2015) (Figure 5.7).

Competition N_2O production measurements on minimal medium over 7 days show that T22 might only delay Fv N_2O production.

A seven-day time course with four N_2O production measurements was conducted on minimal media to retest the initial observations for the key treatments. Flask emission experiments

were performed with minimal medium + sodium nitrite (15 mM) + L-lysine (1 mM), four-time points over seven days in hypoxic conditions. Results throughout the study showed that T22 N_2O emissions were relatively low (23-50 ppm), while *Fv* was able to produce large amounts of N_2O (350-2210 ppm). The T22 and *Fv* competition flasks showed that T22 could decrease the amount of N_2O produced but not eliminate it (Figure 5.8). By day seven, the *Fv* monoculture and T22 and *Fv* competition flasks' N_2O readings were at the same rate and statistically grouped (1750 and 1772 ppm; Figure 5.8). When comparing the *Fv* delay flasks to the T22 + *Fv* flasks with T22 given an advantage, the N_2O readings began to follow the same trend, meaning that over time, the N_2O production is increasing and may not prevent long-term N_2O production (Figure 5.8).

T22 and Fv N_2O production in soil assays

To examine the N_2O emissions of T22 and *Fv* in soil, these strains were tested over 7 days in three different ecological soil types (Table 5.2). Soils were treated with a 10^6/mL spore suspension of T22, *Fv*, T22 and *Fv* WT, MIAE 00042, *Fv* WT with an inoculation delay of 7 days, or T22 and *Fv* WT with a time advantage given to T22 of 7 days. Three samples were taken for each treatment flask (2, 4, and 7 days). N_2O was produced by all fungal strains in all soil types, but the total emissions were relatively low (1.5-50 ppm; Figure 5.9). The most significant difference between the control and fungal N_2O production was seen in the RK1 soil, but even then, the amount of N_2O produced was low.

Discussion

To utilize the biocontrol strain *Trichoderma* T22 for N_2O emission management, there was a need to first characterize its N_2O emissions and potential for denitrification. According to Oakley (2023), some strains of *Trichoderma* contain the genes required to be fungal denitrifiers or N_2O

producers. The results of this study indicate that *Trichoderma* T22 has portions of the denitrification pathway, with a functional NOR1 gene but not NAR1 or DNI1. Therefore, it cannot be considered a complete denitrifier. Instead, it is classified as a potential N_2O producer (Oakley 2023).

Additionally, T22 has previously been used for non-fungal N_2O mitigation using various organic or inorganic nitrogen sources to compare the overall N_2O production in that setting (Haque et al. 2010, Sani et al. 2020). Results from our N_2O assays using T22, the *FvNOR1* mutants, and wild-type strains indicate that while it has a potentially useable NOR1 gene, its N_2O emission ability on the minimal medium was similar to the low-producing *FvNOR1* deletion mutants. This denoted that while the NOR1 gene was present, it did not appear functional in the minimal medium + sodium nitrite (15 mM) + L-lysine (1 mM) we used for N_2O emission studies.

Next, we determined the ability of T22 to manage or inhibit the *Fv* growth, therefore mitigating *Fv* N_2O emissions. Our results showed that on PDA, T22 outpaced and limited the growth of *Fv*. In direct competition flasks, T22 reduced the total N_2O emissions in TvF flasks by over 60% compared to *Fv* monocultures (Figure 5.5). T22 time-advantaged flasks drastically reduced N_2O emissions. However, if *Fusarium* had even a 12 hour growth advantage, T22 could not reduce N_2O emissions to similar levels as the no time-advantaged treatments. These results denote that for the most effective control of N_2O emissions, T22 should be established well before *Fv*. Utilizing T22 (Rootshield) as a seed treatment in corn and wheat (Ladha et al. 2016) has the potential to be used as an N_2O mitigation strategy and to control other fungal denitrificators in the soil.

Maeda et al. (2015) examined over 200 strains of fungi for N_2O emission potential in malt medium flasks and found that 70% of the emitters were taxonomically classified within the order Hypocreales. A large proportion of these fungi were either *Trichoderma* or *Fusarium* spp. Our study evaluated four strains from Maeda et al. (2015) work on minimal medium assays. We hypothesized that we'd observe similar results to those of Maeda et al. (2015) in a malt medium. Still, none of the *Trichoderma* strains tested were found to be N_2O producers in the minimal medium. This highlights the importance of the growth media. N_2O production differed according to the fungal species tested; *Trichoderma* strains produced biomass in minimal medium testing but did not produce N_2O. This contrasted with what was observed by Maeda et al. (2015) when using the four INRAE strains. We hypothesized that while the media was sufficient for *Trichoderma* to grow well, it could not activate the N_2O-production pathway, probably missing a nutrient required for the pathway activation.

The N_2O assessment assay was then repeated by substituting the growing medium with a malt medium. This assay showed that all the tested *Trichoderma* strains produce N_2O on the malt medium. The MIAE strains did not produce on minimal medium but did on the malt medium, as expected from the results from Maeda et al. (2015). Additionally, at 7 days, T22 was the second-highest N_2O producer. These results indicate that the ability of T22, and potentially other fungi, to produce N_2O is nutrient-dependent. This assertion is supported by various fungal N_2O studies that show that N_2O production depends on nitrogen sources (Xu et al. 2014, Jirout 2015, Xu et al. 2018, de Oliveira et al. 2019).

Another assay was performed in a minimal medium + sodium nitrite (15 mM) + L-lysine (1 mM), with four measurements over 7 days instead of just one read at 24 hours post-sealing.

These results showed that T22 was not producing in minimal medium + sodium nitrite (15 mM) + L-lysine (1 mM) even after 7 days, but also showed that over time, the competition flasks reached similar emission levels as the flasks with only *Fv* WT. Given that the trend in N_2O has increased over time, we expect this means that T22 can only delay *Fv* growth temporarily in these conditions. It also appears that even when T22 is given a head start against *Fv* WT, the N_2O emissions rise over time. We expect that if these cultures were continued over time, the delayed readings would eventually meet, similar to the comparison between *Fv* monoculture and T22 and *Fv* combined without advantage flasks.

We wanted to evaluate the N_2O emission capabilities of *Trichoderma* and *Fusarium* in their soilborne natural settings. There are also many studies using T22 for *Fusarium* spp. management of various crops, especially those marketed as Rootshield (Harman et al. 1993, Ferrigo et al. 2014, Innocenti et al. 2015, Modrzewska et al. 2022, Vitti et al. 2022). T22, *Fv* WT, MAIE 00042, and two T22 and *Fv* competition treatments were evaluated in three different ecological soil types: soil from highly managed turfgrass areas (golf greens), minimally managed turfgrass areas (low input landscapes), and row crop agricultural soil. The results showed that all the strains, including T22, produced N_2O in all types of soil tested, but the amounts produced were minor compared to other media. *Fv* and T22 produced N_2O in the soil settings tested at similar levels to MIAE00042.

These results show that T22 can reduce Fv's N_2O emissions, but more research is needed to find the optimal conditions before being utilized for N_2O emission mitigation. T22's ability to produce N_2O under certain conditions is a drawback for its potential as an N_2O mitigator. Therefore, to have a more significant effect on the reduction of agricultural soil N_2O, removing

T22's ability to produce N_2O would be desirable. If a *Trichoderma* were to be used as an N_2O mitigator, it would need to manage various *Fusarium* spp. and outcompete other *Trichoderma* spp. present in many soil samples and crop settings. Given the traits used to select T22 as a biocontrol, including rhizosphere competency and biocontrol capability (Sivan and Harman 1991), including against *Fv* specifically (Ferrigo et al. 2014, Ferrigo et al. 2014). We hypothesize that T22 can act as an N_2O mitigator, and its potential can be improved by removing its N_2O production. T22 has harnessed brand and name recognition, given its vast use and fast-growing capabilities (Stasz et al. 1988, Harman 2011). The commercialization of such a strain would be easier because of the abovementioned factors.

Conclusions

We tested T22, a known biocontrol agent, with the potential to mitigate *Fusarium verticillioides'*s fungal N_2O emissions. This research found that the ability of T22 to produce N_2O is dependent on the source of nitrogen. Additionally, T22 was able to outpace *Fv* growth in PDA plates and reduce the N_2O emissions of *Fv* in competition flasks. This research lays the groundwork for future studies using T22 to mitigate fungal N_2O emissions.

Author Contributions

KO – conceptualization, methodology, investigation, validation, data curation, original draft preparation, review, and editing of final manuscript. TS – conceptualization, review, and editing of final manuscript. TM – methodology, resources, review, and editing of final manuscript. QR – formal analysis, visualization, review, and editing of final manuscript. SG – conceptualization, funding acquisition, supervision, methodology, review, and editing of final manuscript. BO – conceptualization, review, and editing of final manuscript. AME – methodology, review, and

editing of final manuscript. AG – funding acquisition, supervision, methodology, review, and editing of final manuscript.

References

Altschul, S. F., W. Gish, W. Miller, E. W. Myers and D. J. Lipman (1990). "Basic local alignment search tool." Journal of Molecular Biology **215**(3): 403-410.

Bailey, B. A. and R. L. Melnick (2013). The endophytic *Trichoderma*. *Trichoderma*: Biology and applications, CABI Wallingford UK**:** 152-172.

Braun, R. C. (2017). Environmental and management impacts in turfgrass systems: Nitrous oxide emissions, carbon sequestration, and drought and traffic stress Ph.D., Kansas State University.

Braun, R. C. and D. J. Bremer (2018). "Nitrous oxide emissions in turfgrass systems: a review." Agronomy Journal **110**(6): 2222-2232.

Cai, F., C. P. Kubicek and I. S. Druzhinina (2021). Genetic transformation of *Trichoderma* spp. Biofuels and Biodiesel, Springer**:** 171-185.

Coskun, D., D. T. Britto, W. Shi and H. J. Kronzucker (2017). "How plant root exudates shape the nitrogen cycle." Trends in Plant Science **22**(8): 661-673.

de Oliveira, T. s. B., R. C. de Lucas, A. S. d. A. Scarcella, T. Pasin, C. Martinez and M. Polizeli (2019). Perspectives on exploring denitrifying fungi as a model to evaluate nitrous oxide production and reduce emissions from agricultural soils, American Chemical Society.

Djonovic, S., C. Howell and C. Kenerley (2006). "Sm1, a proteinaceous elicitor secreted by the biocontrol fungus *Trichoderma virens* induces plant defense responses and systemic resistance." Mol Plant Microbe Interact **19**: 838-853.

Elena, C. R., V. J. Antonio, H. M. Rosa, M. Enrique and G. Santiago (2006). "A comparison of the phenotypic and genetic stability of recombinant *Trichoderma* spp. generated by protoplast-and *Agrobacterium*-mediated transformation." Journal of Microbiology **44**(4): 383-395.

EPA, U. S. E. P. A. (2023). "Overview of greenhouse gases." EPA, from https://www.epa.gov/ghgemissions/overview-greenhouse-gases.

Ferrigo, D., A. Raiola, E. Piccolo, C. Scopel and R. Causin (2014). "*Trichoderma harzianum* T22 induces in maize systemic resistance against *Fusarium verticillioides*." Journal of Plant Pathology **96**(1).

Ferrigo, D., A. Raiola, R. Rasera and R. Causin (2014). "*Trichoderma harzianum* seed treatment controls *Fusarium verticillioides* colonization and fumonisin contamination in maize under field conditions." Crop Protection **65**: 51-56.

Fu, J., Y. Xiao, Y. F. Wang, Z. H. Liu, Y. F. Zhang and K. J. Yang (2021). "*Trichoderma asperellum* alters fungal community composition in saline–alkaline soil maize rhizospheres." Soil Sci Soc Am J **85**(4): 1091-1104.

Galloway, J. N., A. R. Townsend, J. W. Erisman, M. Bekunda, Z. Cai, J. R. Freney, L. A. Martinelli, S. P. Seitzinger and M. A. Sutton (2008). "Transformation of the nitrogen cycle: Recent trends, questions, and potential solutions." Science **320**(5878): 889-892.

Geng, Y., Y. Yuan, Y. Miao, J. Zhi, M. Huang, Y. Zhang, H. Wang, Q. Shen, J. Zou and S. Li (2021). "Decreased nitrous oxide emissions associated with functional microbial genes under bio-organic fertilizer application in vegetable fields." Pedosphere **31**(2): 279-288.

Grigoriev, I. V., H. Nordberg, I. Shabalov, A. Aerts, M. Cantor, D. Goodstein, A. Kuo, S. Minovitsky, R. Nikitin and R. A. Ohm (2012). "The genome portal of the Department of Energy Joint Genome Institute." Nucleic Acids Res **40**(D1): D26-D32.

Haque, M. M., M. A. Haque, G. Ilias and A. H. Molla (2010). "*Trichoderma*-enriched biofertilizer: a prospective substitute of inorganic fertilizer for mustard (Brassica campestris) production." The Agriculturists **8**(2): 66-73.

Harman, G. E. (2011). "*Trichoderma*—not just for biocontrol anymore." Phytoparasitica **39**(2): 103-108.

Harman, G. E., C. R. Howell, A. Viterbo, I. Chet and M. Lorito (2004). "*Trichoderma* species—opportunistic, avirulent plant symbionts." Nature Rev Microbiol **2**(1): 43-56.

Harman, G. E., T. E. Stasz and N. F. Weeden (1993). Fused biocontrol agents. United States, Cornell Research Foundation Inc. **US5260213A**.

Hirel, B., T. Tétu, P. J. Lea and F. Dubois (2011). "Improving nitrogen use efficiency in crops for sustainable agriculture." Sustainability **3**(9): 1452-1485.

Horgan, B., B. Branham and R. Mulvaney (2002). "Direct measurement of denitrification using 15N-labeled fertilizer applied to turfgrass." Crop Science **42**(5): 1602-1610.

Innocenti, G., R. Roberti and F. Piattoni (2015). "Biocontrol ability of *Trichoderma harzianum* strain T22 against Fusarium wilt disease on water-stressed lettuce plants." BioControl **60**: 573-581.

Jirout, J. (2015). "Nitrous oxide productivity of soil fungi along a gradient of cattle impact." Fungal Ecology **17**: 155-163.

Kashyap, P. L., P. Rai, A. K. Srivastava and S. Kumar (2017). "Trichoderma for climate resilient agriculture." World Journal of Microbiology and Biotechnology **33**(8): 155.

Kim, S. and A. Miasnikov (2013). Method for introducing nucleic acids into fungal cells. US, Danisco US Inc. **US20100304468A1**.

Kuć, J. (2001). "Concepts and direction of induced systemic resistance in plants and its application." Eur J Plant Pathol **107**: 7-12.

Ladha, J. K., A. Tirol-Padre, C. K. Reddy, K. G. Cassman, S. Verma, D. S. Powlson, C. van Kessel, D. de B. Richter, D. Chakraborty and H. Pathak (2016). "Global nitrogen budgets in cereals: A 50-year assessment for maize, rice and wheat production systems." Scientific Reports **6**(1): 19355.

Lange, L. (2014). "The importance of fungi and mycology for addressing major global challenges." IMA Fungus **5**(2): 463-471.

Lavrent'ev, R., S. Zaitsev, I. Sudnitsyn and A. Kurakov (2008). "Nitrous oxide production by fungi in soils under different moisture levels." Moscow University soil science bulletin **63**(4): 178-183.

Maeda, K., A. Spor, V. Edel-Hermann, C. Heraud, M.-C. Breuil, F. Bizouard, S. Toyoda, N. Yoshida, C. Steinberg and L. Philippot (2015). "N2O production, a widespread trait in fungi." Scientific Reports **5**(1): 1-7.

Marik, T., C. Tyagi, D. Balázs, P. Urbán, Á. Szepesi, L. Bakacsy, G. Endre, D. Rakk, A. Szekeres and M. A. Andersson (2019). "Structural diversity and bioactivities of peptaibol compounds from the *Longibrachiatum* clade of the filamentous fungal genus *Trichoderma*." Front Microbiol **10**: 1434.

Modrzewska, M., M. Bryła, J. Kanabus and A. Pierzgalski (2022). "*Trichoderma* as a biostimulator and biocontrol agent against *Fusarium* in the production of cereal crops: Opportunities and possibilities." Plant Pathology **71**(7): 1471-1485.

Mothapo, N., H. Chen, M. A. Cubeta, J. M. Grossman, F. Fuller and W. Shi (2015). "Phylogenetic, taxonomic and functional diversity of fungal denitrifiers and associated N2O production efficacy." Soil Biology and Biochemistry **83**: 160-175.

Mothapo, N. V., H. Chen, M. A. Cubeta and W. Shi (2013). "Nitrous oxide producing activity of diverse fungi from distinct agroecosystems." Soil Biology and Biochemistry **66**: 94-101.

Oakley, B. A. (2023). Denitrification in *Fusarium*: A crossroads between fungal biology and emission of a major greenhouse gas.

Pachauri, R. K. and A. Reisinger (2007). "Climate change 2007: Synthesis report. Contribution of working groups I, II and III to the fourth assessment report of the Intergovernmental Panel on Climate Change." Climate Change 2007. Working Groups I, II and III to the Fourth Assessment.

Persoon, C. H. (1794). "Disposita methodical fungorum." Romers Neues Mag Bot **1**: 81-128.

Prather, M. J., J. Hsu, N. M. DeLuca, C. H. Jackman, L. D. Oman, A. R. Douglass, E. L. Fleming, S. E. Strahan, S. D. Steenrod, O. A. Søvde, I. S. Isaksen, L. Froidevaux and B. Funke (2015). "Measuring and modeling the lifetime of nitrous oxide including its variability." Journal of Geophysical Research **120**(11): 5693-5705.

Prime, G. Geneious Prime

Sani, M. N. H., M. Hasan, J. Uddain and S. Subramaniam (2020). "Impact of application of *Trichoderma* and biochar on growth, productivity and nutritional quality of tomato under reduced NPK fertilization." Annals of Agricultural Sciences **65**(1): 107-115.

Shoun, H., S. Fushinobu, L. Jiang, S.-W. Kim and T. Wakagi (2012). "Fungal denitrification and nitric oxide reductase cytochrome P450nor." Philosophical Transactions of the Royal Society B: Biological Sciences **367**(1593): 1186-1194.

Shoun, H., D.-H. Kim, H. Uchiyama and J. Sugiyama (1992). "Denitrification by fungi." FEMS Microbiology Letters **94**(3): 277-281.

Signor, D. and C. E. P. Cerri (2013). "Nitrous oxide emissions in agricultural soils: A review." Pesquisa Agropecuária Tropical **43**: 322-338.

Singh, H., B. Singh, S. Singh, S. Singh and B. Sarma (2009). "Biological control of plant diseases: Status and prospects." Recent Advances in Biopesticides: Biotechnological Applications; New India Pub.: New Delhi, India **322**.

Sivan, A. and G. Harman (1991). "Improved rhizosphere competence in a protoplast fusion progeny of *Trichoderma harzianum*." Microbiol **137**(1): 23-29.

Stasz, T., G. Harman and N. Weeden (1988). "Protoplast preparation and fusion in two biocontrol strains of *Trichoderma harzianum*." Mycologia **80**(2): 141-150.

Survey, U. S. G. (2023). Mineral commodity summaries 2023. Mineral Commodity Summaries. Reston, VA**:** 210.

Te'o, V., P. Bergquist and K. Nevalainen (2002). "Biolistic transformation of *Trichoderma reesei* using the Bio-Rad seven barrels Hepta Adaptor system." Journal of Microbiological Methods **51**(3): 393-399.

Van Wees, S. C., S. Van der Ent and C. M. Pieterse (2008). "Plant immune responses triggered by beneficial microbes." Curr Opin Plant Biol **11**(4): 443-448.

Vitti, A., V. Bevilacqua, G. Logozzo, R. Bochicchio, M. Amato and M. Nuzzaci (2022). "Seed coating with *Trichoderma harzianum* T-22 of Italian durum wheat increases protection against Fusarium culmorum-induced crown rot." Agriculture **12**(5): 714.

Walling, E. and C. Vaneeckhaute (2020). "Greenhouse gas emissions from inorganic and organic fertilizer production and use: A review of emission factors and their variability." Journal of Environmental Management **276**: 111211.

Wang, C., B. Amon, K. Schulz and B. Mehdi (2021). "Factors that influence nitrous oxide emissions from agricultural soils as well as their representation in simulation models: A review." Agronomy **11**(4): 770.

Wang, Y., H. Chen, L. Ma, M. Gong, Y. Wu, D. Bao and G. Zou (2022). "Use of CRISPR-Cas tools to engineer *Trichoderma* species." Microbial Biotechnology **15**(10): 2521-2532.

Wuebbles, D. J., D.W. Fahey, K.A. Hibbard, D.J. Dokken, B.C. Stewart, and T.K. Maycock, eds. (2017). Climate science special report: Fourth National Climate Assessment, volume I. . U. U. S. G. C. R. Program).

Xu, S., S. Feng, H. Sun, S. Wu, G. Zhuang, Y. Deng, Z. Bai, C. Jing and X. Zhuang (2018). "Linking N2O emissions from biofertilizer-amended soil of tea plantations to the abundance and structure of N2O-reducing microbial communities." Environmental Science & Technology **52**(19): 11338-11345.

Xu, S., X. Fu, S. Ma, Z. Bai, R. Xiao, Y. Li and G. Zhuang (2014). "Mitigating nitrous oxide emissions from tea field soil using bioaugmentation with a *Trichoderma viride* biofertilizer." The Scientific World Journal **2014**: 793752.

Xu, S., S. Zhou, S. Ma, C. Jiang, S. Wu, Z. Bai, G. Zhuang and X. Zhuang (2017). "Manipulation of nitrogen leaching from tea field soil using a *Trichoderma viride* biofertilizer." Environmental Science and Pollution Research **24**(36): 27833-27842.

Figures

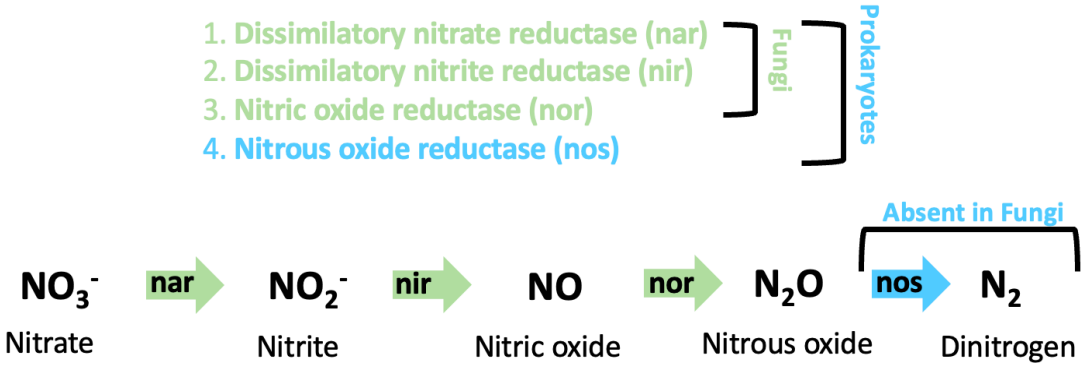

Figure 5.1: Genes and steps in denitrification pathway. Green portions occur in both fungi and prokaryotes, while blue (step four) is absent in fungi.

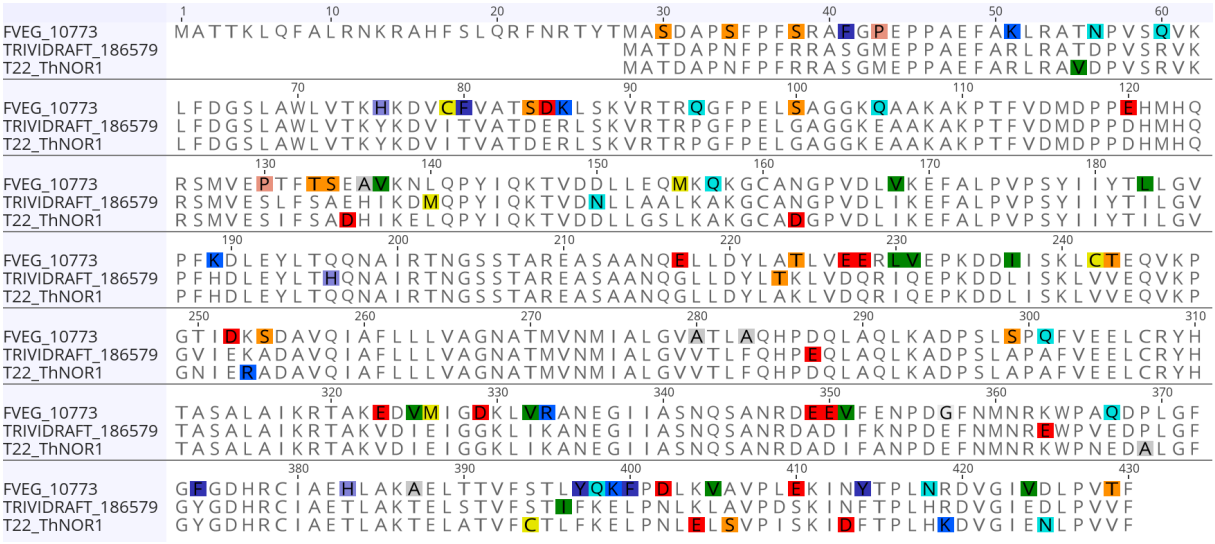

Figure 5.2: Protein alignments for N_2O pathway genes in T22. Pairwise alignment of *Trichoderma* T22 TaNOR1 protein sequence against FVEG_10773 and TRIVIDRAFT_186579. Color denotes a difference in amino acids between those sequences.

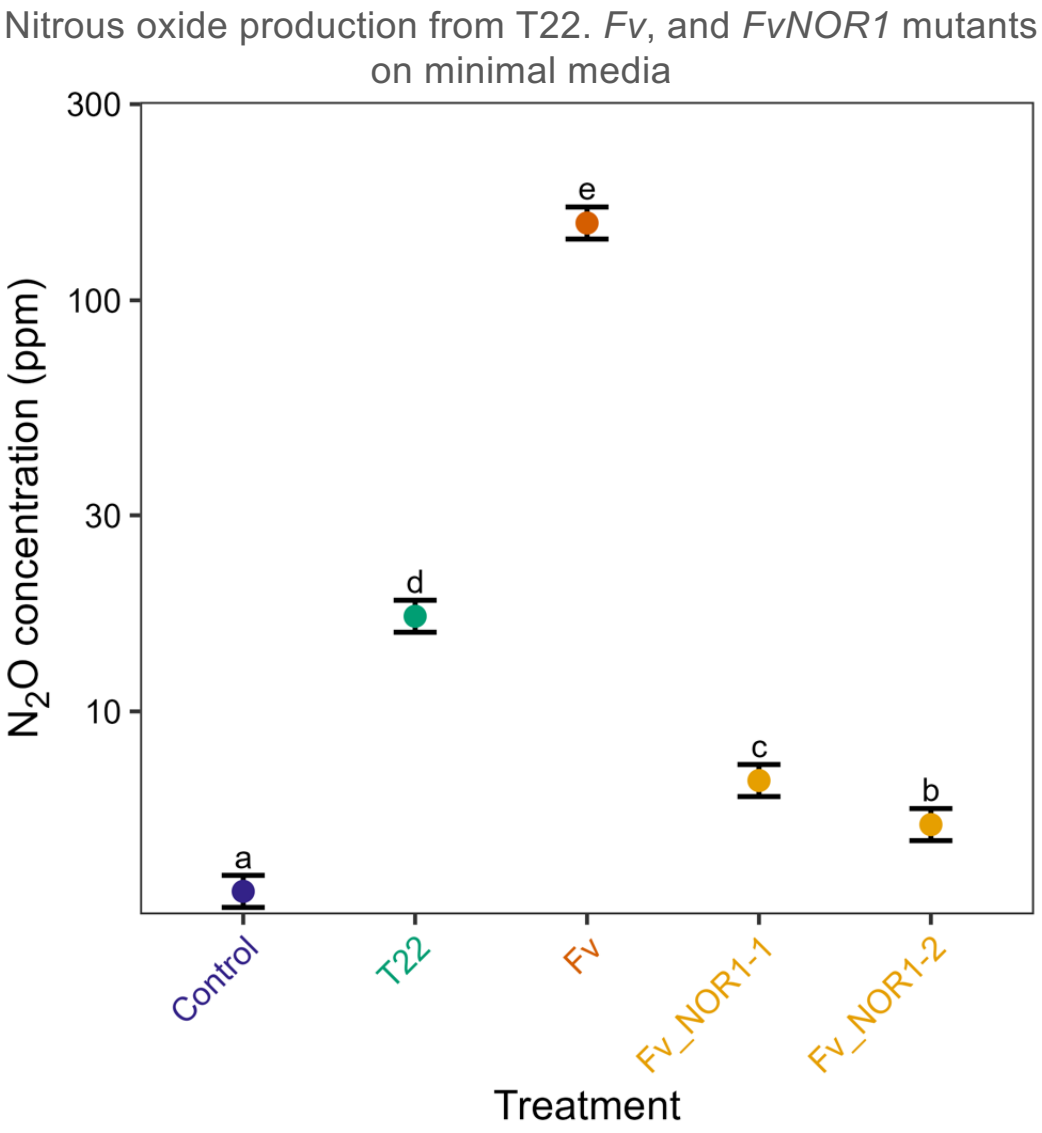

Figure 5.3: *Trichoderma* T22 N_2O production compared to *FvNOR1* mutants. N_2O expression on T22 compared to *F. verticillioides* mutants and wild *Fusarium* strains from Oakley et al. (2025) on minimal medium plus sodium nitrite (15 mM) + L-lysine (1 mM).

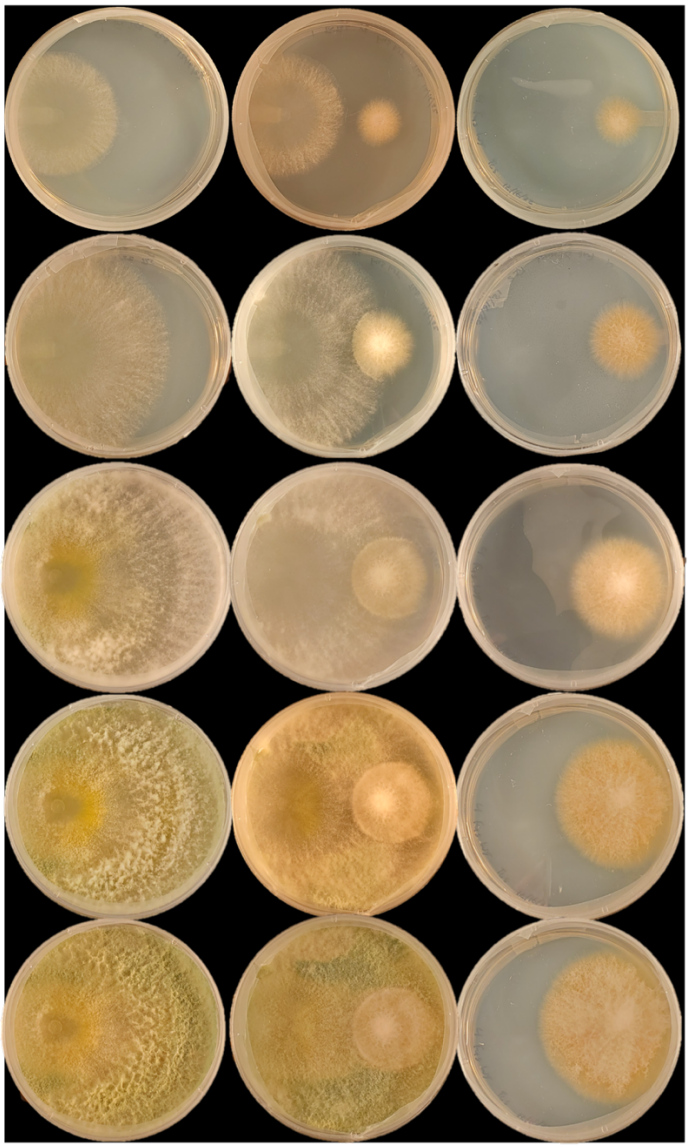

Figure 5.4: Competition plates of T22 vs Fv WT.
Trichoderma T22 (left), *Fusarium verticillioides* WT (right), and *F. verticillioides* and T22 (center) competition assays on potato dextrose agar plates after two, three, four, five, and six days at 27 °C.

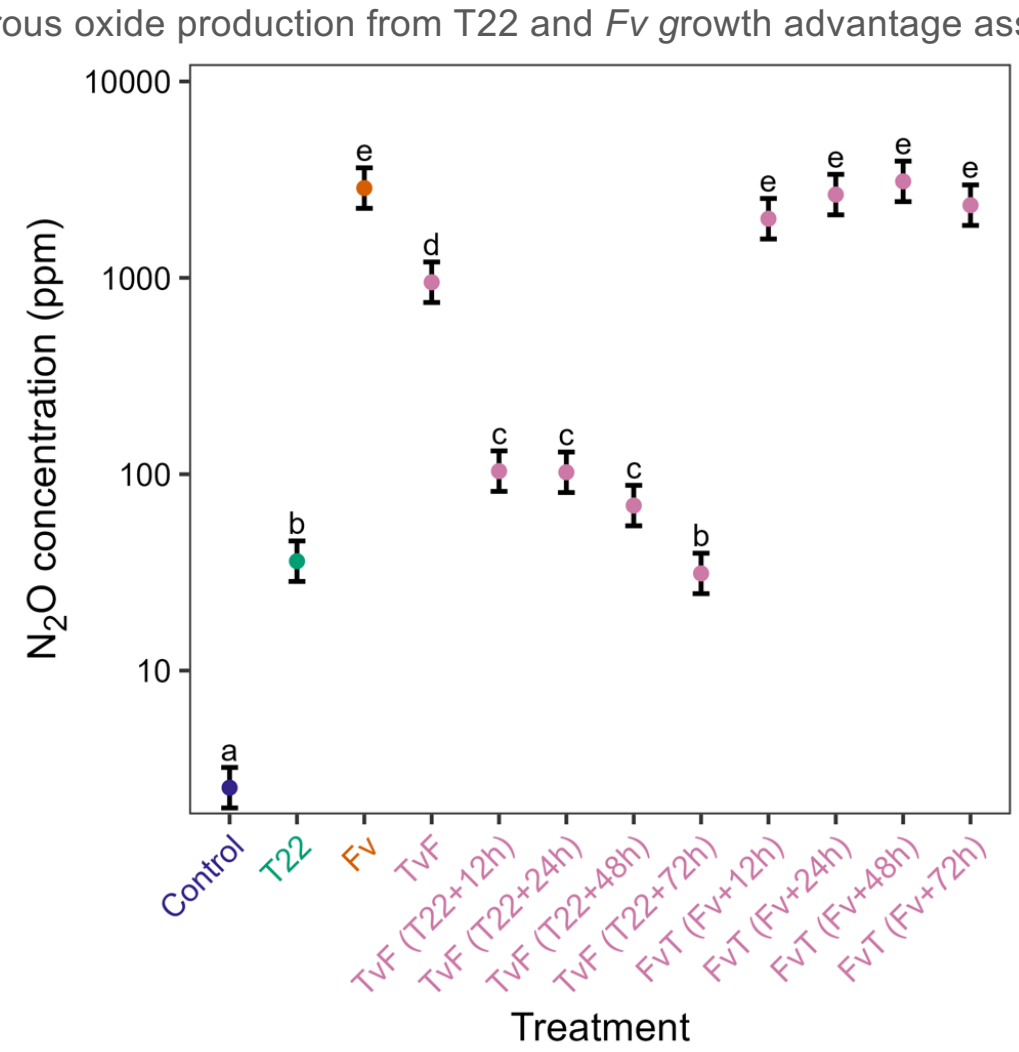

Figure 5.5: Competition and growth advantage assay N_2O production results. Preliminary results for *F. verticillioides* and T22 N_2O emissions in competition assays on minimal medium plus sodium nitrite (15 mM) + L-lysine (1 mM). *Trichoderma* T22 was given a time advantage of 12, 24, 48, or 72 hours over *Fusarium* in the TvF assays and *Fusarium* was given a time advantage of 12, 24, 48, or 72 hours over *Trichoderma* in the FvT assays.

Nitrous oxide production from T22 and *Fv* compared to high N_2O

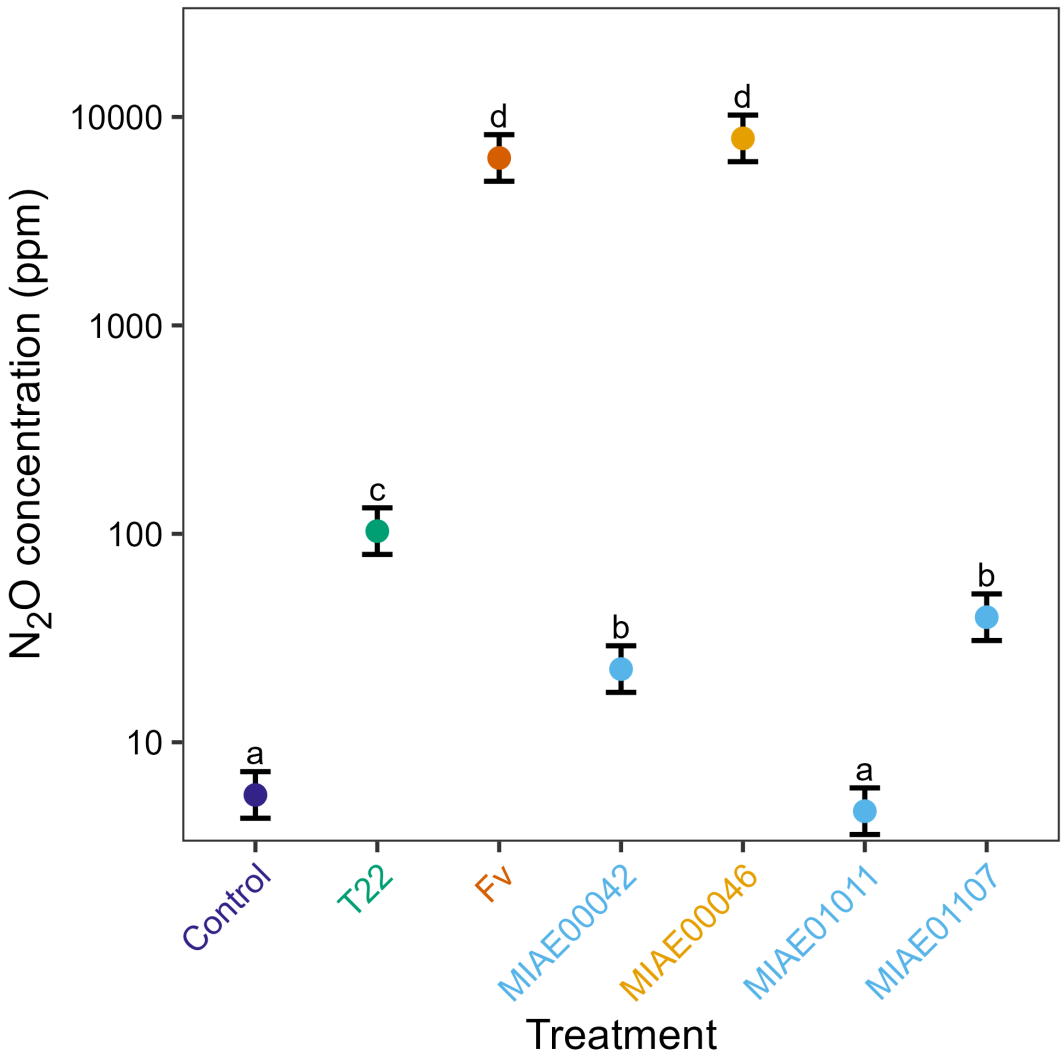

Figure 5.6: N_2O production from T22 and *Fv* compared to high N_2O producing strains on minimal medium plus sodium nitrite (15 mM) + L-lysine (1 mM).

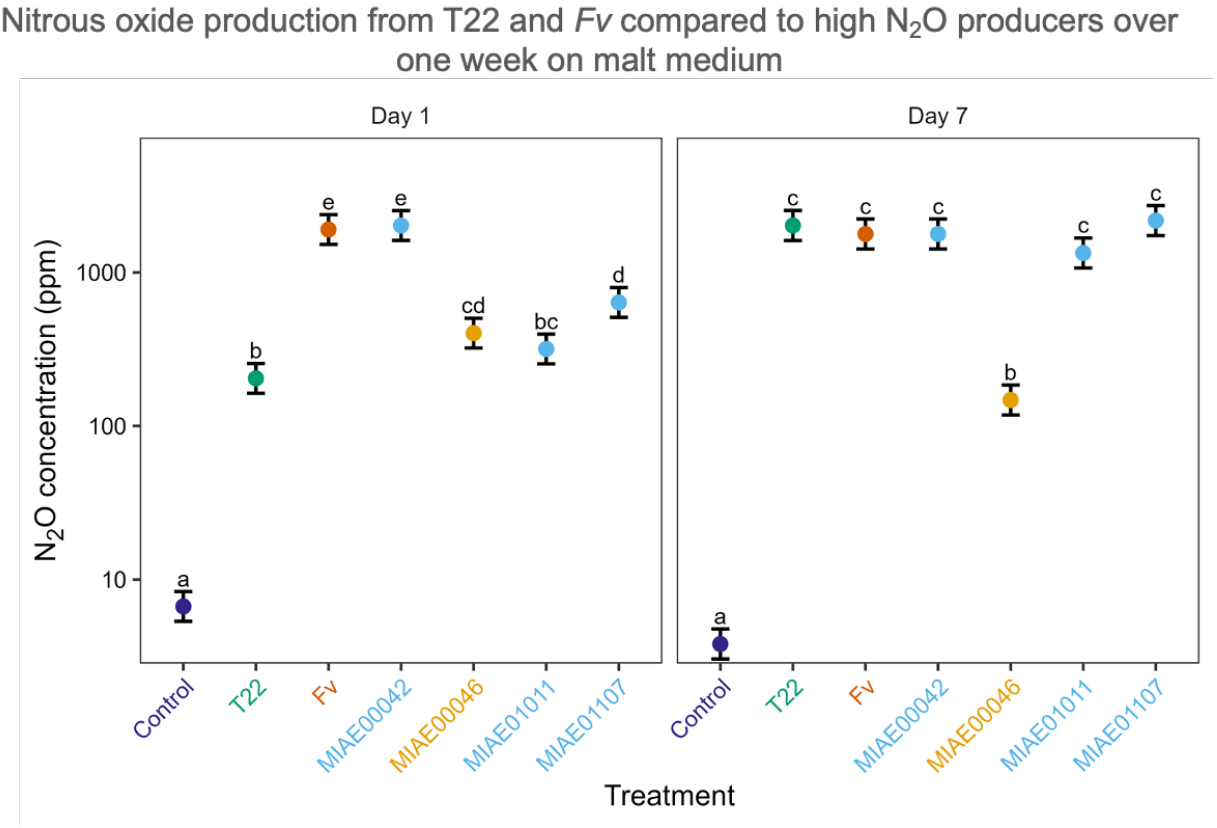

Figure 5.7: N_2O production from T22 and *Fv* compared to high N_2O producers over one week on malt medium + sodium nitrite (5 mM) assays. N_2O emissions results after one and seven days sealed for *F. verticillioides*, T22, and the four highest-producing strains from Maeda et al. (2015) in malt medium supplemented with sodium nitrite (5 mM).

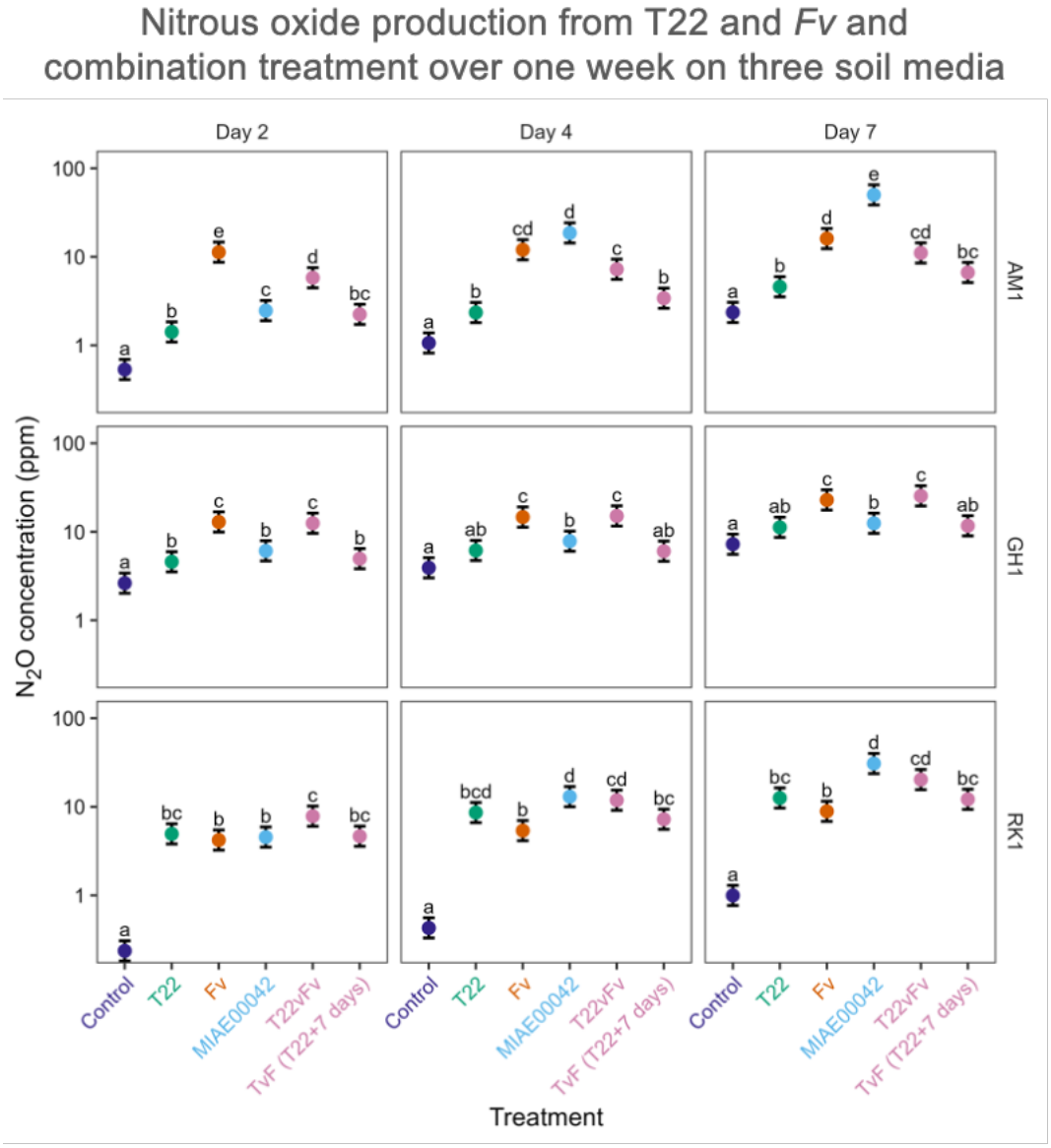

Figure 5.8: N_2O production from various fungi on three soil samples over one week. Strains of fungi were either grown alone (T22, Fv, MIAE00042) or together (T22vFv, TvF [T22+7days]) on three different soil types with sodium nitrite added.

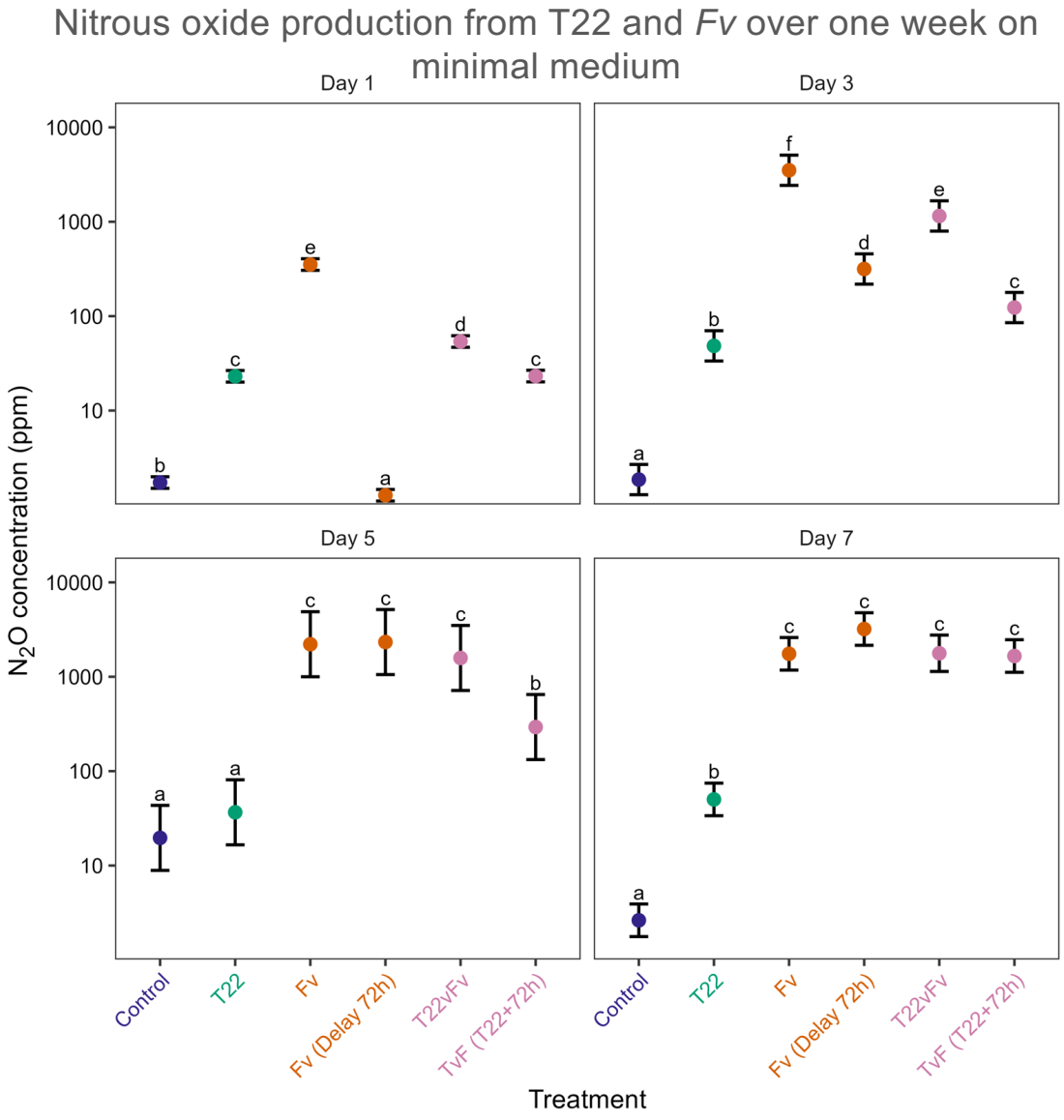

Figure 5.9: N_2O production over one week on minimal medium plus sodium nitrite (15 m + L-lysine (1 mM).Tables

Table 5.1: Fungal strains used in this study. ATCC is the American Type Culture Collect INRAE is the National Research Institute for Agriculture, Food and Environment collectio France.

Strain name	Species	Source	Description
T22	*Trichoderma afroharzianum*	ATCC	Commercial strain in RootShield
MIAE 00042	*Trichoderma harzianum*	INRAE	High N_2O producer; strain in Mae
MIAE 01011	*Trichoderma harzianum*	INRAE	High N_2O producer; strain in Mae

E 01015	*Trichoderma* sp.	INRAE	Low N_2O producer; strain in Maeda et al. 2015
E 01092	*Trichoderma* sp.	INRAE	Medium N_2O producer; strain in Maeda et al. 2015
E 01093	*Trichoderma* sp.	INRAE	Medium N_2O producer; strain in Maeda et al. 2015
E 01095	*Trichoderma* sp.	INRAE	Medium N_2O producer; strain in Maeda et al. 2015
E 01102	*Trichoderma* sp.	INRAE	Low N_2O producer; strain in Maeda et al. 2015
E 01107	*Trichoderma* sp.	INRAE	High N_2O producer; strain in Maeda et al. 2015
E 01115	*Trichoderma* sp.	INRAE	Low N_2O producer; strain in Maeda et al. 2015
E 00995	*Fusarium oxysporum* f. sp. *lycopersici*	INRAE	Low N_2O producer; strain in Maeda et al. 2015
E 00046	*Fusarium oxysporum*	INRAE	High N_2O producer; strain in Maeda et al. 2015
E 01003	*Fusarium oxysporum*	INRAE	Medium N_2O producer; strain in Maeda et al. 2015
T M3125	*Fusarium verticillioides*	Dr. Scott Gold	Wild type strain used in TRMU unit
nor1-1	*Fusarium verticillioides*	Dr. Scott Gold	NOR1 deletion mutant; hygromycin resistance
nor1-2	*Fusarium verticillioides*	Dr. Scott Gold	NOR1 deletion mutant; hygromycin resistance

Table 5.2: Soil testing results for the three soil samples used for this study. 23_RK1 is from a corn field, 24_AM1 is from a highly managed turf green, and 24_GH1 is from a low-managed grass stand. Soil testing was performed at the University of Georgia Agricultural & Environmental Services Laboratories in Athens, GA, USA.

	ppm $CaCO_3$/pH			Mehlich 1 mg/kg (ppm)						%			%				g water per g soil
Sample	**LBC**	**LBC eq**	**P^H**	**Ca**	**K**	**Mg**	**Mn**	**P**	**Zn**	**OM**	**C**	**N**	**Sand**	**Silt**	**Clay**	**Soil Type**	**Water Holding**
23_RK1	235	674	5.81	536	26.3	78.6	9.03	56.2	4.35	1.30	0.79	0.06	89.1	8.02	2.90	Sand	0.42
24_AM1	393	1140	4.94	303	49.7	40.8	38.81	36.4	0.99	3.20	1.62	0.54	58.2	23.96	17.80	Sandy Loam	0.68
24_GH1	413	1198	4.99	346	51.1	72.0	16.57	16.2	1.18	4.58	1.90	0.18	56.2	21.88	21.88	Sandy Clay Loam	0.80

CHAPTER 6

CONCLUDING REMARKS AND FUTURE PERSPECTIVES

Plant pathology is a broad field that aims to protect plant growers from many diseases and plant problems through various management strategies. My graduate research explored several areas, including molecular assay design, genomic analysis, and biological experimental design in multiple pathosystems. Here, I developed (1) two different molecular methods of dollar spot detection, (2) an in-depth genomic analysis of the two fusion participant strains, and (3) an analysis of T22's potential for use in N_2O emission mitigation. These results include two peer-reviewed

my research began in 2021, the pathogens that cause dollar spot in the continental US, *Clarireedia jacksonii* and *Clarireedia monteithiana*, were newly renamed. At the time, detection depended on either visual signs and symptoms or qPCR, which did not differentiate between the two species. There was a key need for new molecular methods of detection that allowed differentiation between the two species and allowed for same-day in-field detection. Novel dollar spot detection assays are needed to address two primary concerns. The first is that the two species causing dollar spot in the U.S. can't be differentiated from one another without waiting several days for sequencing, and the second is that dollar spot detection can only be performed in a laboratory setting, which delays rapid identification.

To answer the speciation problem, I developed a co-dominant cleaved amplified polymorphic sequences (CAPS) assay that differentiated between *C. jacksonii* and *C. monteithiana* by targeting a single nucleotide polymorphism (SNP) found within the calmodulin gene (CaM). Results are viewed on a gel, and the difference in species can be seen with a different band pattern displayed between the two species. This involved primer designing, testing, and optimization. Specificity and sensitivity were also tested. This assay was developed and tested using pure fungal culture samples but has shown significant promise and should be tested in leaf tissue or field samples.

This research included developing a probe-based loop-mediated isothermal amplification (LAMP) assay that could detect both *C. jacksonii* and *C. monteithiana*, the test species that cause dollar spots within the continental US. This assay allowed for molecular detection directly in the field with leaf tissue. The research included designing and testing primers and probes, various tissues, and optimization. This included both specificity and sensitivity testing. Positive results can

be viewed as a red liquid in the tube under blue wavelengths or using a machine such as a Genie III with real-time fluorescent quantification. To our knowledge, it was the first LAMP assay to use TaqMan probes to visualize a color difference. This result can be obtained in just over an hour and performed with reagents, pipettes, a hot water bath, and a blue light flashlight. Overall, both assays allow for faster, more precise detection to aid in dollar spot management and fulfill the objective set out to complete.

Objective two (Chapter 4): Evaluate the genomic structure and protoplast participant contribution to *Trichoderma* strain T-22 through whole genome SNP analysis of reported protoplast fusion participants.

Trichoderma is an important fungus often associated with soil and plant rhizosphere relationships. It has been studied intensely over the last century, and strains have been altered in laboratories to improve their biocontrol and biofertilizing traits since at least the 1980s. One such strain is T22, created via protoplast fusion, which has been sold commercially under several names since its generation and patent in 1990. This strain has been used extensively in various studies, but little has been studied about the strains from which it originated. The parental strains, T12 and T95, were analyzed in this research to understand the genetic background of T22 better and to identify potential gene targets for future biocontrol strain generation.

This objective aimed to identify the genomic contributions of T12 and T95 to the biological control agent T22. The strain T22 was initially patented as a protoplast fusion of T12 and T95, and while T22 had been sequenced, the two fusion participant strains had not. My research aimed to sequence those strains and compare the three genomes to one another to determine what portions came from which of the two protoplast fusion participants. The results of this study concluded that

while it was expected that there would be significant genomic contributions from both fusion participants, we instead found that there was no evidence of T95 contributing to T22's genome. This was supported by both the SNP analysis and the structural variation analysis. Additionally, the SNPs that differed between T12 and T22 were very limited. These SNPs were examined as potential targets for future *Trichoderma* line development. These genetic differences likely contribute to T22 having rhizosphere competency, a trait initially thought to have been inherited from T95. These results will help design future studies involving *Trichoderma* by focusing on these identified SNPs and host genes to better understand the biological control capacity of this fungus.

Objective three (Chapter 5): Test the use of *Trichoderma* biocontrol agent T22 to reduce fungal N_2O production in fertilized soils.

Trichoderma has been used intensively for managing pathogens and improving plant health overall; the proposed research wanted to explore its ability to mitigate the greenhouse gas and nitrogen loss bioproduct nitrous oxide (N_2O). Nitrous oxide is a significant fungal emission of concern within agriculture. Our research aimed to mitigate the fungal N_2O emissions of *Fv* through treatment with the T22 strain of *Trichoderma*.

This research aimed to understand if T22 was a good biological control candidate to mitigate the nitrous oxide (N_2O) emissions from *F. verticillioides* (Fv). T22 is a well-known biological control agent labeled for *Fusarium* management. My research tested if T22 could limit Fv's growth and N_2O emissions. The results found that T22 produces N_2O in some conditions, which may be nutrient-dependent. Additionally, it found that T22 could reduce the N_2O emissions of Fv, but the reduction can be temporary in some settings. We also found that Fv and T22 produce

some N_2O in the tested soil settings. Overall, these experiments showed promise for T22 to mitigate Fv N_2O emissions, but further research would need to be performed to develop a better fungal N_2O mitigator. These results can help inform future fungal N_2O emission mitigation research.